NASA

DYNAMICS EXPLORER SUMMARY PLOT USER'S GUIDE

December 1983

National Aeronautics and
Space Administration

Goddard Space Flight Center
Greenbelt, Maryland 20771

DYNAMICS EXPLORER SUMMARY PLOT USER'S GUIDE

November 1983

Compiled by: R. M. Candey and J. R. Thieman
ORI, Incorporated
1400 Spring Street
Silver Spring, Maryland 20910

Reviewed by: R. A. Hoffman
Dynamics Explorer Project Scientist
Code 696
Goddard Space Flight Center
Greenbelt, Maryland 20771

PREFACE

This Dynamics Explorer Summary Plot User's Guide was produced to aid the scientist who views the microfiche summary plots. In addition to general explanations of the summary plots in the introduction chapters, the plots for the individual instruments are described in separate chapters employing a common format. The information was compiled from data supplied by the DE Instrumenters.

It is difficult to anticipate questions or areas of confusion which may arise to a casual user or to a person less familiar with a particular instrument. Therefore, any and all suggestions are welcome and should be forwarded to the undersigned. Based on these suggestions, revisions to the Guide will be issued.

R. A. Hoffman
DE Project Scientist

Dynamics Explorer Summary Plot User's Guide

Table of Contents

DYNAMICS EXPLORER-1 SUMMARY PLOTS
INTRODUCTION

1.1 GENERAL EXPLANATION OF THE SUMMARY PLOTS

The Dynamics Explorer summary plots are designed to provide the scientist with a method for selecting interesting events and time periods which are likely to produce results upon detailed analysis. This is accomplished primarily by searching for particular signatures in the data.

Summary plot generation involves the extraction of a subset of the telemetry data and conversion to geophysical parameters using relatively simple algorithms. The results are summarized in plot form and displayed by the Information International FR-80 COM recorder device on microfiche. Data from all acquisition periods will eventually be processed in summary plot form.

All data appearing in the plots are unverified, and simplifying approximations are used in the conversion of the telemetry data to the plotted parameters. For these reasons the data should not be used for analysis purposes without consultation with the appropriate instrumenters (names and addresses are given at the beginning of each chapter).

For further information about the program and instruments, the researcher is referred to the special Dynamics Explorer issue of Space Science Instrumentation, 5, No. 4, 1981. Copies are available from the DE Project Scientist.

1.2 SUMMARY PLOTS FORMATS

1.2.1 General

Each microfiche contains data from one pass, the time interval that a tape recorder on the spacecraft is turned on for a continuous period. For a long pass the data may continue onto a second fiche.

A fiche title appears across the top in large bold characters. For example: "SPP DE01 81326 A081 0389", where:

SPP	Summary Plot Production
DE01	DE-1 fiche
81326	Year (YY) and day number (DDD)
A081	Magnetic tape number for the tape generated on the Sigma-9 for plotting on the FR-80
0389	Orbit number

Early production fiche may contain some variations to this format.

Four rows of frames are used to plot the data from DE-1, each column on a common time scale of one hour per frame (see Figure 1.1). Universal Time (UT) runs continuously between columns of frames, with the first column of plots beginning on an even hour. One additional frame (fifth row, last column) is used for a full pass summary of a subset of the data.

The first column of frames is a glossary containing information on the contents of each row. The glossary in the fifth row is common to all rows. The bottom row contains test patterns used for quality control purposes.

1.2.2 Polar Plot Frame

The frame in the last column, second row from the bottom, contains a polar plot of the orbit in geographic latitude and radial distance. A letter "A" designates the beginning of the pass.

1.2.3 Production Information Frame

The frame in the lower right hand corner of the fiche contains fiche production information.

Top line:	Spacecraft number and orbit number
Second line:	Date of pass (at time of tape recorder turn-on)
Third line:	Summary plot version number (see Section 1.5) and date version implemented (blank for early versions)
Fourth line:	Date fiche produced on the Sigma-9

1.2.4 Blank Frames

Data from the Spin-Scan Auroral Imager (SAI) are not plotted in the hour frames. At times the SAI is the only instrument being operated, requiring the spacecraft tape recorder to be on. In such cases, the hour frames may appear on the fiche for the other instrument data, but will contain no data plotted. See orbit 262, from 0100 to 0300 UT, for example.

At other times the tape recorder may remain on although all instruments are temporarily off. Blank frames will then appear between data periods. For example, see orbit 336 with the frame starting at 0500 UT. On other passes, only a subset of the instruments may be on and data will appear only in certain rows. For example, see orbit 333 from 1140 to 1230 UT, when only MAG-A and RIMS data appear (first and fourth rows). Finally, certain modes of operation for particular instruments produce data for which algorithms are not included, thus yielding blank frames.

1.3 ORBIT DEFINITION

Orbits are numbered sequentially with orbit number 1 beginning at the first ascending node (spacecraft crossing the geographic equator northbound). Thereafter, each orbit begins at the ascending node. The orbit assigned to a pass is determined by the location of the spacecraft at the time the tape recorder is turned on (not the time of first appearance of data). Thus it is possible for the majority of the data of a pass to have been acquired during the next numbered orbit. For example, see orbit 450, during which the instruments were turned on at the end of orbit 450, but most data were actually acquired during orbit 451 (the orbit number on each frame does change appropriately). Obviously, if more than one tape recorder operation occurs during an orbit, more than one fiche can have the same orbit number.

1.4 INSTRUMENT DATA PLOTS

First row	MAG-A ΔB_z
	PWI E_x, WBR AGC, LWR Gain, PWI Flag, AC-A, SFR, SA, Electron gyro frequency
Second row	HAPI log electron and ion energy spectrograms, log total ion and electron particle fluxes
Third row	EICS H^+ & O^+ flux at 90^o pitch angle and maximum flux designated by pitch angle range if not at 90^o pitch angle, for energy ranges 0-1, 1-4, 4-16 keV
Fourth row	RIMS ion densities, ram angle & ion count rate/angle spectrograms for H^+ and He^+
Fifth row	Full pass plots of MAG-A, PWI, HAPI, RIMS data
Sixth row	Spacecraft orbit plot and SAI filter data
Seventh row	Test patterns and fiche production data

See the Glossary for explanation of the abbreviations.

Spectrograms show the time variations of spectra. At each level of the spectrogram, an area is filled in, with the intensity and width determined by the value of the flux at that level and time and by the time resolution of the measurements. For HAPI, there may be up to 32 levels. There are 24 ranges of ram angles for RIMS and frequencies for PWI. For SFR, there are 128 frequency ranges and for SA 8 ranges of frequencies at which counts are plotted.

1.5 VERSIONS

As algorithms for the instrument data have improved or software problems solved, the summary plot production programs have been given new version numbers (see 1.2.3). The primary changes which affect the summary plots from the user's perspective are listed in Table 1.1 for each version.

1.6 PROBLEMS

As the fiche are produced, occasional problems are found in either the formats or the data plotted. These are investigated and corrections made to the programs when appropriate. An example of a data-related problem appears in orbit 982 (Version 3.3) with the PWI spectrogram, in which the same data are plotted during the first 8 minutes of each frame. When appropriate, such passes are reprocessed and new fiche produced. All fiche produced with Versions prior to 3.6 will eventually be rerun.

The file TMSTAT (see Dynamics Explorer Telemetry Status File Scanning Program User's Guide, July 1983) contains a "Variance" field for comments on problems with the Summary Plot fiche or reasons why certain data do not appear.

Telemetry synchronization losses can cause short data drop-outs, and noisy telemetry can cause spurious points on the plots.

The Invariant Latitude (IL) reads "999" when McIlwain's L value is greater than 100.

1.7 INSTRUMENT ORIENTATION

Figure 1.2 shows the general orientation of the instruments aboard DE-1.

TABLE 1.1 Summary Plot Algorithm Changes

Version	Day	Instrument	Corrections and Changes
3.0	82162	MAG-A:	Correction introduced to phase angle of magnetic field for small offset of sensor axes to spacecraft axes. (N.B.: This correction was introduced incorrectly and affects E_x, HAPI, EICS and RIMS data until Version 3.4)
		PWI:	E_x changed to linear scale from log scale
		RIMS:	New grey scale
		Glossary:	Added input file information
3.1	82175	PWI:	Corrected PWI mode information on top frame
		Glossary:	Added grey scale table dates
3.2	82216	MAG-A:	Correction introduced to ΔB_z to correct sign (N.B.: from Version 3.0 to this version, sign of ΔB_z was incorrect)
		RIMS:	Modified algorithm to handle additional modes
		Quality Control:	Two areas of grey shades added to test frames for densitometer measurements of the grey scale
3.3	82223	Glossary:	Satellite darkness indicator explained
3.4	82307	MAG-A:	Corrected calculation of phase angle to magnetic field. Affects E_x, HAPI, EICS, and RIMS data
		RIMS:	Modifications to acquire spectrograms after switch of mode during pass
3.5	83047	PWI:	Algorithm changed to eliminate saturated spectrograms when filter bank not available
3.6	83056	Geomagnetic Latitude:	Corrected code for calculation
3.7	83076	Nadir Pulses:	Introduced test to eliminate spurious nadir pulses
		EICS:	Eliminated points plotted at 0 when instrument power off (Note: occasionally on EICS, memory load was missed because of unavailable ground station contact with spacecraft, causing EICS to remain off)
3.8	83104		No user impacts
3.9	83143	MAG-A:	Dual scale introduced for ΔB_z
		HAPI:	Total flux integral started at 20 eV instead of 5 eV to eliminate photoelectrons
4.0	83174		No user impacts
4.1	83220	PWI:	Added electron gyrofrequency to PWI spectrogram. PWI FLAG and LWR GAIN plotted every two major frames instead of every one (Note: due to program error, the calculated points do not appear)

SPP DE01 81326 A081 0389

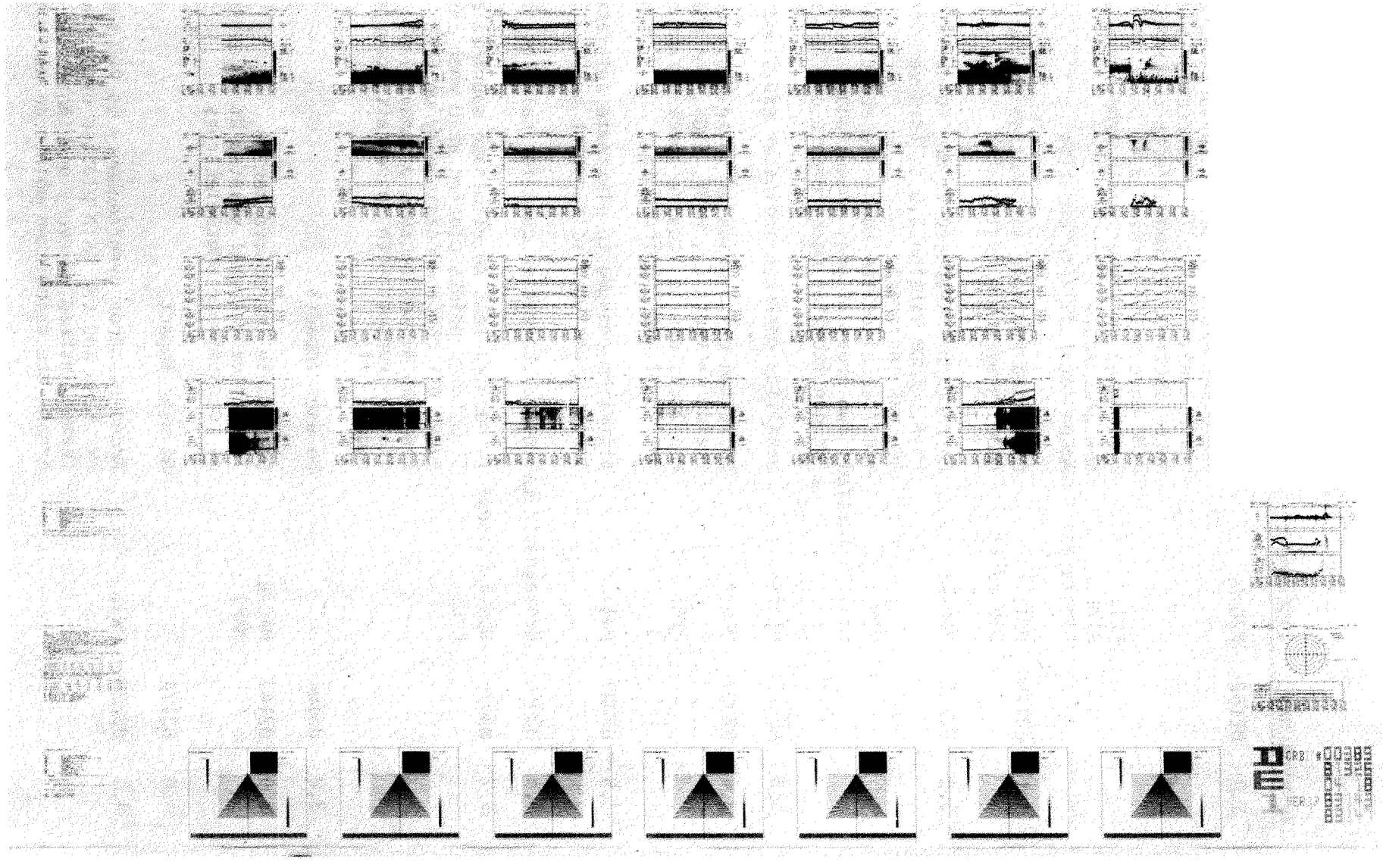

Figure 1.1: Summary plot microfiche layout

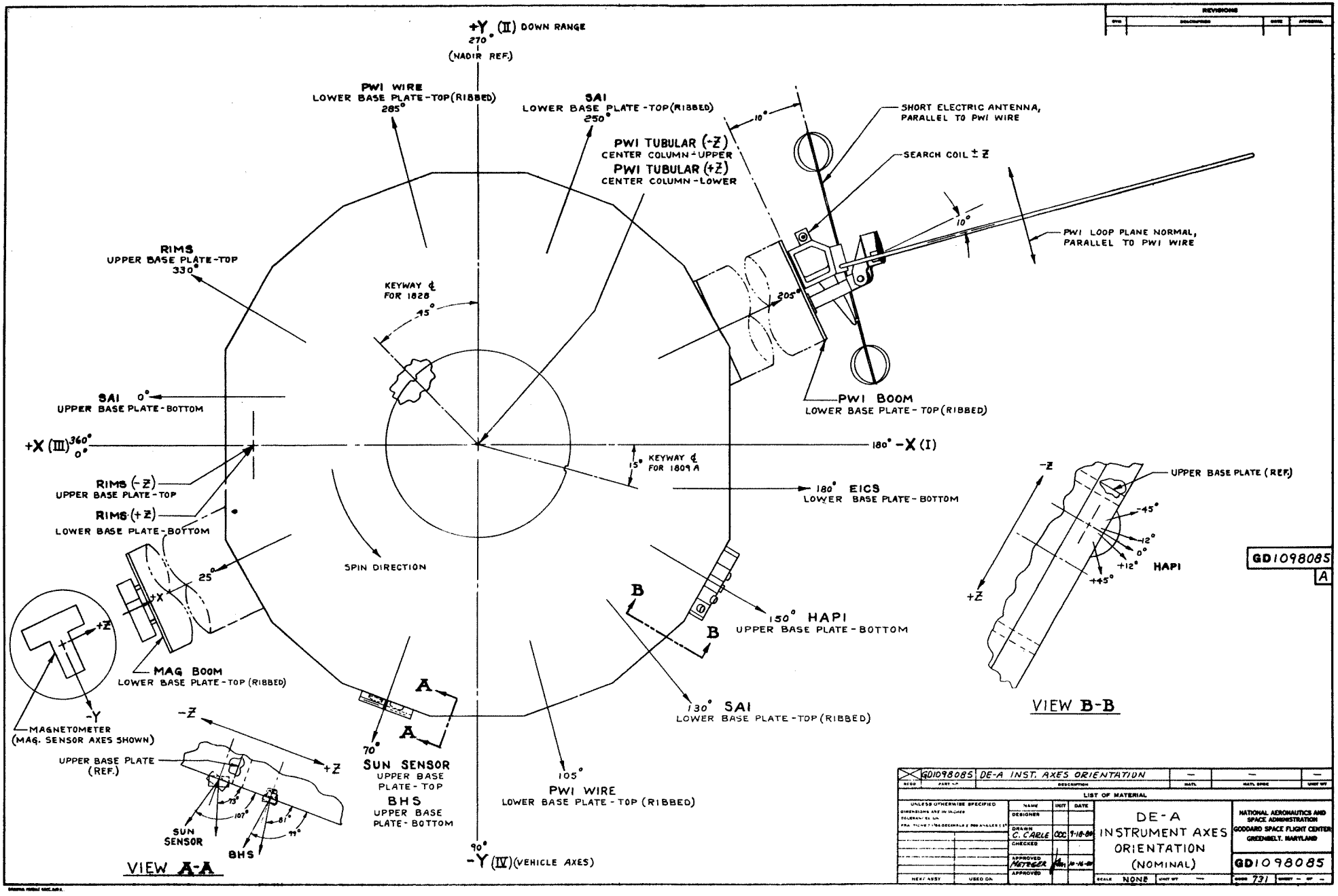

Figure 1.2: Orientation of the instruments on DE-1

CHAPTER 2
MAGNETOMETER (MAG)-A

2.1 FURTHER INFORMATION:

Contact: Brian Ledley (301) 344-6259
Code 696
Goddard Space Flight Center
Greenbelt, MD 20771

References: Farthing, W.H., M. Sugiura, B.G. Ledley, and L.J. Cahill, Jr., "Magnetic Field Observations on DE-A and -B", Space Science Instrumentation, 5, 551 (1981).

2.2 SUMMARY PLOT PARAMETERS:

- o B_z Measured magnetic field
  --Component along the spin axis, nominally in the East-West direction.
- o ΔB_z Bz minus MAGSAT model internal field
  --Provides a high resolution display of changes in B_z and a sensitive parameter for field-aligned currents (FAC).
- o Full pass plot
  --Provides an overall picture of ΔB_z along the entire pass.

2.3 PARAMETERS NOT PLOTTED:

- o Other components of the magnetic field
  --None plotted since complicated algorithms are required to calculate all three components of the difference field by despinning the coordinate system.

2.4 MEASUREMENT UNITS

- o Geophysical Units: Directly in nanoTeslas (nT).
- o Range of Valid Data: All on-scale ΔB_z.
- o Summary Plot Sampling Rate: Once per spin (6 seconds).
- o Summary Plot Resolution: The resolution on the ±750 nT and ±500 nT scale plots is limited to the summary plot resolution of about 1/500 of full scale, i.e., about 3 nT. This is the same as the instrument resolution when the instrument is in its highest range mode. For the ±100 nT scale plots, the resolution is either 3 nT, when the instrument is in its highest range mode, or 0.25-0.5 nT (the summary plot resolution), when the instrument is in its more sensitive modes.

- o Accuracy of Trends on Plots: Long term trends are not meaningful.

- o Instrument Orientation: See Figure 1.2. B_z is positive in the spacecraft +Z direction, which is West when traveling South to North and East when traveling North to South.

- o Summary Plot Algorithm: The non-orthogonal field components along each sensor's effective axis are combined by a linear matrix multiplication to describe a vector in spacecraft coordinates. Only the Z-axis component is used in the ΔB_z calculation for the summary plots.

2.5 MODES

- o Three instrument resolution modes:
  --$\pm$1.5 nT with a range of +62,000 nT
  --$\pm$0.2 nT with range of +1000 nT
  --$\pm$0.02 nT with range of $\pm$80 nT
  --The two high resolution modes are used for wave studies at high altitudes.

2.6 CORRECTED FOR:

- o Orientation of the triaxial magnetometer sensor axes
  --Long term stability is expected to be about 0.1 degrees.

- o Spacecraft magnetic field
  --Expected to be below the instrument's resolution.

- o Cross coupling between sensors
  --Corrected for in the definition of sensor axis directions.

- o Thermal effects
  --Calibration includes the temperature dependence of the sensors.

2.7 UNCORRECTED FOR:

- o Spacecraft attitude
  --ΔB_z depends on the accuracy to which B_z lies East-West, since ΔB_z is B_z minus the model East-West component.

2.8 DISPLAY ANOMALIES:

- Scale changes with altitude
  --Originally a 500 nT plot scale was chosen for ΔB_z to provide a high resolution display. To reduce the frequency of off-scale plots and provide better resolution at high altitudes, two scales were employed for plots generated after May 1983 (summary plot Version 3.9, see Section 1.5). These scales are +750 nT, used when the spacecraft is at low altitudes, and $\pm$100 nT used at high altitudes when the signatures of field-aligned currents are smaller.

- Off-scale ΔB_z
  --Due to attitude description errors, model field errors, and occasional large field-aligned current signatures. Saturated plots may be replaced at a future date. See Figure 2.1, day 81302, orbit 304, starting at 0335 UT, for an example.

- North pole effect on ΔB_z
  --Discontinuity in ΔBz on crossing the geographic poles due to the subtraction of the East-West component of the model field. See Figure 2.2, day 82177, orbit 1146, at 0824 UT, for example.

2.9 INTERPRETATIONS:

Substantial variation in "standard" patterns exist. The following are given only as possible cases and should not be construed as definitive.

- VLF waves
  --See Figure 2.3, day 82211, orbit 1264, from 0211 to 0300 UT, for example.

- Field-aligned currents
  --See Figure 2.4, day 82204, orbit 1239, at 0350 UT, for example. A decreasing ΔB_z corresponds to an upward current and an increasing ΔB_z corresponds to a downward current. Currents cannot always be modeled by infinite current sheets. Therefore caution is required in deducing the direction of the current.

2.10 COMMENTS

- PWI E_x data are often helpful in identifying field-aligned current regions.

- Ignore saturated plots and extremely rapid changes from one limit of the scale to the other (either attitude data or reference field values are wrong).

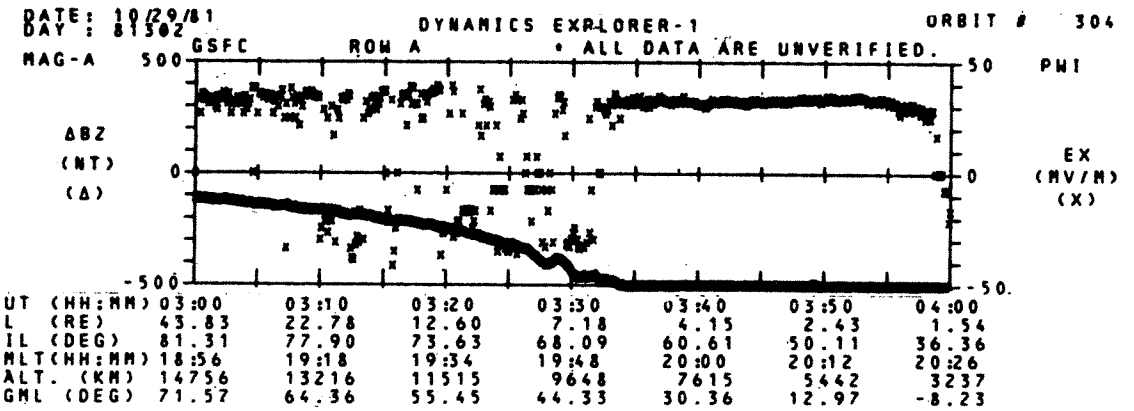

Figure 2.1: Example of saturated ΔB_z plots

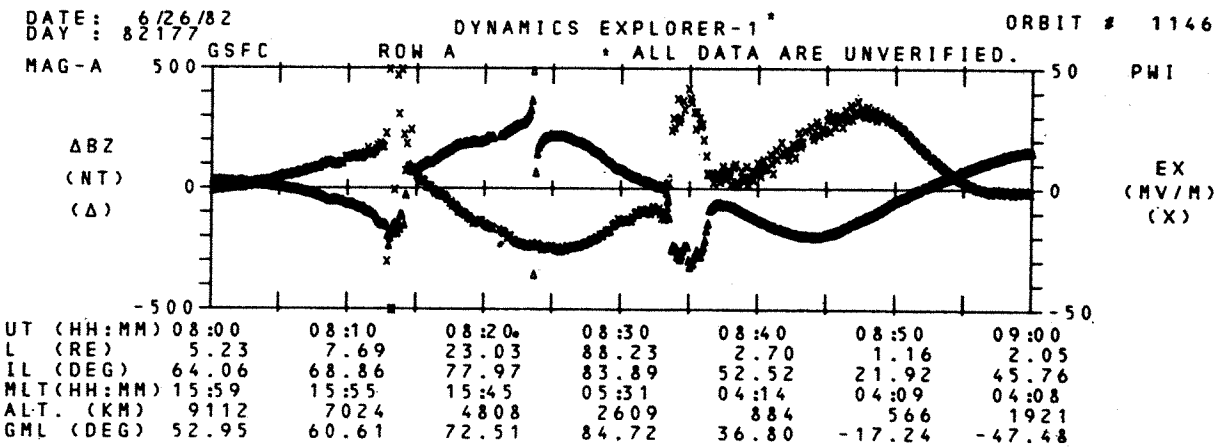

Figure 2.2: Example of North Pole effect

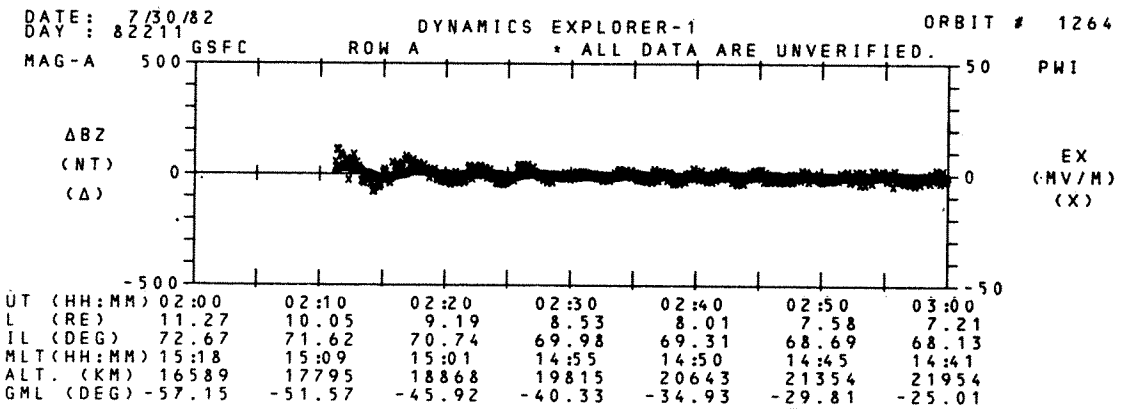

Figure 2.3: Example of VLF wave

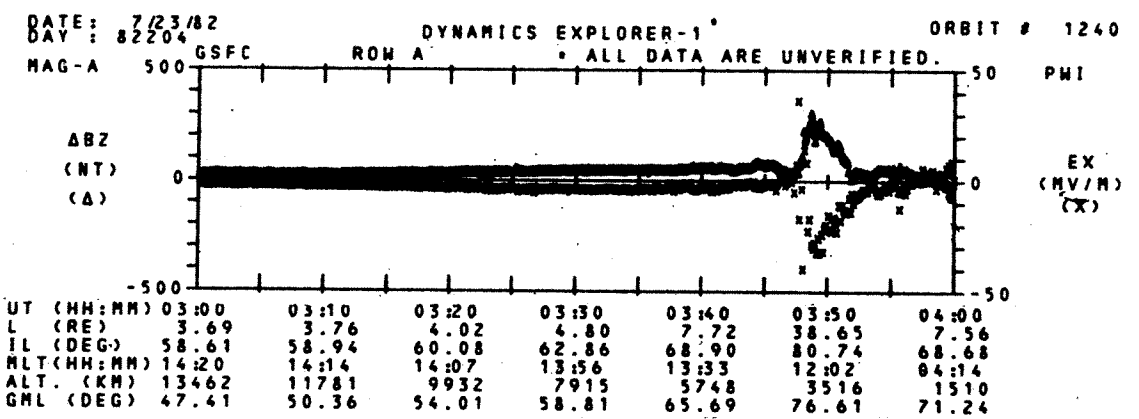

Figure 2.4: Example of field-aligned currents

CHAPTER 3

PLASMA WAVE INSTRUMENT (PWI)

3.1 FURTHER INFORMATION:

Contact: Stanley D. Shawhan (319) 353-3294
Richard L. Huff (319) 353-7413
Department of Physics and Astronomy
University of Iowa
Iowa City, Iowa 52242

References: Shawhan, S.D., D.A. Gurnett, D.L. Odem, R.A. Helliwell, and C.G. Park, "The Plasma Wave and Quasi-static Electric Field Instrument (PWI) for Dynamics Explorer-A", Space Science Instrumentation, 5, 535 (1981).

3.2 SUMMARY PLOT PARAMETERS:

- o E_x Electric field perpendicular to B
  --From the spin-plane wire antennas. This is the most reliable determination and is comparable to other determinations of plasma convection velocity by $v_c = (E \times B)/B^2$.

  --Full pass plot shows changes along the entire orbit.

- o WBR AGC Automatic Gain Control of the Wide Band Receiver
  --Indicates the broadband signal strength of noise in the passband. Antenna data are also given.

- o PWI Flag Analog data downlink flag
  --(a line at about 4 Volts in the WBR AGC panel) Indicates Wide Band Receiver (WBR) data transmitted.

- o LWR AGC Gain from the Linear Wideband Receiver
  --Another indication of noise. Antenna data are also given.

- o PWI AC-A AC wave digital spectrogram from the Sweep Frequency Receiver (SFR) and the Spectrum Analyzer (SA)
  --Usually connected to the E_x (long wire) antenna and provides the best frequency survey of wave activity from 1.8 Hz to 400 kHz. Antenna data are also given.

- o Electron gyrofrequency
  --Calculated from the model field, beginning with Version 4.1 (although not plotted yet due to program error).

o The following passbands are used:

Number	WBR Mode	WBR Channel	LWR Channel
0	10 KHz + FM	Baseband	3-6 KHz
1	40 KHz	31.25 KHz	6-10 KHz
2	10 KHz only	62.5 KHz	10-16 KHz
3	FM	125 KHz	3.11 KHz
4		250 KHz	
5		500 KHz	
6		1 MHz	
7		2 MHz	

3.3 PARAMETERS NOT PLOTTED:

o Step frequency and low frequency correlations
--The second receiver spectrum, with E_z or loop antennas, does not show much overall difference from the PWI AC-A plot.

o Wide band receiver data
--Infeasible to display 512 frequency bins with 50 msec resolution; the data are available only 20-40 percent of the time and are not digitized. The analog data is available from the University of Iowa.

3.4 MEASUREMENT UNITS

o Geophysical Units: E_x is in physical units of mV/m. Spectrogram time and frequency ranges are given on the plots.

o Range of Valid Data: Spectrogram grey scale amplitude covers 100 dB (20 dB/Volt) and 1 to 1000,000 Hz. The plotted range for E_x is $\pm$50 mV/m, 0-5 Volts for WBR AGC and 8 levels for LWR Gain.

o Summary Plot Sampling Rate: The instrument samples E_x 16 times a second, but only one point per spin is plotted. The instrument resolution for the spectrograms is 32 seconds per spectrum.

o Summary Plot Resolution: E_x is quantized over 256 counts which gives an instrument resolution of 100 nV/m. The frequency resolution of the spectrogram is less than 100 Hz for 4 per decade and greater than 100 Hz for 64 instead of 128 steps. There are 128 frequency ranges for SFR and 8 ranges of SA frequencies.

o Accuracy of Trends on Plots: E_x is accurate to within $\pm$10 percent (plus antenna effects) in low density plasma less than 10 per cm^3. The spectrograms are accurate to the grey scale limit.

o Orientation of Antennas: See Figure 1.2. The spacecraft orientation is corrected for in the DC E_x plot and does not affect the rest of the summary data.

o Summary Plot Algorithm: A simple algorithm is used to derive E_x for plotting in which single points are selected when E_x is perpendicular to B using the magnetic nadir. All other PWI summary data are raw values.

3.5 MODES

o Antennas:
  --Long wire in spin plane, E_x, provides the best detail for electrostatic and electromagnetic waves.
  --Short dipole, E_s, is very insensitive and is unreliable below 100 Hz.
  --Tubular boom along spin axis, E_z, is 30 dB less sensitive than the long wire antenna.
  --Search coil, H, is for less than 100 Hz electromagnetic waves.
  --Loop, B, is for greater than 100 Hz electromagnetic waves.

o Receivers and Correlators:
  --Wideband analog spectrum, WBR; only WBR AGC is plotted.
  --Linear wideband analog spectrum, LWR; only LWR AGC is plotted.
  --Narrowband step frequency spectrum, SFC, can lock frequency step through four frequency bands related by 1:8:64:512.
  --Narrowband low frequency spectrum, LFC, can lock frequency step through two bands related by 1:10.

o Both high and low gain are available simultaneously.

o Manual and automatic antenna modes:
  --Auto-antenna sequences through all antennas in 48 seconds. Manual is the usual mode for all PWI sub-systems. Some auto antenna select passes have been made, but these require special processing; summary data are confusing and often appear as a checkerboard pattern. See Figure 3.1, day 81261, orbit 163, from 1800 to 1832 UT, for example. The mode was used from 1622 to 1832 UT.
  --Manual and automatic gain modes for LWR; auto-ranging gain is the usual operational mode. Manual gain is used for calibration and for Stanford real-time exercises.
  --Manual and automatic step select; auto step select (sweeping) is the usual mode for SFR's and LFC's. Manual step select has been used, but it requires special processing.

o Step rates
  --32 seconds/sweep; usual operational mode.
  --8 seconds/sweep; not used.

3.6 CORRECTED FOR:

o Nothing.

3.7 UNCORRECTED FOR:

- o v x B component in E_x
  --Not subtracted out in the summary plots.

- o Sensors in spacecraft shadow
  --Affects the reliability of E_x and E_z in an unpredictable manner. No effect on AC spectrograms.

- o Contact potential differences
  --Produces unpredictable changes to E_x and E_z.

- o Cross talk between channels

- o Low frequency noise from solar array effects
  --Seen on all AC spectrograms.

- o Radiated magnetic field from spacecraft
  --Seen in AC spectrograms when connected to the B loop. Possible harmonics from the pulse-width generator.

3.8 DISPLAY ANOMALIES:

- o Internal calibration of the instrument
  --Used infrequently.

- o Saturated plot points in E_x
  --Related to spacecraft charging. See Figure 3.2, day 82045, orbit 685 (Version 3.4), from 1703 to 1710 UT, for example.

- o Incorrect E_x scale before Version 3.0
  --Changed from log to linear scale in Version 3.0.

- o Version 3.0 to 3.4 E_x plots are invalid due to a programming error in calculating the pitch angle from the magnetometer.

3.9 INTERPRETATIONS:

Substantial variation in "standard" patterns exist. The following are given only as possible cases and should not be construed as definitive.

- o Plasmaspheric hiss
  --See Figure 3.3, day 81281, orbit 230, from 0140 to 0155 UT, for an example covering the 1-10 kHz frequency range.

- o Auroral kilometric radiation (AKR)
  --Usually seen in every orbit. In general, emissions above 100 kHz are AKR by definition except for UHR, solar bursts, etc. See Figure 3.4, day 81309, orbit 329, beginning at 0540 UT, broadening down to 100 kHz at 0638 UT. Saturation of the SFR occurs throughout, producing a cut-off at 60 kHz.

- o Plasma frequency
  --Cut-off can be seen in Figure 3.4, day 81309, orbit 329, from 0600 to 0625 UT. The cut-off is at about 12 kHz, bounding auroral hiss below and probably Z-mode above.

- o Upper Hybrid Resonance (UHR)
  --See Figure 3.5, day 81281, orbit 231 for an example. UHR is off the top of the frequency scale at 0950 UT and becomes visible at decreasing frequencies until 1000 UT when it approaches the local electron cyclotron frequency at about 30 kHz. The local electron gyro frequency shows as a faint line on top of the spectrograms. This may not show on the printed example.

- o VLF ground transmitter signals
  --See Figure 3.5, day 81281, orbit 231, from 0836 to 0856 UT, for an example at about 20 kHz.

- o Chorus
  --Broadband structure decreasing from about 12 kHz to about 300 Hz in Figure 3.5, day 81281, orbit 231, from 0915 to 1000 UT, for example.

3.10 COMMENTS

- o Observe correlations of E_x with VEF1. WBR AGC data can be correlated with E_x, magnetometer and particle measurements; LWR AGC data can be correlated with ground transmitters in the passband.

- o Distinguishing polarization, propagation direction, and electrostatic versus electromagnetic energy require both spectrograms with special processing.

- o If ΔB_z is suspect, E_x may be suspect also.

- o Due to power limitations, the duty cycle of PWI is about 50 percent and real-time analog data is limited to 20-40 percent.

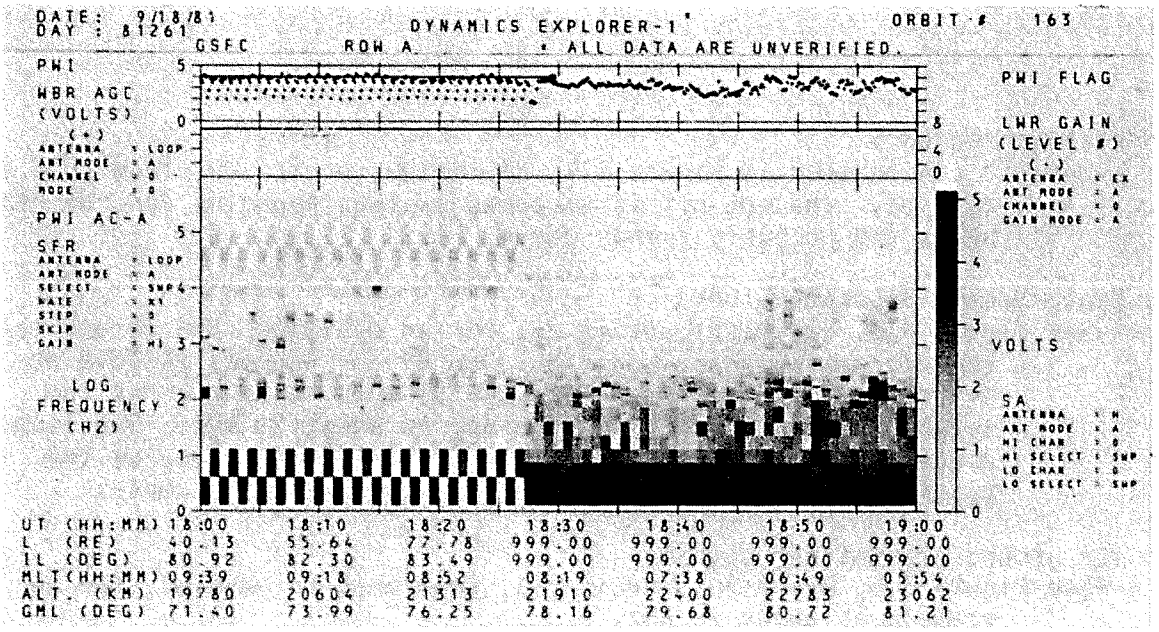

Figure 3.1: Example of auto-antenna select mode

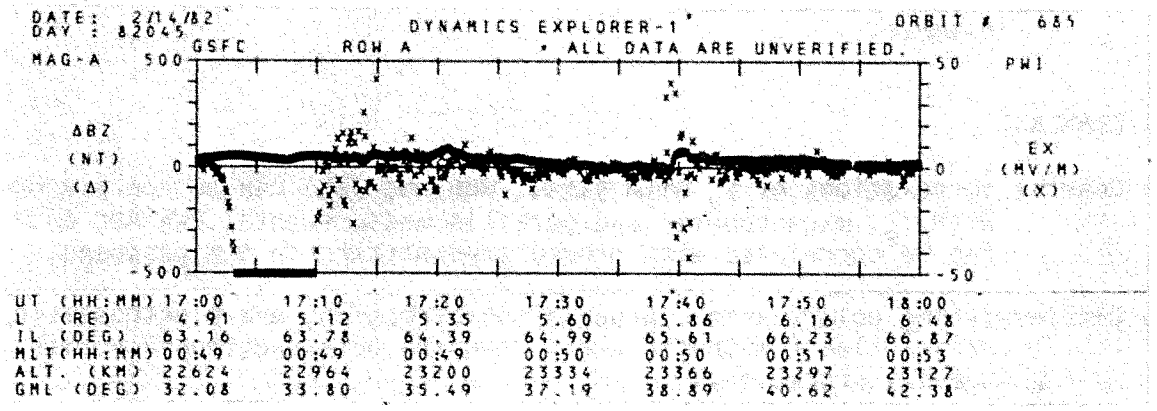

Figure 3.2: Example of saturated plot points in E_x

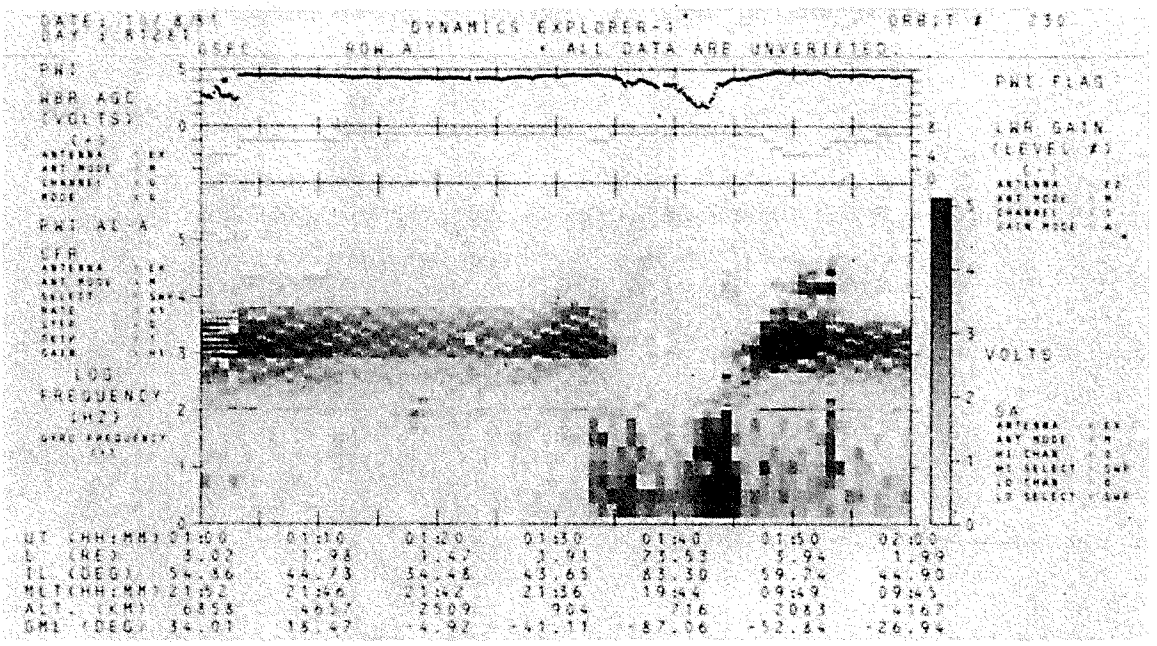

Figure 3.3: Example of plasmaspheric hiss

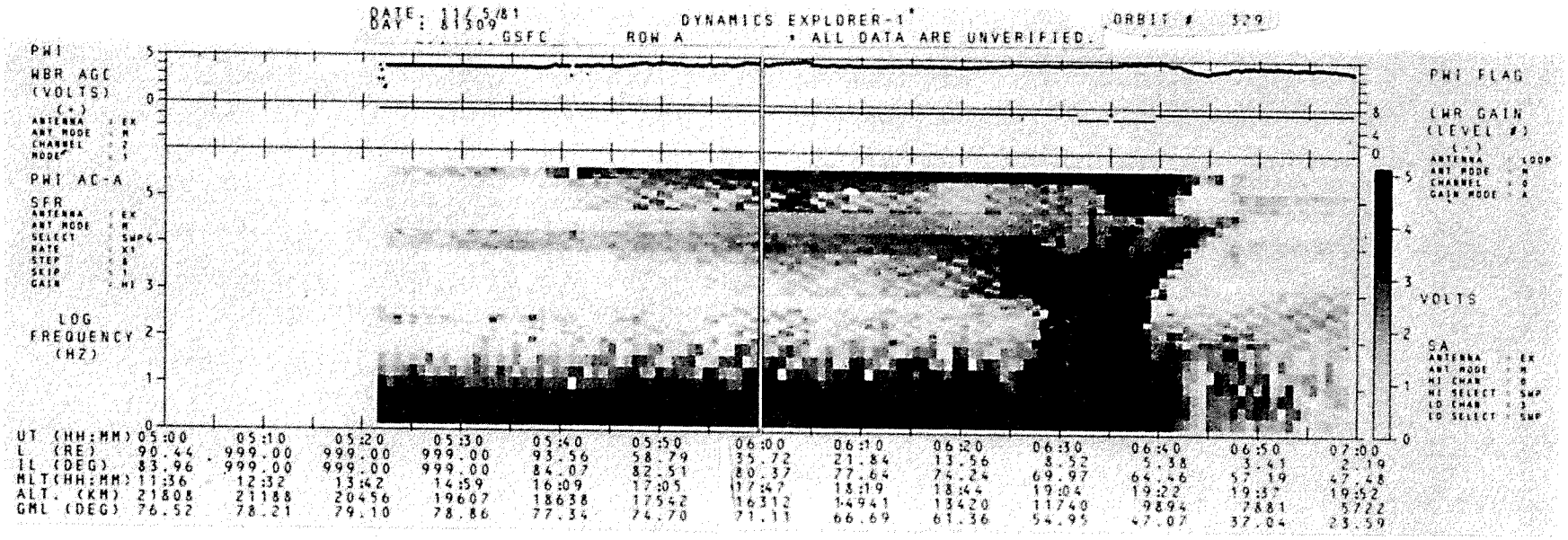

Figure 3.4: Example of strong AKR and plasma frequency cut-off

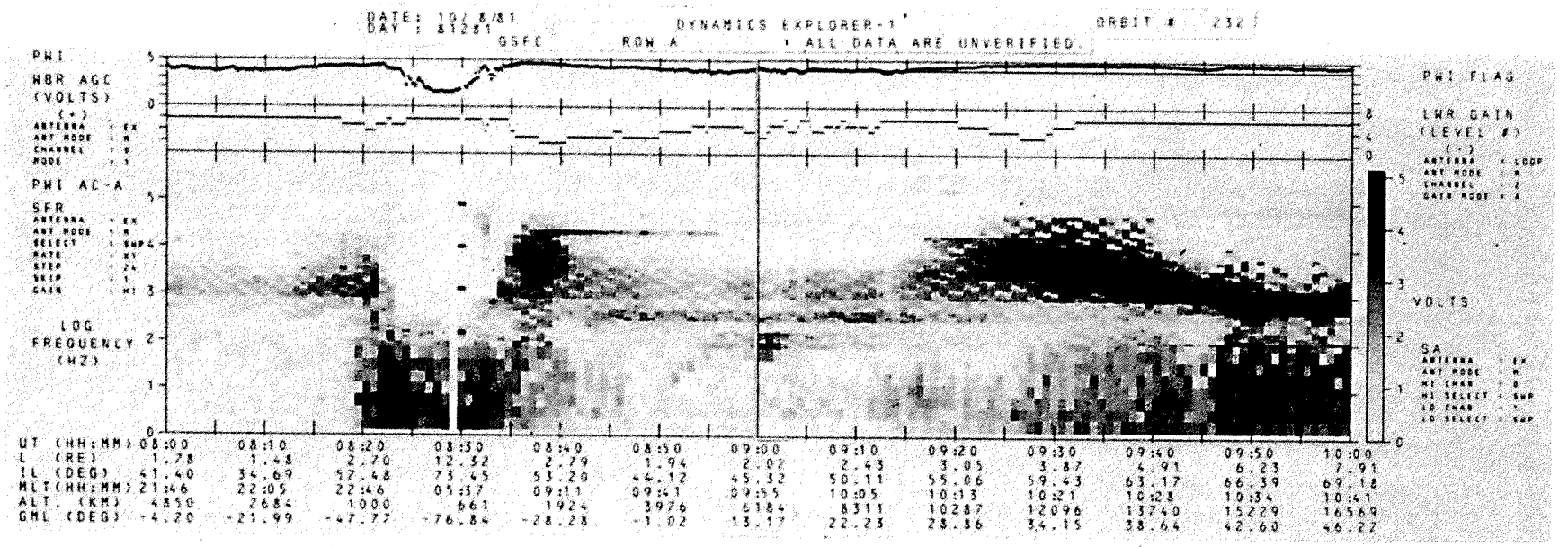

Figure 3.5: Example of UHR, VLF ground transmitter signals and chorus

CHAPTER 4

HIGH ALTITUDE PLASMA INSTRUMENT (HAPI)

4.1 FURTHER INFORMATION:

Contact: James L. Burch (512) 684-5111 x2526
Southwest Research Institute
P.O. Drawer 28510
San Antonio, TX 78284

References: Burch, J.L., J.D. Winningham, V.A. Blevins, N. Eaker, W.C. Gibson, and R.A. Hoffman, "High-Altitude Plasma Instrument for Dynamics Explorer-A", Space Science Instrumentation, 5, 455 (1981).

4.2 SUMMARY PLOT PARAMETERS:

- o Ion and electron energy flux spectrograms near 90 degree pitch angle
  --90 degree pitch angle provides a sensitive indication of the presence of both trapped and isotropic distributions.

- o Total particle flux line plot near 0 degree pitch angle
  --Integrates both ions and electrons over 5 eV (20 eV with Version 3.9) to 25 keV.
  --Included because particle flux is closely related to current density and responds equally to particles of all energies. Energy flux, on the other hand, is more strongly affected by higher energy particles.

- o Total energy flux line plot near 90 degree pitch angle on full pass summary plot
  --Shows the integrated energy flux.

4.3 PARAMETERS NOT PLOTTED:

- o Spectra as a function of other pitch angles and separate analyzers
  --Insufficient space and resolution.

- o Flow velocities
  --Calculated under certain conditions, but requires algorithms too complicated for summary plots.

4.4 MEASUREMENT UNITS

- o Geophysical Units: Energy in electron Volts (eV), energy flux in ergs/(cm^2 sec sr eV) and particle flux in particles/(cm^2 sec sr).

o Range of Valid Data:

--Energy	5×10^{-7} eV to $31{,}000$ eV
--Energy flux	10^{6} to 10^{11} ergs/(cm^2 sec sr eV)
--Total particle flux	10^{-4} to 10^{2} particles/(cm^2 sec sr)
--Full pass plot	10^{-4} to 10^{2} ergs/(cm^2 sec sr eV)

o Summary Plot Sampling Rate: One spectra or point per spin (6 seconds).

o Summary Plot Resolution: Divided into 32 energy flux levels.

o Accuracy of Trends on Plots: Determined by counting statistics.

o Instrument Orientation: See Figure 1.2. Limits pitch angle range (i.e., minimum pitch angle) sampled by the instrument.

o Summary Plot Algorithm: For counting efficiency e_i at energy E_i (in eV), and C, the counts per accumulation interval of 64 steps per second, the differential energy flux is

$F_i = (1.14 \times 10^{6})(1.602 \times 10^{-12})(C)/(e_i)$, the total energy flux is $E = \sum F_i \, dE$, and the total number flux is $\sum \frac{(1.14 \times 10^{6})(C)}{(e_i)(E)} \, dE$

4.5 MODES

o High temporal resolution modes used for summary plots
  --Two stepping rates (64/second and 32/second).
  --Two energy ranges (E > 5 eV and E > 50 eV). The E > 50 eV mode is used for perigee passes to avoid high counting rates at low energies from rammed ions.

4.6 CORRECTED FOR:

o Nothing.

4.7 UNCORRECTED FOR:

o Spacecraft magnetic and electric fields
  --Spacecraft magnetic fields distort the angular distributions of electrons with energies below about 100 eV. Spacecraft potentials are normally below 10 Volts, although some cases of 50 Volt charging have been seen. In general, the electrons with E < 10 eV are spacecraft photoelectrons.

o Background light and high energy penetrating particles and X-rays
  --Occasional sun pulses are seen, but with low count rates. The instrument is turned off in the heart of the radiation belt. No high energy background has been seen.

o Photoelectrons
  --Both atmospheric and spacecraft photoelectrons are measured.

4.8 DISPLAY ANOMALIES:

o Occasional grey scale problem
  --Grey scales should be visible down to 10^{-6} ergs cm^{-2} sec^{-1} sr^{-1} eV^{-1}. On many summary plots (particularly the ones produced early in the program) the grey scale is visible only down to about 10^{-5}. In these cases the ion fluxes are generally invisible.

o Saturation of the ion and electron spectrograms below 50 eV
  --This plotting problem was corrected before Version 3.9. See Figure 4.1, day 81287, orbit 254 at 2100 UT, for example. The problem always commences at the start of a plotting frame and occurs for both electrons and ions.

4.9 INTERPRETATIONS:

Substantial variation in "standard" patterns exist. The following are given only as possible cases and are not definitive.

o High fluxes in the ion spectrogram below 50 eV
  --Near perigee, these are rammed ionospheric ions. See Figure 4.2, day 81276, orbit 213 at 0510 to 0525 UT for example. As opposed to the plotting problem described in Section 4.8, these high fluxes only appear in the ion plots.

o Striations at high energies at perigee
  --Ram effect due to high internal gas pressures and low level corona at high deflection voltages. See Figure 4.2, day 81276, orbit 213, from 0505 to 0515 UT, for example.

o Spacecraft photoelectrons (generally below 10 eV)
  --Shows as a bright band at the bottom of the electron spectrogram when the spacecraft is in sunlight. See Figure 4.3, day 81276, orbit 213, from 0107 to 0200 UT, for example.

o Distinct sine wave in sunlight for the total particle flux line plots
  --Apparently caused by the 90 degree pitch angle selecting process and strong photoelectron angular dependence with slightly different pitch angles. See Figure 4.3, day 81276, orbit 213, from 0140 to 0150 UT, for example.

4.10 COMMENTS

o Pitch angle is defined as the angle between the particle velocity vector and the magnetic induction vector (B). Particles with 0 degree pitch angle move down the field line in the northern hemisphere and up the field line (away from the earth) in the southern hemisphere.

o No data after day 81335 due to high voltage power failure.

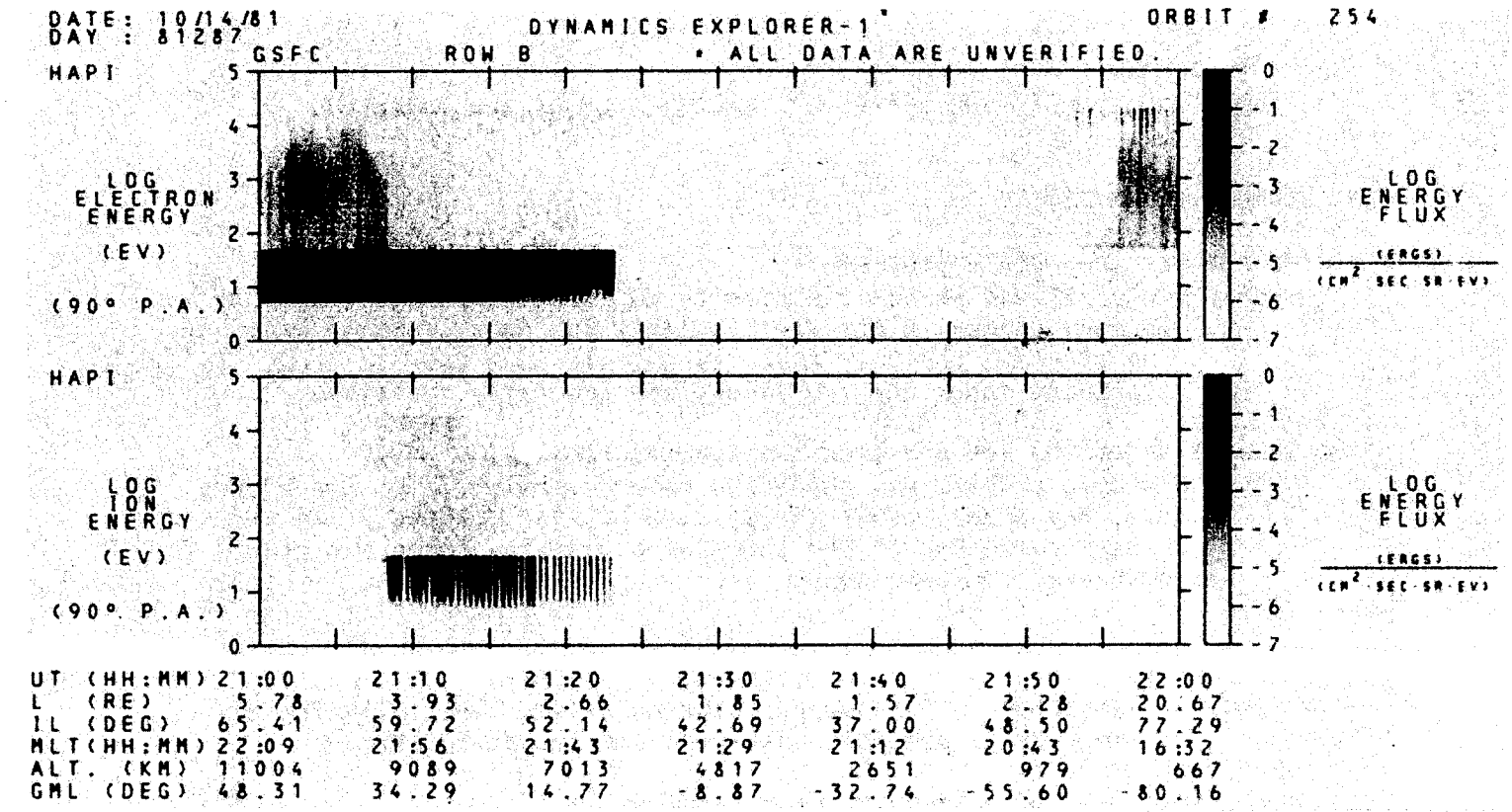

Figure 4.1: Example of spectrogram saturation

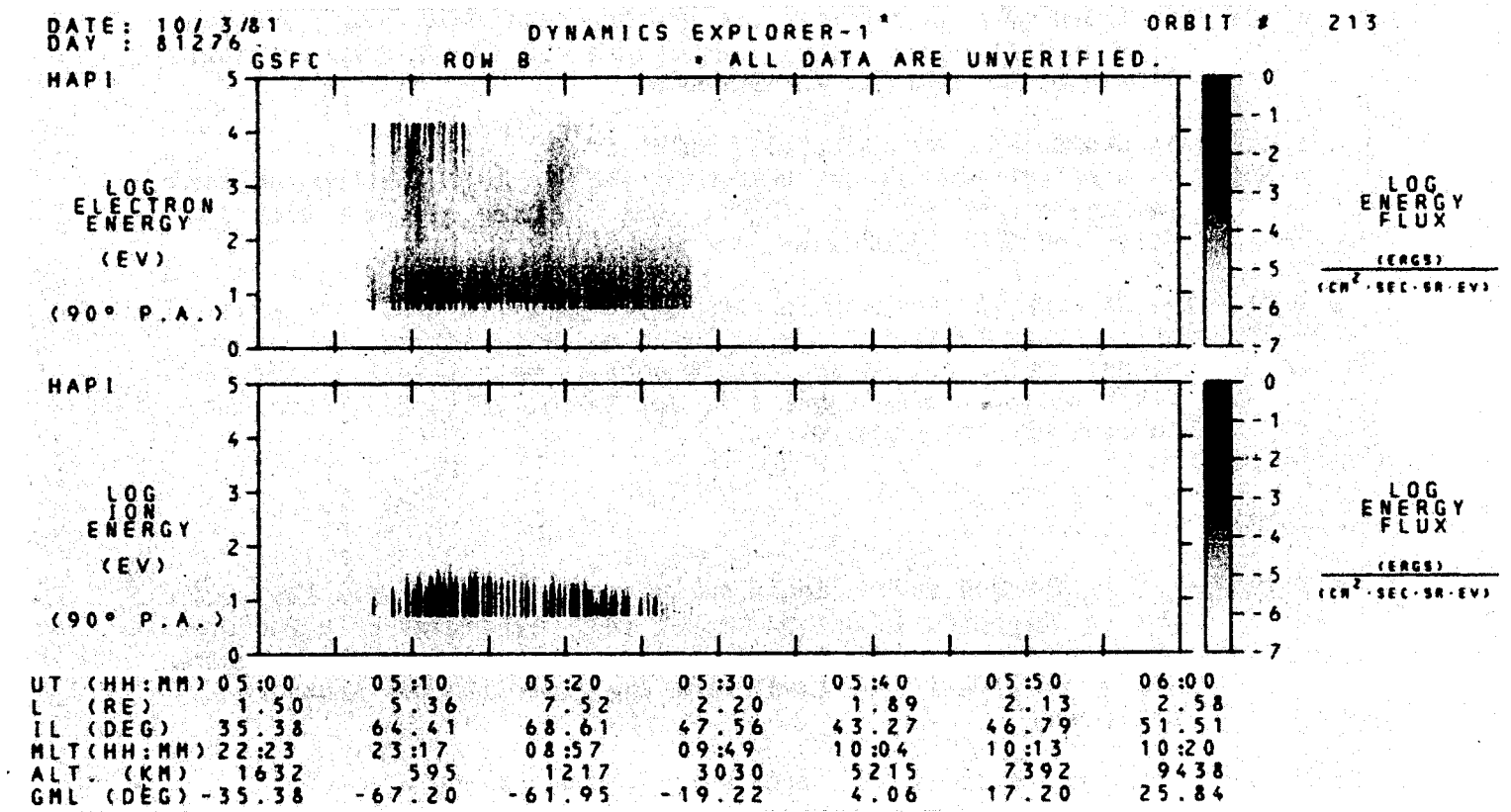

Figure 4.2: Example of rammed ionospheric ions and striations at high energies

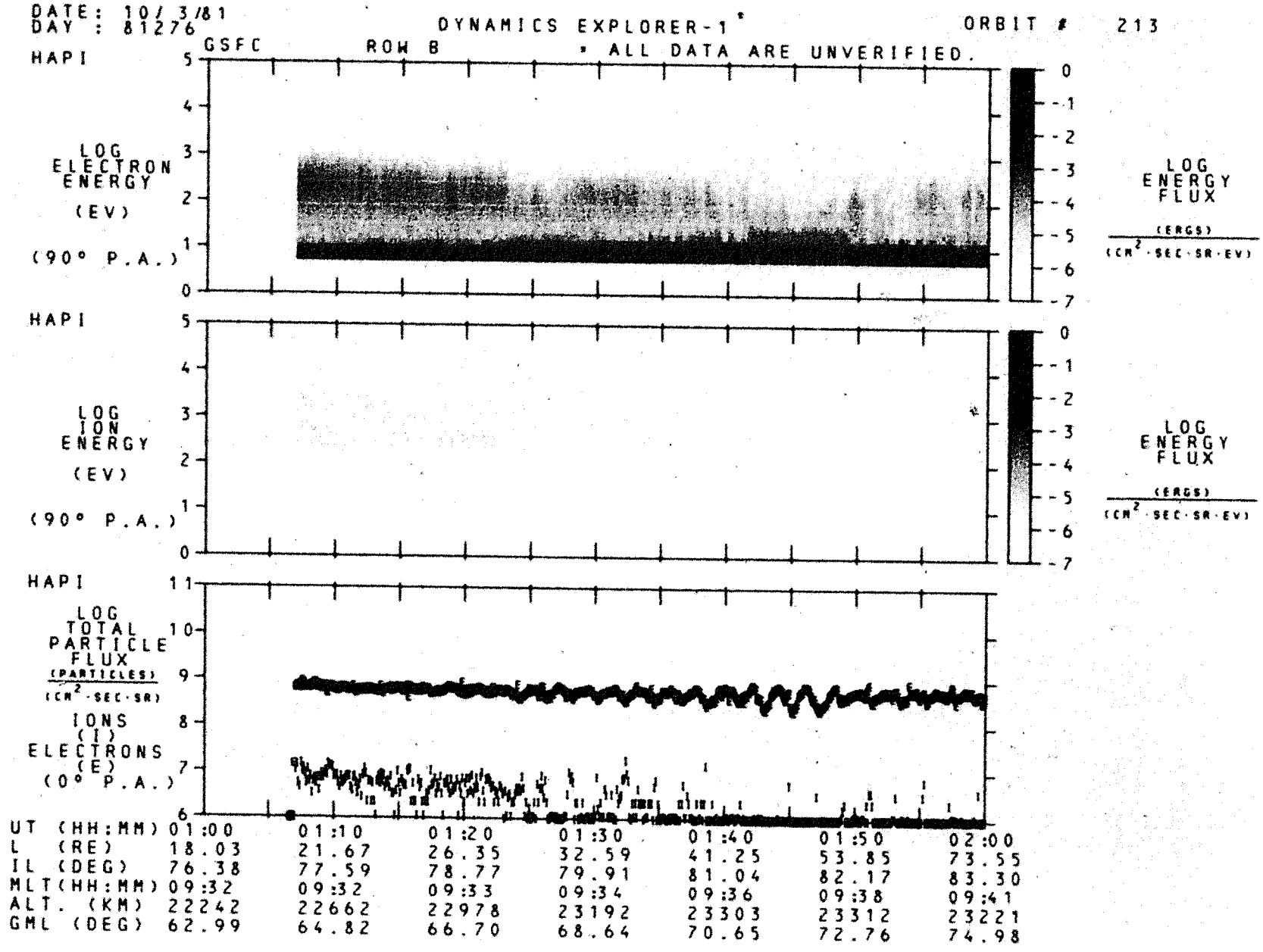

Figure 4.3: Example of photoelectrons and sine wave in sunlight

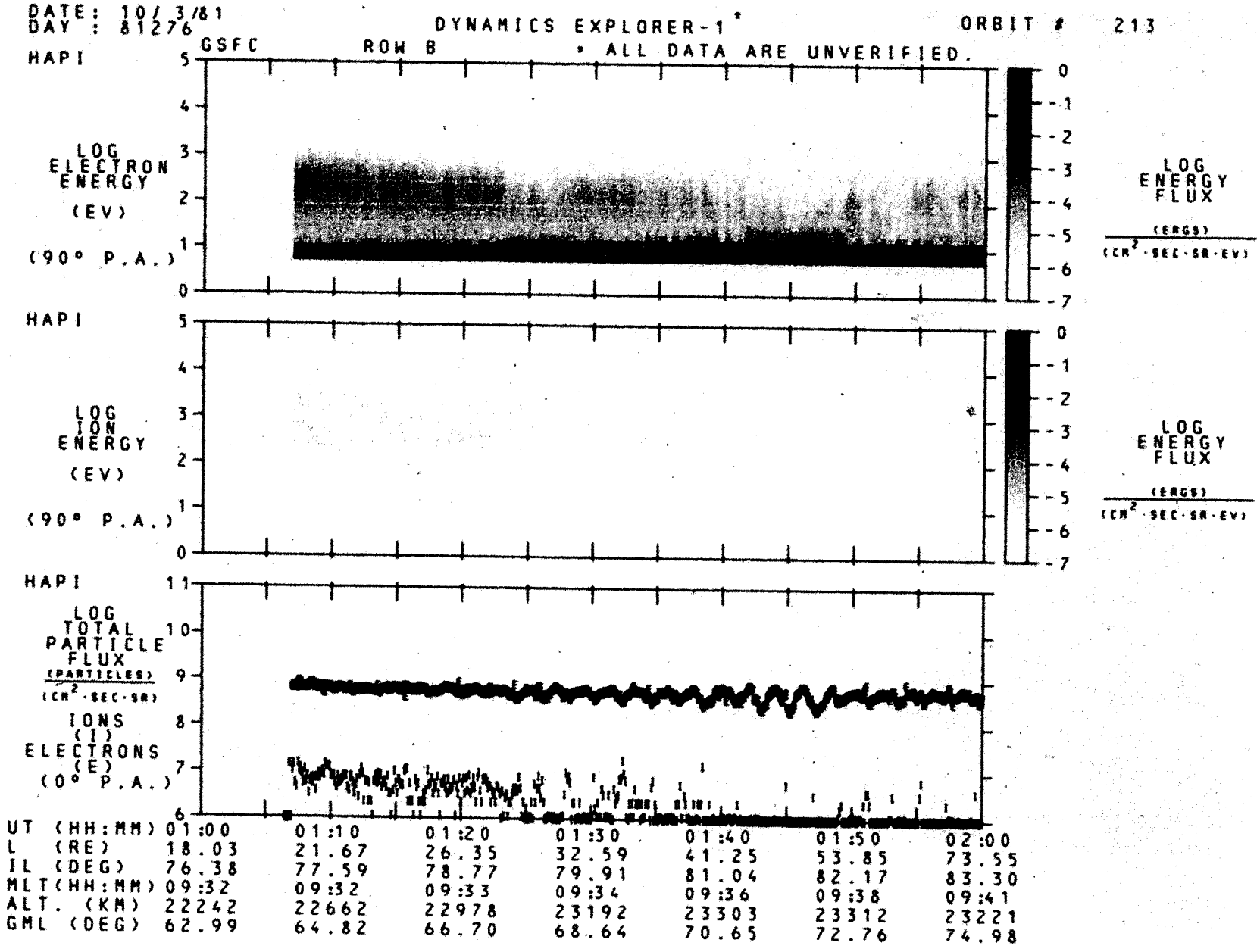

Figure 4.3: Example of photoelectrons and sine wave in sunlight

CHAPTER 5

ENERGETIC ION COMPOSITION SPECTROMETER (EICS)

5.1 FURTHER INFORMATION:

Contact: W.K. Peterson (415) 858-4069
Department 52-12, Building 255
Lockheed Palo Alto Research Laboratory
3251 Hanover Street
Palo Alto, CA 94304

References: Shelley, E.G., D.A. Simpson, T.C. Sanders, E. Hertzberg, H. Balsinger, and A. Ghielmetti, "The Energetic Ion Composition Spectrometer (EICS) for the Dynamics Explorer-A", Space Science Instrumentation, 5, 443 (1981).

5.2 SUMMARY PLOT PARAMETERS:

- 90 degree pitch angle counting rate data
  --Represents the largest fraction of phase space and generally represents the maximum of the distribution for other than upward flowing ion events.

- H^+ and O^+ ion data
  --Major ion species, also chosen since data for other species require further processing to be reliable.

- Maximum counting rate identified with pitch angle range
  --Allows identification of field-aligned beams and conics.

- The mode is written at the bottom of the plots every 20 minutes or any time it changes. See the glossary for an explanation of the mode numbers.

5.3 PARAMETERS NOT PLOTTED:

- Only three energy channels are plotted with plotting in counts per sample minus background instead of flux in order to limit the number of plot frames and the computer time required to generate them.

5.4 MEASUREMENT UNITS

- Geophysical Units: A paper by Yau et al. is being written on the subject of converting the summary plot counts/sample to meaningful geophysical parameters.

- o Range of Valid Data: 1 to 10^5 counts/second for H^+ and O^+ in O-1, 1-4, 4-16 keV bands with pitch angles from 0 to 180 degrees.

- o Summary Plot Sampling Rate: One summary set every 96 seconds, a compromise for efficient computation.

- o Summary Plot Resolution: Pitch angle of maximum flux is divided into 20 degree increments. The mode determines the number of samples represented by each plotted point after a variable background has been subtracted. In general, the resolution of the 96 second averages is much better than that available on the plots. There are cases, especially in the radiation belts, where the opposite is true, however.

- o Accuracy of Trends on Plots: Primarily event identifier type data.

- o Instrument Orientation: See Figure 1.2. Instrument looks in the -X spacecraft direction normal to the spin axis. Pitch angle is defined as the angle from the ram direction in the X-Y plane and is calculated assuming $B_z = 0$.

- o Summary Plot Algorithm: H^+ and O^+ fluxes are averaged over three representative energy ranges in each of eight pitch angle ranges and plotted for the maximum pitch angle.

5.5 MODES

- o Modes are described in detail in the DE Science Data Processing System Sigma-9 file MODES.EICS. Neither of the FAST cusp modes, CPFT2 and CPFT1, sample O^+ and it is missing from the summary data when these modes are used. In addition, the CPFT1 mode does not sample H^+.

- o Early in the mission, and later during times when operation personnel changed, there were periods when EICS was incorrectly commanded. The usual, but not unique, signature of this in the summary plots is a series of very closely spaced mode identifier numbers at the bottom of the EICS frame. There are several different signatures of an incorrectly commanded instrument; one of the most obvious is shown in Figure 5.1, day 82116, orbit 932, from 0600 to 0800 UT.

- o Calibration mode
  --Results in a short data gap. In the first months of operation, the instrument was sometimes incorrectly left in the calibration mode for several hours. During these periods only three H^+ energy steps are sampled. These periods have mode identifier numbers between 55 and 63.

- The LOAD SCAN mode (usually 69) has a very long cycle time (64 seconds) compared to the spin period (6 seconds). During the 96 second summary plot averaging period, there is inadequate sampling of the full range of mass-energy-angle parameters. This results in a great deal of scatter in the 90° O^+ and H^+ summary plots, unless the flux intensity is stable and the spectra are very flat in both energy and angle. See Figure 5.2, day 82028, orbit 624, for an example of mode identifier 69.

5.6 CORRECTED FOR:

- Penetrating radiation
  --Background counting rate.

5.7 UNCORRECTED FOR:

- Differential spacecraft charging
  --Below the resolution of the summary plots but affects the relative angular displacements for different energy ions.

- Photo-ionization of residual gases in the pre-acceleration region of the spectrometer
  --Produces the anomalous count rate for O^+ and H^+ in the lowest energy channel once per spin and only when the local time of the orbit plane is within two hours of noon or midnight. This could produce the false signature of a field-aligned or conic distribution under conditions of low ambient fluxes.

- Detector saturation
  --Caused by high flux rate in the lowest energy channel due to the ram of high density O^+ at altitudes below 10,000 km. This also can produce an invalid signature of anisotropic distributions.

5.8 DISPLAY ANOMALIES:

- All zeros being plotted
  --Produced when the instrument mode samples only species other than O^+ and H^+.

- Overlay of mode numbers
  --Produced during mode changes or instrument memory load periods. See Figure 5.3, day 82051, orbit 705 at 1515 and 1540 UT.

- Incorrect pitch angle calculations
  --EICS summary plot data are not valid for Versions 3.0 to 3.4.

5.9 INTERPRETATIONS:

Substantial variation in "standard" patterns exist. The following are given only as possible cases and should not be construed as definitive.

- o O^+ fluxes out of the polar cap
  --Identified by a long series of 8's in the low energy O^+ frame. See Figure 5.4, day 81312, orbit 341 from 1400 to 1500 UT, for example.

- o Extended O^+ low energy conics
  --Identified by 6's and 7's in the low energy O^+ frame at the North Pole and strings of 2's and 3's at the South Pole. See Figure 5.5, day 81281, orbit 230 from 0400 to 0410 UT, for example at the North Pole.

- o The summary plots have too limited resolution to identify H^+ flux broadened by wave particle interaction.

5.10 COMMENTS

- o There is no simple recipe that can be used to ensure the validity of the EICS summary plot data. After significant experience involving the intercomparison of summary plots with data that have been processed in detail, one can learn to recognize most anomalies. For the inexperienced, the EICS summary plots should be used only as a first order indication of the characteristic H^+ and O^+ fluxes. Before any significant effort is put into an analysis project based on the EICS summary plot data, their validity and interpretation should be verified with an EICS team member. In most cases more detailed processing will be required.

- o The 80 to 100 degree bin for maximum flux angle is plotted with an "o".

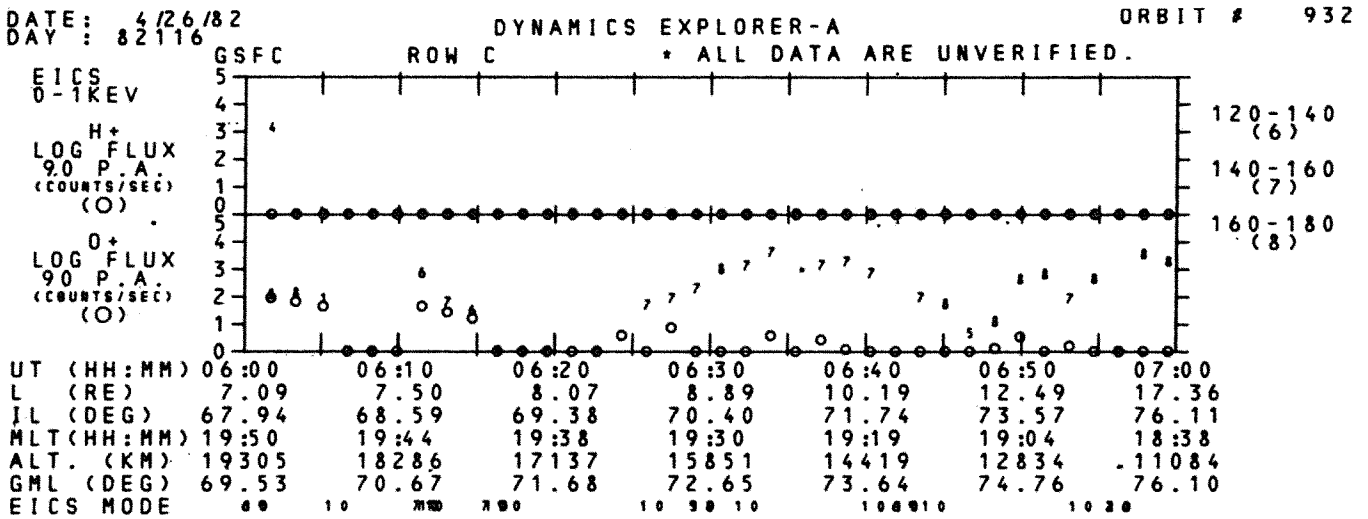

Figure 5.1: Example of incorrectly commanded instrument

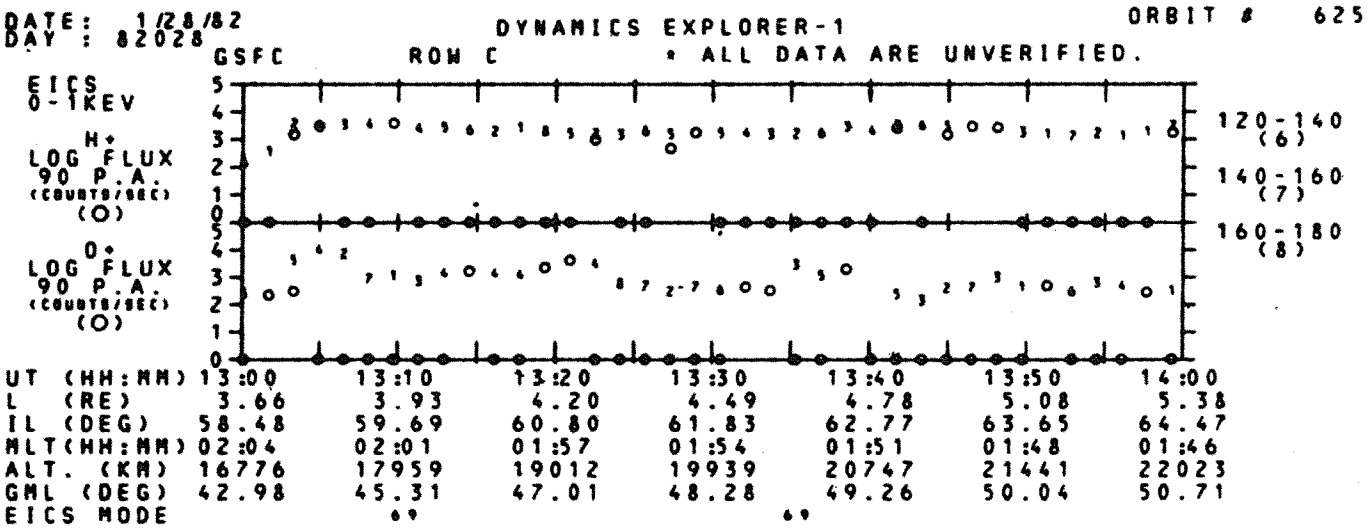

Figure 5.2: Example of LOAD scan mode scatter

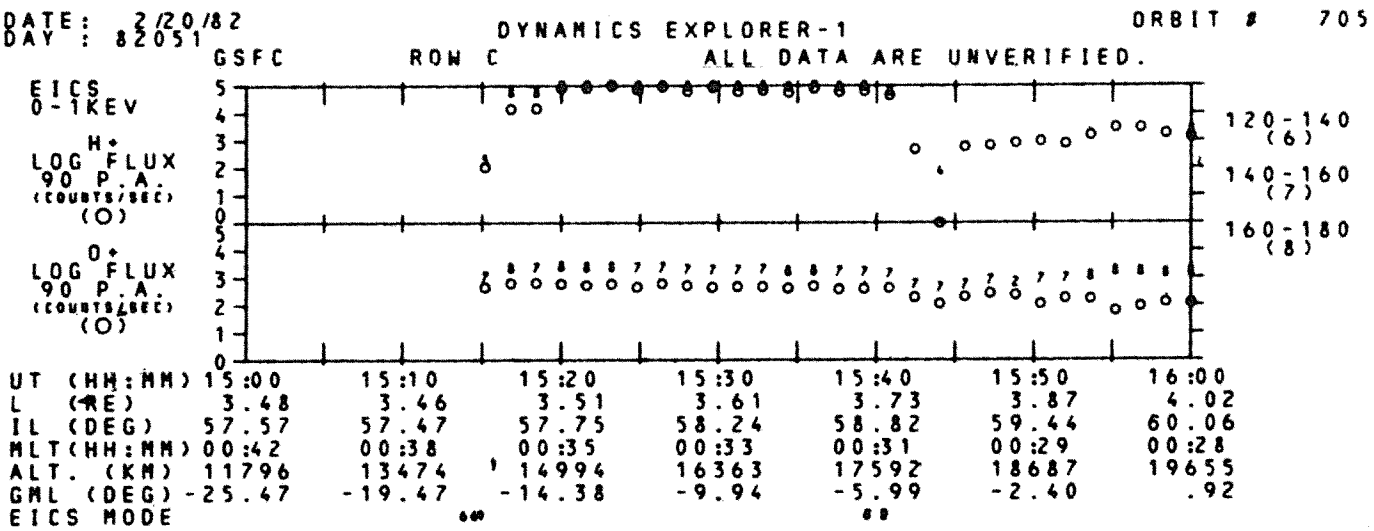

Figure 5.3: Example of overlay of mode numbers

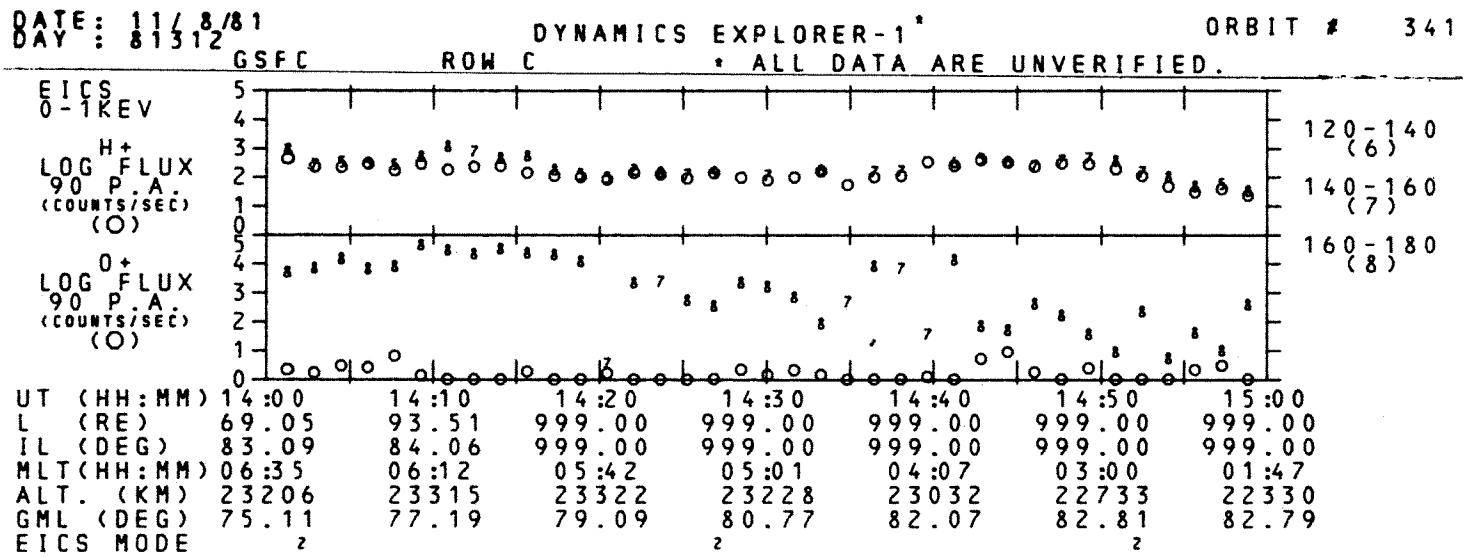

Figure 5.4: Example of O^+ fluxes out of the polar cap

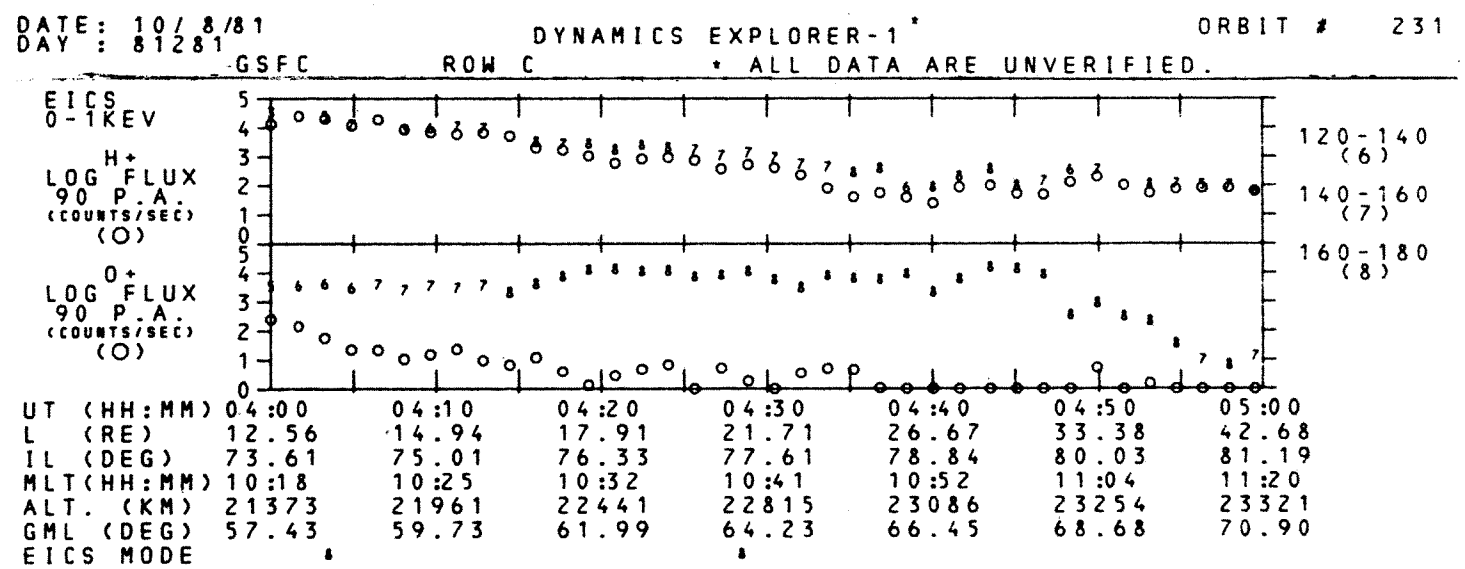

Figure 5.5: Example of extended O^+ low energy conics

CHAPTER 6

RETARDING ION MASS SPECTROMETER (RIMS)

6.1 FURTHER INFORMATION:

Contact: Hunter Waite (205) 453-3037
E S53
Marshall Space Flight Center, AL 35812

References: Chappell, C.R., S.A. Fields, C.R. Baugher, J.H. Hoffman, W.B. Hanson, W.W. Wright, and H.D. Hammack, "The Retarding Ion Mass Spectrometer on Dynamics Explorer-A", Space Science Instrumentation, 5, 477 (1981).

6.2 SUMMARY PLOT PARAMETERS:

- Estimated ion density for O^+, H^+, He^+, He^{++}, O^{++}
  --Energy spectra as a function of spacecraft spin phase angle are measured for each species.

- Spin phase angle spectrograms for H^+ and He^+ as a function of angle with respect to the ram direction
  --Provides the pitch or ram angle characteristics of the low energy plasma. Inside the plasmasphere, peak fluxes occur in the direction of the spacecraft velocity vector, indicating a cold isotropic plasma. Outside the plasmasphere, the ions are generally field-aligned in character.

- Magnetic and Anti-magnetic field directions
  --Plotted on the spin phase plots to aid in the determination of pitch angle characteristics of the low energy plasma outside the plasmasphere, i.e., peaks along the field line direction or peaks perpendicular to the field line (trapped distributions).

6.3 PARAMETERS NOT PLOTTED:

- Ion temperature
  --Requires extensive processing and curve fitting.

- Bulk ion flow
  --Also requires extensive data analysis in order to determine a meaningful result.

- Each of the three sensor heads individually
  --Lack of display space and processing time prevented this data display.

6.4 MEASUREMENT UNITS

- o Geophysical Units: Estimated densities are in ions per cm^3 with phase angles in degrees.

- o Range of Valid Data: Densities range from 0.1 to 1000 ions/cm^3 and the angle range is $\pm$180 degrees with count rate of 1 to 10^4 counts.

- o Summary Plot Sampling Rate: The instrument samples both a high and low mass in all three heads every 1/64 of a second. A 32 point programmable energy and mass scan combination takes a half second. A complete mass, energy and angle scan takes 16 seconds. The summary plot sampling rate is 16 seconds.

- o Summary Plot Resolution: Density resolution is 3 points per decade on a log scale from 10^{-2} to 10^5 cm^{-3}; angle resolution is 24 levels.

- o Accuracy of Trends on Plots: The estimated densities inside the plasmasphere are good to within a factor of two under most situations. However they are almost meaningless outside the plasmasphere. The spin angle spectrograms are only used to find qualitative trends.

- o Instrument Orientation: See Figure 1.2. Phase angles are measured from the ram direction in the spacecraft X-Y plane.

- o Summary Plot Algorithm: Simple algorithm and curve fitting routines are employed to derive the bulk ion densities and pitch angle spectrograms. Selecting the peak count rate for a given spin and dividing the estimated flux by the spacecraft velocity yields the estimated ion density. This estimation works well inside the plasmasphere, but outside the plasmasphere this density is merely an indication of the peak counting rate.

6.5 MODES

- o Limited resolution combined energy/mass survey mode
  --Nominal mode, contains energy and spin information with a resolution of 16 seconds.

- o Comprehensive mass analysis with no energy analysis (M modes)
  --Provides resolution of half second. During such modes no data can be displayed on the summary plots.

- o High resolution energy/pitch angle analysis for H^+ and He^+
  --Provides resolution of 6 seconds. Can be displayed on the summary plots, but estimated densities for O^+, O^{++}, He^{++} are not available.

6.6 CORRECTED FOR:

- o Nothing.

6.7 UNCORRECTED FOR:

- o Spacecraft magnetic and electric fields
  --Positive charging of the spacecraft outside the plasmasphere can prevent detection of low energy plasma (less than 10 eV). Since peak fluxes are not corrected for spacecraft potential effects, the estimated density calculations can be significantly affected, particularly outside the plasmasphere.

- o Changes in the sensitivities of high and low mass multipliers
  --Relative count rate between the two is not reliable on an absolute scale since the summary plot algorithm does not allow for this correction.

6.8 DISPLAY ANOMALIES:

- o Biased count rate grey scale
  --Biased toward low count rates so that density enhancements within the plasmasphere do not show up.

- o Data drop-out on the spectrograms
  --The instrument cuts-off for very high count rates to protect itself, thereby causing some data drop-outs at low altitudes.

- o Untrustworthy pitch angle
  --For Versions prior to 3.4, the direction and anti-direction of the magnetic field on the plots may at times be inaccurate, making the identification of field-aligned plasma flows outside the plasmasphere a more difficult task. Version 3.0 to 3.4 summary plots are invalid due to a programming error in calculating pitch angles. (See Section 1.5).

6.9 INTERPRETATIONS:

Substantial variation in "standard" patterns exist. The following are given only as possible cases and should not be construed as definitive.

- o Plasmapause
  --The increase in plasma density inside L = 5. The density gradient is usually sharper on the nightside (see Figure 6.1A, day 81281, orbit 231, at 0735 UT, for example) than on the dayside (see Figure 6.1B, from 0930 to 1000 UT, for example).

- o Polar wind
  --Can best be detected during negative biasing of the aperture (to overcome the positive spacecraft potential). See Figure 6.2, day 81287, orbit 254, at 2340 UT, for example.

- o Possible sun pulse
  --Straight line of low count rates in the spectrograms when the spacecraft orbital plane is near the noon/midnight meridian. See Figure 6.3, day 81295, orbit 282, from 1920 to 2000 UT, for example at 120 to 135 degrees in H^+.

- o Trapped particles
  --Peak at 90 degrees to magnetic field and seen mostly at the geomagnetic equator. See Figure 6.4, day 82075, orbit 790, from 1510 to 1540 UT, for an example in H^+.

- o Broad field-aligned flows
  --See Figure 6.5, day 81312, orbit 342, from 1935 to 2010 UT, for an example in H^+.

- o Field-aligned conical distributions
  --At 20-40 degree pitch angle. See Figure 6.6, day 81340, orbit 438, from 1112 to 1120 UT, for example.

6.10 COMMENTS

- o Location of the plasmasphere
  --Shows as a dramatic increase in the counting rate and estimated density with a peak flux in the ram direction.

- o Degradation of the channeltron detectors
  --Indicated by a high relative counting rate of He^+ as compared to H^+ on the spin phase angle spectrograms. This may lead to a misinterpretation of relative ion concentrations from the summary plots. This information can in most cases be reconstructed from the full data set and inquiries should be made to the RIMS science team.

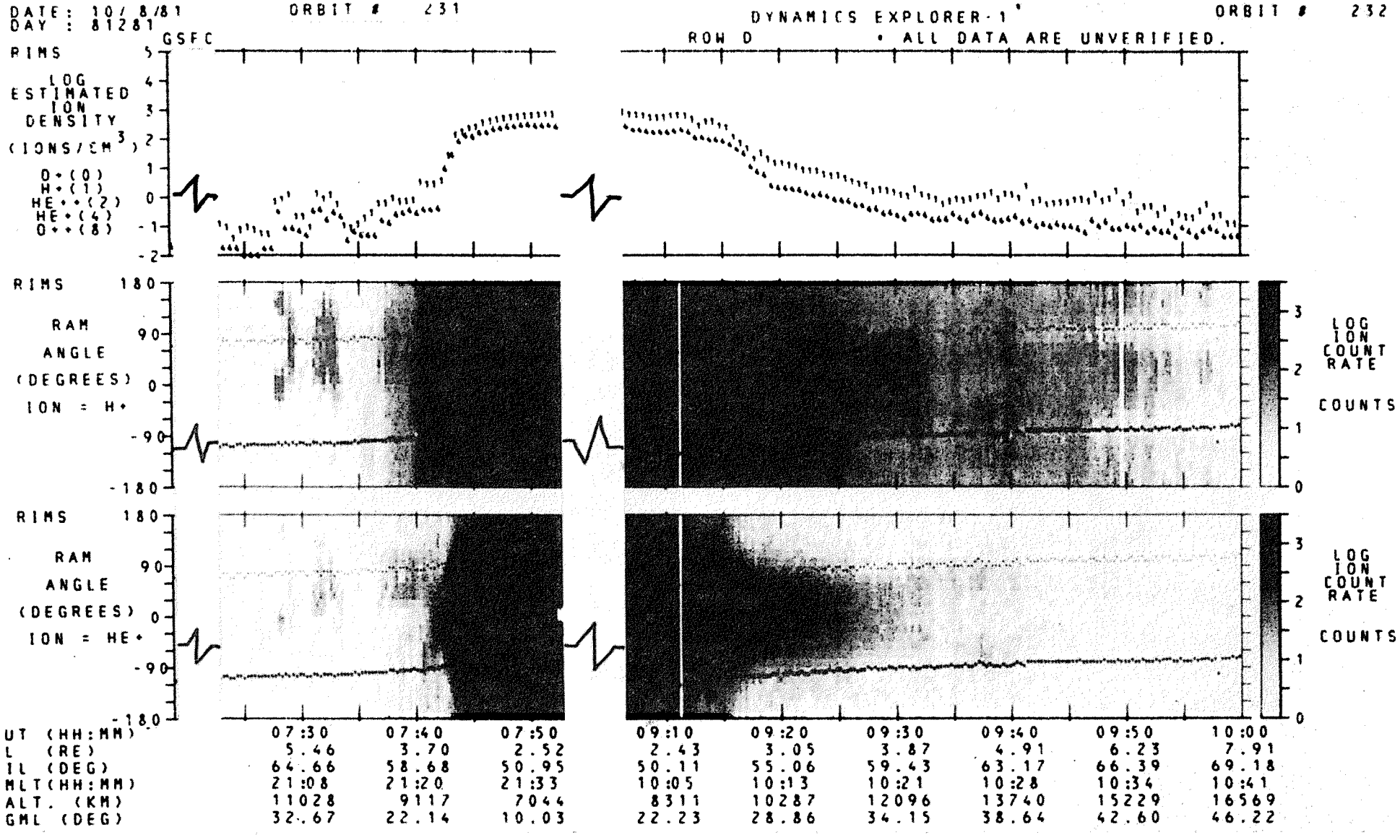

Figure 6.1A: Example of nightside plasmapause

Figure 6.1B: Example of dayside plasmapause

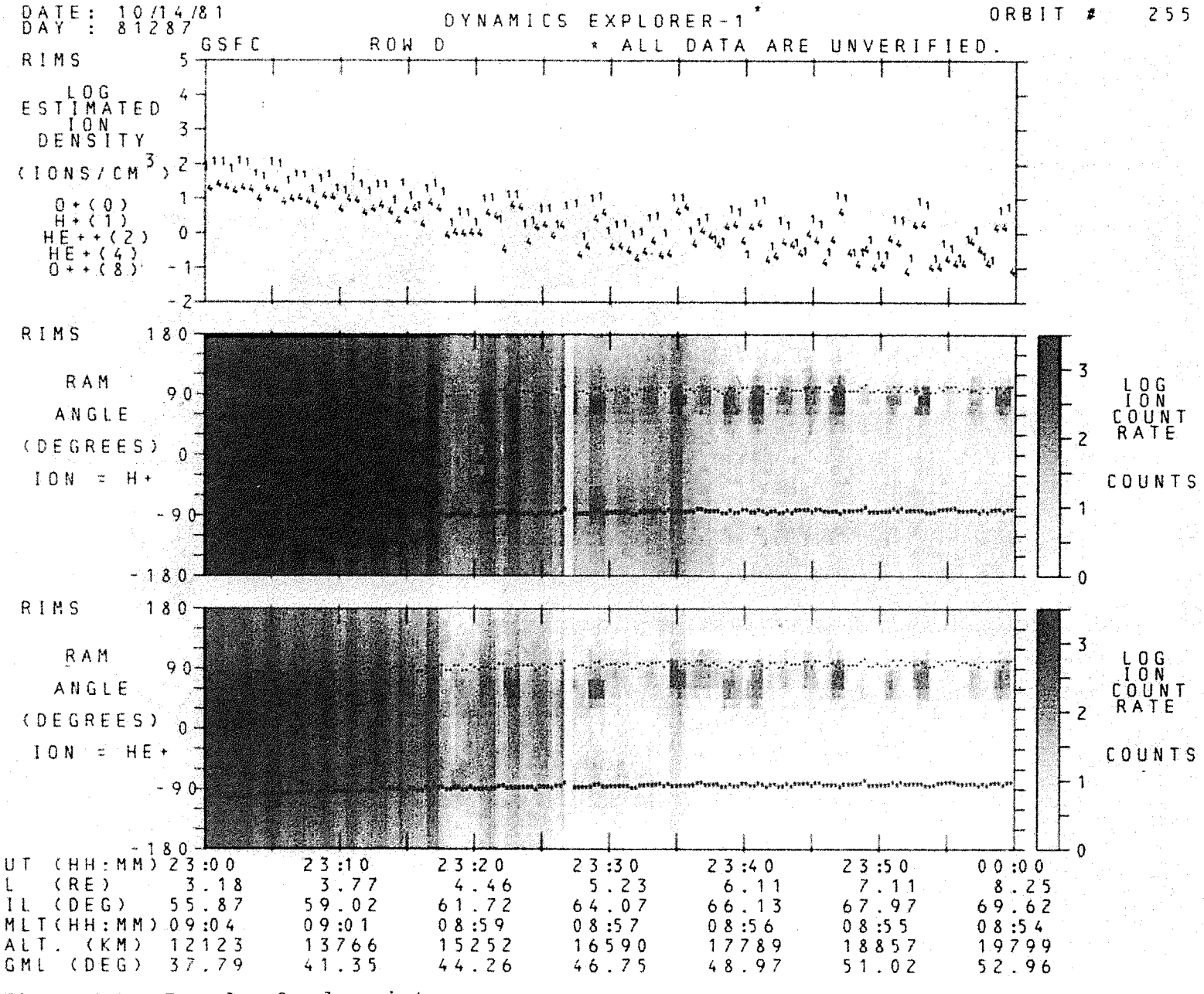

Figure 6.2: Example of polar wind

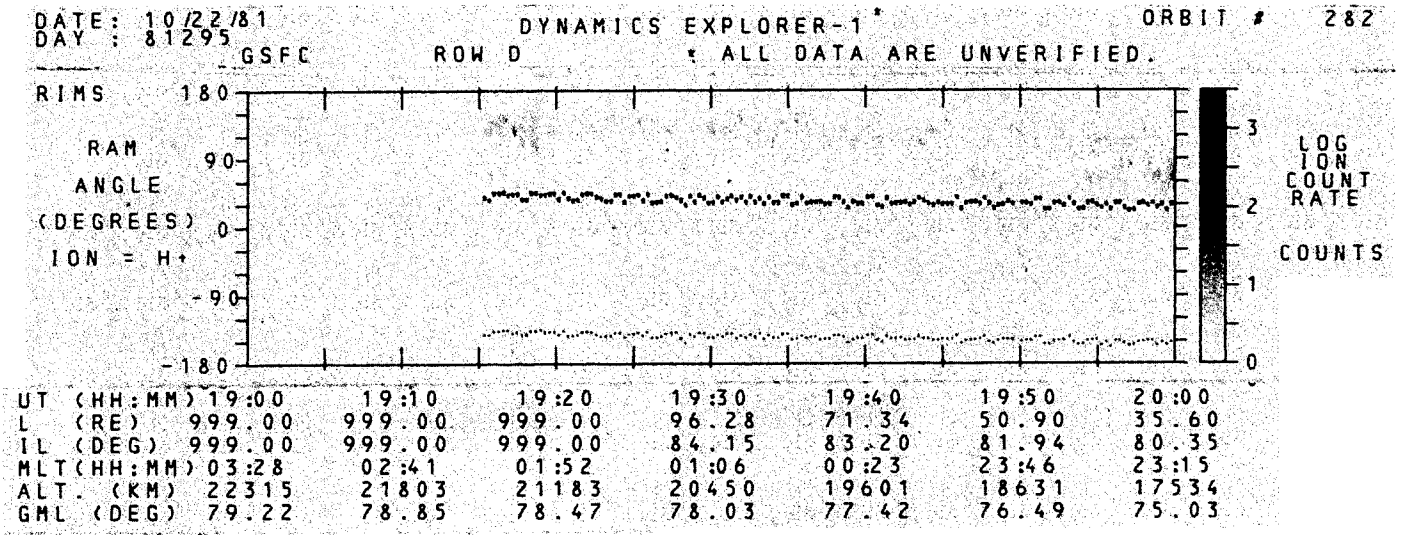

UT (HH:MM)	19:00	19:10	19:20	19:30	19:40	19:50	20:00
L (RE)	999.00	999.00	999.00	96.28	71.34	50.90	35.60
IL (DEG)	999.00	999.00	999.00	84.15	83.20	81.94	80.35
MLT(HH:MM)	03:28	02:41	01:52	01:06	00:23	23:46	23:15
ALT. (KM)	22315	21803	21183	20450	19601	18631	17534
GML (DEG)	79.22	78.85	78.47	78.03	77.42	76.49	75.03

Figure 6.3: Example of possible sun pulse

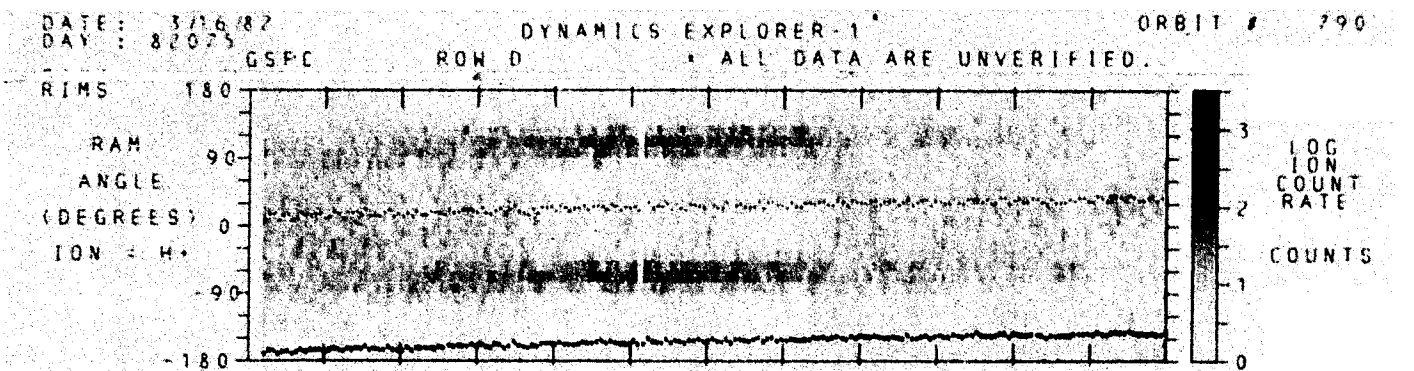

UT (HH:MM)	15:00	15:10	15:20	15:30	15:40	15:50	16:00
L (RE)	4.05	4.13	4.23	4.33	4.44	4.56	4.68
IL (DEG)	60.20	60.54	60.91	61.28	61.67	62.06	62.46
MLT(HH:MM)	22:59	22:58	22:58	22:58	22:59	22:59	23:00
ALT. (KM)	19317	20210	20985	21646	22197	22641	22980
GML (DEG)	11.83	14.59	17.09	19.40	21.56	23.62	25.61

Figure 6.4: Example of trapped particles

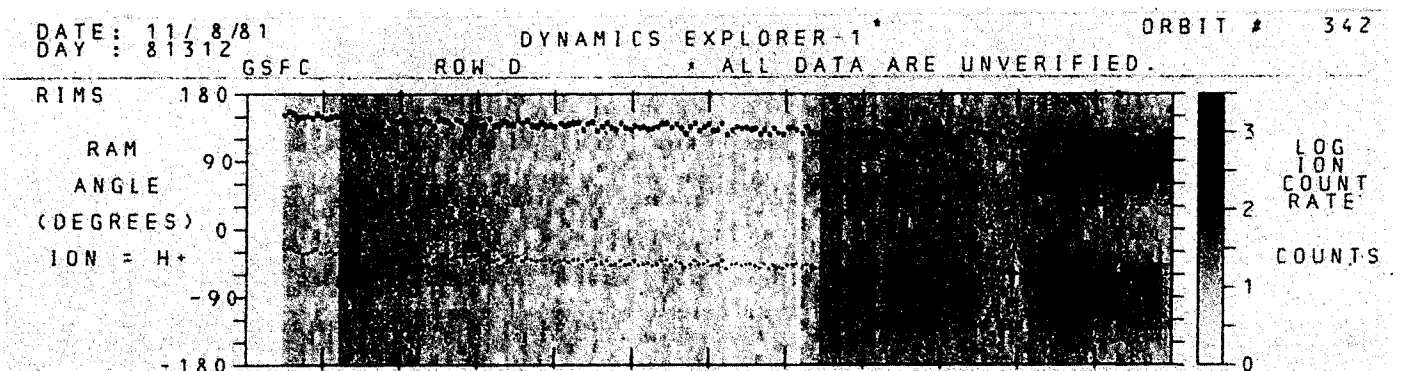

UT (HH:MM)	19:00	19:10	19:20	19:30	19:40	19:50	20:00
L (RE)	3.96	4.57	5.25	6.00	6.83	7.74	8.75
IL (DEG)	59.82	62.12	64.14	65.91	67.49	68.93	70.24
MLT(HH:MM)	07:19	07:15	07:10	07:06	07:03	06:59	06:56
ALT. (KM)	14643	16043	17301	18424	19419	20291	21047
GML (DEG)	52.34	54.08	55.43	56.54	57.50	58.39	59.24

Figure 6.5: Example of broad field-aligned flows

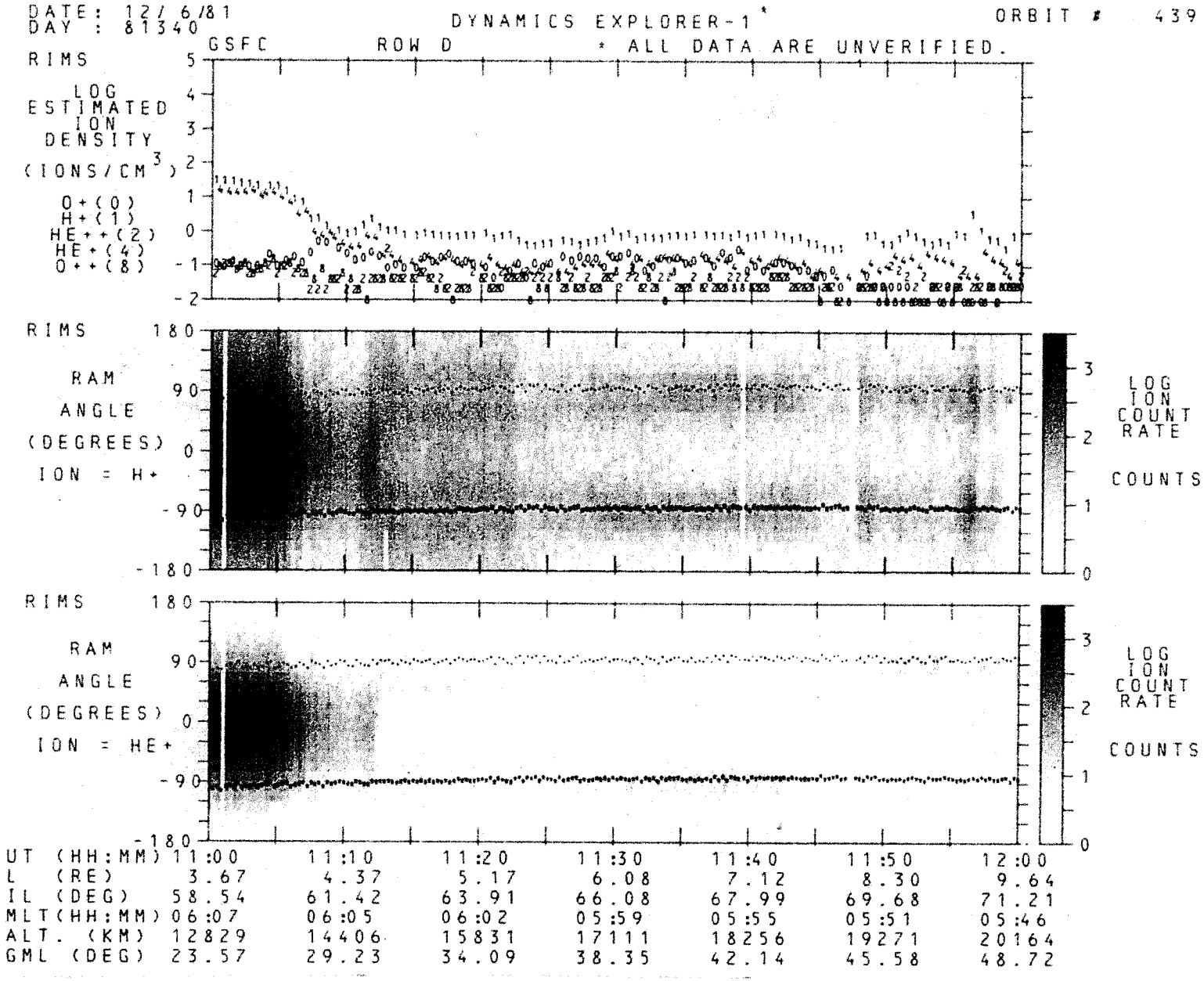

Figure 6.6: Example of field-aligned conical distributions

CHAPTER 7

SPIN-SCAN AURORAL IMAGER (SAI)

7.1 FURTHER INFORMATION:

Contact: Louis A. Frank (319) 353-5029
John D. Craven (319) 353-5514
Department of Physics and Astronomy
University of Iowa
Iowa City, Iowa 52242

References: Frank, L.A., J.D. Craven, K.L. Ackerson, M.R. English, R.H. Eather, and R.L. Carovillano, "Global Auroral Imaging Instrumentation for the Dynamics Explorer Mission", Space Science Instrumentation, 5, 369 (1981).

7.2 SUMMARY PLOT PARAMETERS:

- o Filter wheel position numbers
  --1 2 3 4 5 6 7 8 9 A(10) B(11) C(12). See the glossary for filter characteristics. Two filters can be identified for each six minute interval.
  --0 indicates Optical Path Impeded (OPI) or invalid filter wheel position data sample (often due to a tape-recorder change-over or bad telemetry).
  --N indicates no imaging in progress.
  --X indicates the detector is off.
  --* indicates more than two filters were identified in the time interval.
  --V indicates the default flag for when the filter could not be identified because of bad data or the filter wheel was not properly positioned.

- o Satellite in darkness
  --Shown as a line above the filter numbers.

7.3 MEASUREMENT UNITS

- o Summary Plot Sampling Rate: The plots will identify the two filters in use during each six minute interval.

- o Instrument Orientation: See Figure 1.2.

7.4 INTERPRETATIONS

- o Two filters can be identified in a six minute interval when there is a mode change in the interval.

- o One, two, or three photometers may be operating at one time. In general, all three are operating simultaneously. The second most common mode uses Photometer C (vacuum UV) only.

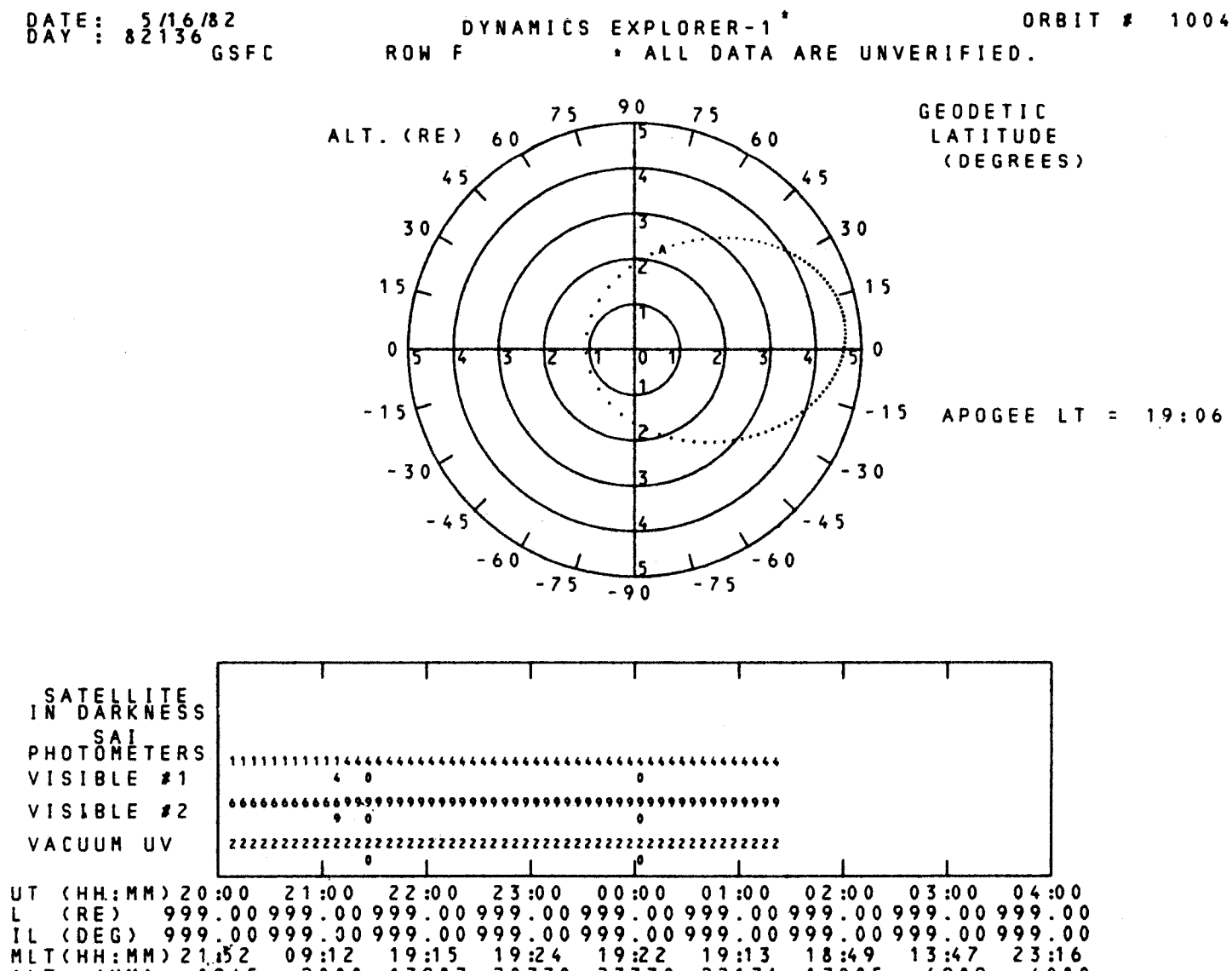

Figure 7.1: Sample SAI summary plot

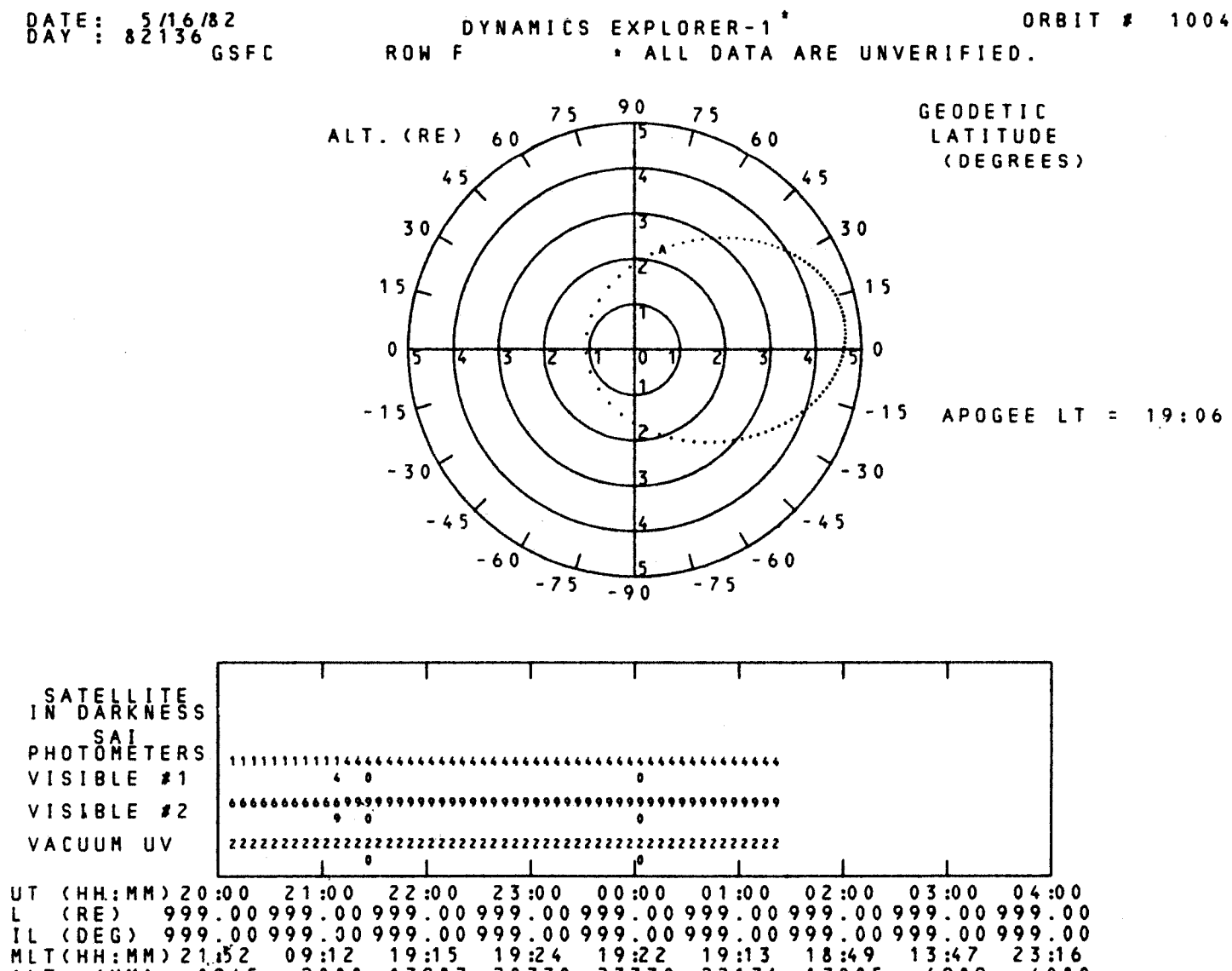

Figure 7.1: Sample SAI summary plot

DYNAMICS EXPLORER-2 SUMMARY PLOTS

INTRODUCTION

8.1 GENERAL EXPLANATION OF THE SUMMARY PLOTS

The Dynamics Explorer summary plots are designed to provide the scientist with a method for selecting interesting events and time periods which are likely to produce results upon detailed analysis. This is accomplished primarily by searching for particular signatures in the data.

Summary plot generation involves the extraction of a subset of the telemetry data and conversion to geophysical parameters using simple algorithms. The results are summarized in plot form and displayed by the Information International FR-80 COM recorder device on microfiche. Data from all acquisition periods will eventually be processed in summary plot form.

All data appearing in the plots are unverified, and simplifying approximations are used in the conversion of the telemetry data to the plotted parameters. For these reasons the data should not be used for analysis purposes without consultation with the appropriate instrumenters (names and addresses are given at the beginning of each chapter).

Further information about the program and instruments can be found in the special Dynamics Explorer issue of Space Science Instrumentation, 5, No. 4, 1981. Copies are available from the DE Project Scientist.

8.2 SUMMARY PLOTS FORMATS

8.2.1 General

Each microfiche contains data from one pass, the time interval that a tape recorder on the spacecraft is turned on for a continuous period. For a long pass the data may continue onto a second fiche.

A fiche title appears across the top in large bold characters. For example: "SPP DE02 81299 B051 1236", where:

SPP	Summary Plot Production
DE02	DE-2 fiche
81299	Year (YY) and day number (DDD)
B051	Magnetic tape number for a tape generated on the Sigma-9 for plotting on the FR-80
1236	Orbit number

Early production fiche may contain some variations to this format.

Five rows of frames are used to plot the data from DE-2, each column on a common time scale of ten minutes per frame (see Figure 8.1). Universal Time (UT) runs continuously between columns of frames, with the first column

of plots beginning on an even ten minutes. One additional frame (sixth row, last column) is used for orbit plots of the spacecraft trajectory.

The first column of frames is a glossary containing information on the contents of each row. The glossary in the sixth row is common to all rows.

The bottom row contains test patterns used for quality control purposes.

8.2.2 Polar Plot Frame

The frame in the last column, second row from the bottom, contains both a polar plot of the trajectory, in invariant latitude and magnetic local time, and a rectangular plot of the subsatellite point in geographic coordinates. The letters "A" and "B" indicate the first point in time plotted on each graph for the DE-1 and DE-2 satellites, respectively.

In the polar plot, points were plotted every 45 seconds until Version 4.5, after which the points appear every minute on the minute to correspond to orbit parameters listed below each data plot.

8.2.3 Production Information Frame

The frame in the lower right hand corner of the fiche contains fiche production information.

Top line:	Spacecraft number and orbit number
Second line:	Date of pass (at time of tape recorder turn-on)
Third line:	Summary plot version number (see Section 8.5) and date version implemented (blank for early versions)
Fourth line:	Date fiche produced on the Sigma-9

8.2.4 Blank Frames

At times the tape recorder may remain on although all instruments are temporarily off. Blank frames will then appear between data periods. See orbit 1231, from 2001 to 2008:30 UT, for example.

8.3 ORBIT DEFINITION

Orbits are numbered sequentially with orbit number 1 beginning at the first ascending node (spacecraft crossing the geographic equator northbound). Thereafter, each orbit begins at the ascending node. The orbit assigned to a pass is determined by the location of the spacecraft at the time the tape recorder is turned on (not the time of first appearance of data). Thus it is possible for the majority of the data of a pass to have been acquired during the next numbered orbit. For example, see the fiche for orbit 681. Obviously, if more than one tape recorder operation occurs during an orbit, more than one fiche can have the same orbit number. For examples, see orbit 972 with tape numbers B057 (North) and B058 (South) and orbit 976 with tape numbers B061 (North) and B062 (South).

Occasionally the tape recorder may be left on even though all the instruments are off temporarily. Although the second data acquisition period may occur after the spacecraft has crossed the equator northbound, that data will remain labeled by the previous orbit number. However, the next orbit number will appear should the data continue onto a second fiche.

8.4 INSTRUMENT DATA PLOTS

First row	MAG-B B_z and ΔB_z VEFI $E_{x_{sc}}$ IDM V(VI), V(HI)
Second row	LAPI log electron and ion energy spectrograms, log total ion and electron particle fluxes
Third row	VEFI log voltage in 8-16 Hz and 4-16 kHz LANG log temperature, ion density RPA log $\Delta N_i/N_i$
Fourth row	WATS wind to the East and upward FPI ionic and neutral winds, temperature
Fifth row	NACS N2 density, normalized N2 and He density, O/N2 density ratio, TINF
Sixth row	Spacecraft orbit plot data
Seventh row	Test patterns and fiche data

See the Glossary for explanation of the abbreviations.

Spectrograms show the time variations of spectra. At each level of the spectrogram, an area is filled in, with the intensity and width determined by the value of the flux at that level and time and by the time resolution of the measurements. For LAPI, there were up to 32 energy levels per scan before day 81327; after that, there were 16 energy levels per scan.

8.5 VERSIONS

As algorithms for the instrument data have improved or software problems solved, the summary plot production programs have been given new version numbers (see Section 8.2.3). The primary changes which affect the summary plots from the user's perspective are listed in Table 8.1 for each version.

8.6 PROBLEMS

As the fiche are produced, occasional problems are found in either the formats or the data plotted. These are investigated and corrections made to the programs. When appropriate, such passes are reprocessed and new fiche produced.

The file TMSTAT (see Dynamics Explorer Telemetry Status File Scanning Program User's Guide, July 1983) contains a "Variance" field for comments on problems with the Summary Plot fiche or reasons why certain data do not appear.

Telemetry synchronization losses can cause short data drop-outs, and noisy telemetry can cause spurious points.

8.6.1 Orbit Parameters

The Invariant Latitude (IL) reads "999" when McIlwain's L value is greater than 100.

8.6.2 Spinning Passes

The instrument algorithms were not designed to correctly plot data on those occasions when the spacecraft spun at 1 RPM. Fiche produced from such operations are readily identifiable. See orbit 1532 for example.

8.6.3 Fiche Titles

The fiche titles are manually added at the FR-80. Especially for fiche produced early in the program, a number of errors and format variations occurred. Most significant are missing or incorrect orbit numbers.

8.7 SPACECRAFT INVERSIONS

Every six months the spacecraft was inverted about the X-axis (Y and Z axes changed direction) for thermal control purposes. While the main maneuver required less than one day, the period for which the Z-axis of the spacecraft was not normal to the orbit plane extended over several days.

DE-2 Inversion Maneuvers

Mode		Inversion Period		
From	To	Start	Primary Maneuver	End
Inverted	Normal	81241	81244	81249
Normal	Inverted	82050	82055	82064
Inverted	Normal	82239	82243	82246

8.8 INSTRUMENT ORIENTATION

Figure 8.2 shows the general orientation of the instruments aboard DE-2.

Table 8.1: Summary Plot Algorithm Changes

Version & Day			Corrections and Changes
3.0	82124	VEFI:	Corrected 8-16 Hz and 4-16 kHz plots for gain and axis identification
		LAPI:	Algorithm changed to handle spacecraft telemetry word enable failure on day 81327. Corrected occasional problem of interchange of electron and ion spectrograms. Changed GM scale
		LANG:	Constants changed for calculations of temp. and density
		FPI:	Algorithm changed for temperature scale and eliminated brightness parameter from plots
4.0	82137	LAPI:	Algorithm changes to account for a failure in one high voltage power supply system
		WATS:	Allowed rollover of data points when they go offscale
		Glossary:	Added input file information dates
4.1	82162		No user impacts
4.2	82175	Glossary:	Added date of grey scale definition
4.3	82201	MAG-B:	Corrected problem of sign error in model field subtraction when spacecraft was inverted
		WATS:	Scale changed. Corrected wind directions for spacecraft inversions
		FPI:	Algorithm changed to increase statistical accuracy and eliminate noise and/or useless data
		Glossary:	Satellite darkness indicator explanation added
4.4	82223	MAG-B:	Program aborts if MAGSAT2 model field not present. Prevents repeated renormalizations of ΔB_z
4.5	82337	VEFI/IDM:	Removed points plotted as saturated values when the instruments were off
		LAPI:	Grey scale changed to match HAPI for low fluxes
		Polar Plot:	Changed from one point each 45 seconds to one point every minute on the minute
4.6	83004	NACS:	Corrected data extraction routine to recover more data
4.7	83047	LAPI:	Eliminates streaks across spectrogram when it was off
4.8	83153		No user impacts
4.9	83174		No user impacts
5.0	83216	LANG:	Temperature not plotted for ion density below 10^4
5.1	83260	RPA:	Changed range of LOG ΔNI/NI from (-3 to +3) to (-4 to +2). Added "32-86 Hz" to label. Note, "0" of scale was inadvertantly not moved
5.2	83313	RPA:	Corrected error in scale label for LOG ΔNI/NI

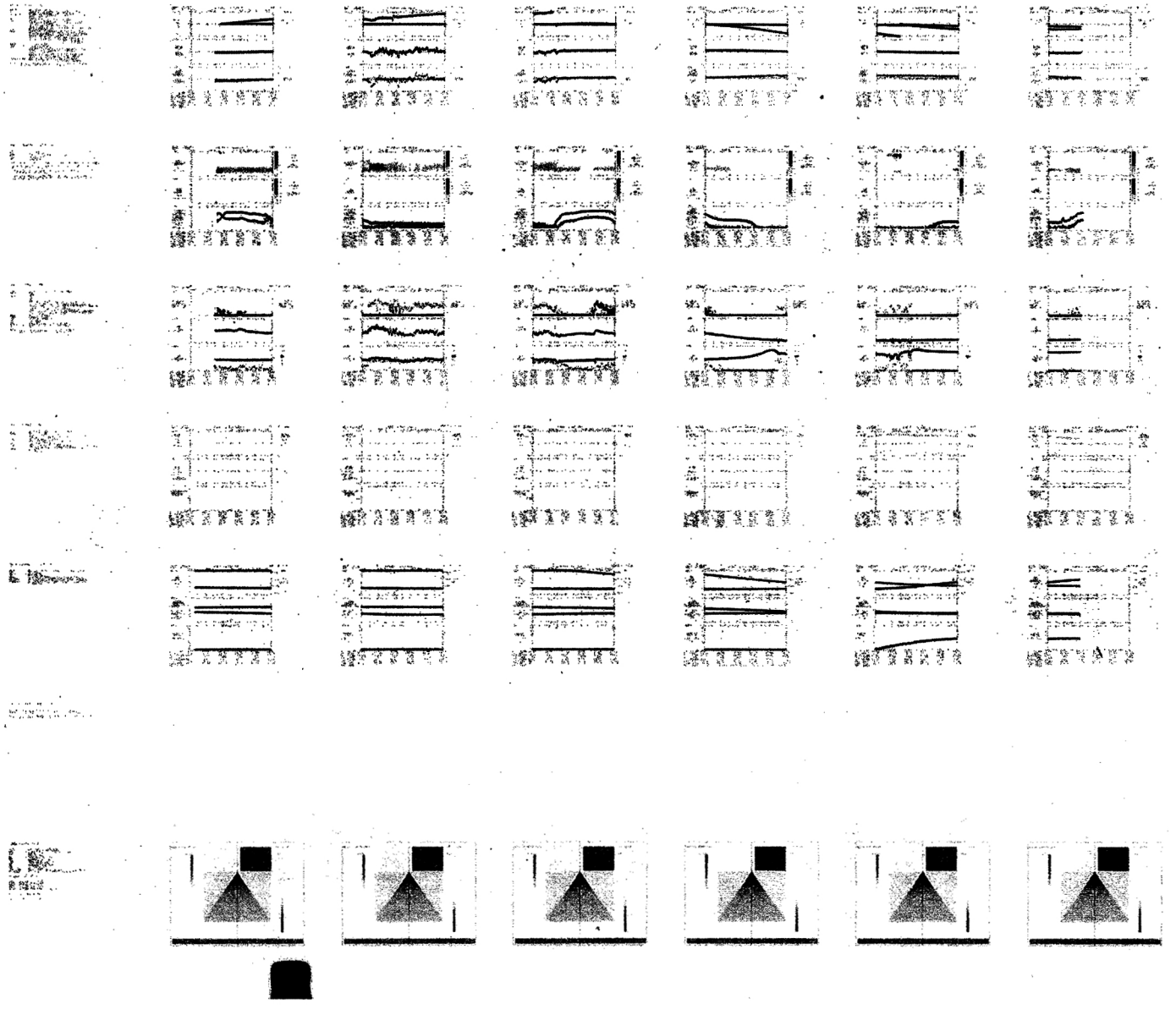

Figure 8.1: Summary plot microfiche layout

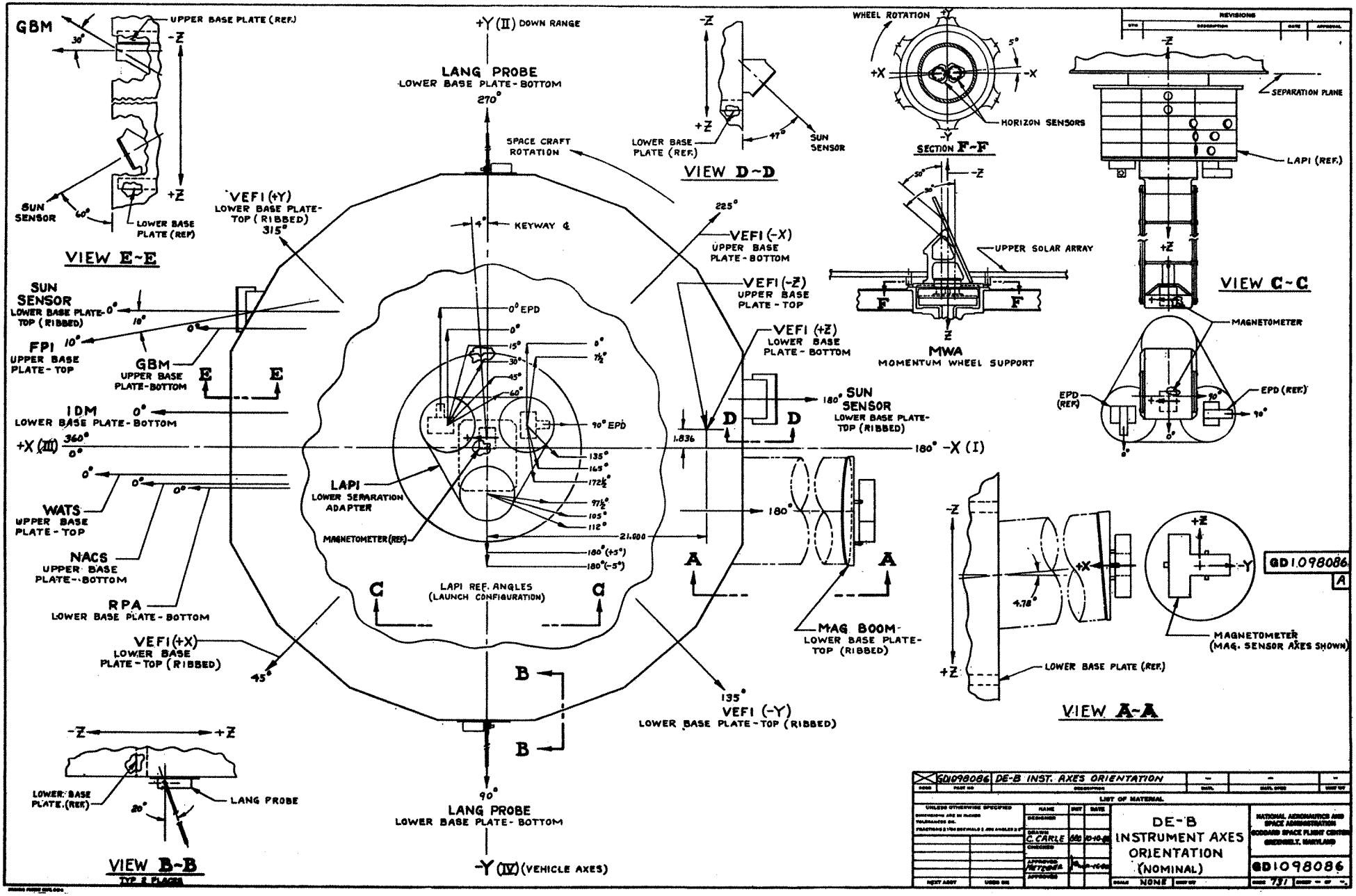

Figure 8.2: Orientation of the instruments on DE-2

- Instrument Orientation: See Figure 8.2. B_z is in the spacecraft Z direction which is East when traveling South to North and West when traveling North to South. This is reversed when the spacecraft is inverted; see Version 4.3 algorithm change.

- Summary Plot Algorithm: The non-orthogonal field components along each sensor's effective axis are combined by linear matrix multiplication to describe a vector in spacecraft coordinates. Only the Z-axis component is used in the summary plots.

9.5 MODES

- None.

9.6 CORRECTED FOR:

- Orientation of the triaxial magnetometer sensor axes
  --Long term stability is expected to be about 0.1 degrees.

- Spacecraft magnetic field
  --Expected to be below the instrument's resolution.

- Cross coupling between sensors
  --Corrected for in the definition of sensor axis directions, as determined during ground calibrations.

9.7 UNCORRECTED FOR:

- Spacecraft attitude
  --ΔB_z depends on the accuracy to which B_z lies East-West (normal to the orbit plane), since ΔB_z is B_z minus the model East-West component.

- Spacecraft attitude oscillations
  --Roughly 30 second period oscillations. See Figure 9.1, day 82009, orbit 2356, from 0840 to 0850 UT, for example.
  --Roughly five second period oscillations in ΔB_z (less than 10 nT) are apparent in Figure 9.2, day 82122, orbit 4056, from 0740 to 0746 UT, for example. Thirty second oscillations are also evident.

- Instrument Orientation: See Figure 8.2. B_z is in the spacecraft Z direction which is East when traveling South to North and West when traveling North to South. This is reversed when the spacecraft is inverted; see Version 4.3 algorithm change.

- Summary Plot Algorithm: The non-orthogonal field components along each sensor's effective axis are combined by linear matrix multiplication to describe a vector in spacecraft coordinates. Only the Z-axis component is used in the summary plots.

9.5 MODES

- None.

9.6 CORRECTED FOR:

- Orientation of the triaxial magnetometer sensor axes
  --Long term stability is expected to be about 0.1 degrees.

- Spacecraft magnetic field
  --Expected to be below the instrument's resolution.

- Cross coupling between sensors
  --Corrected for in the definition of sensor axis directions, as determined during ground calibrations.

9.7 UNCORRECTED FOR:

- Spacecraft attitude
  --ΔB_z depends on the accuracy to which B_z lies East-West (normal to the orbit plane), since ΔB_z is B_z minus the model East-West component.

- Spacecraft attitude oscillations
  --Roughly 30 second period oscillations. See Figure 9.1, day 82009, orbit 2356, from 0840 to 0850 UT, for example.
  --Roughly five second period oscillations in ΔB_z (less than 10 nT) are apparent in Figure 9.2, day 82122, orbit 4056, from 0740 to 0746 UT, for example. Thirty second oscillations are also evident.

9.8 DISPLAY ANOMALIES:

- o Renormalization of ΔB_z
  - --When ΔB_z exceeds ± 1100 nT (2 percent of the maximum expected B_z scale), it is renormalized (minus ± 1100 nT) to keep the plot on scale.
  - --Due to: Spacecraft Z-axis not normal to orbit plane. Attitude control was maintained to 0.5 degrees out of normal.
    Bad attitude description.
    Model field not available (for fiche produced before Version 4.4).
  - --See Figure 9.2, day 82122, orbit 4056, from 0740 to 0747:30 UT, for example.

- o North/South pole effect on ΔB_z
  - --Caused by change in sign with change of direction from North to South (or South to North) in crossing the pole. See Figure 9.2, day 82122, orbit 4056, at 0748 UT, for example.

9.9 INTERPRETATIONS:

Substantial variation in "standard" patterns exist. The following are given only as possible cases and should not be construed as definitive.

- o Field-aligned currents
  - --See Figure 9.3, day 82325, orbit 7171, from 1810 to 1814 UT, for example.

Spacecraft Orientation	Decreasing ΔBz	Increasing ΔBz
Normal	Upward	Downward
Inverted	Downward	Upward

9.10 COMMENTS

- o VEFI plots and LAPI energy-time spectrograms are useful in identifying field-aligned current regions.

- o Ignore slopes in ΔB_z associated with plot rollovers which are due to attitude description or model field errors.

- o Only summary plots produced after Version 4.3 should be used.

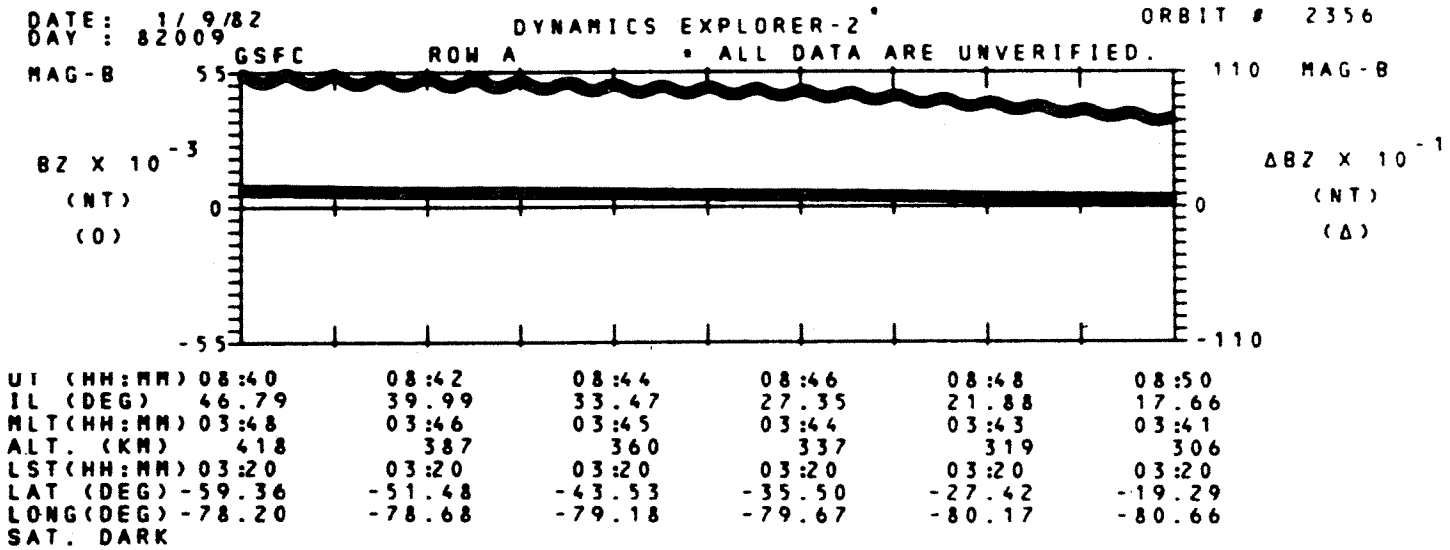

UT (HH:MM)	08:40	08:42	08:44	08:46	08:48	08:50
IL (DEG)	46.79	39.99	33.47	27.35	21.88	17.66
MLT(HH:MM)	03:48	03:46	03:45	03:44	03:43	03:41
ALT. (KM)	418	387	360	337	319	306
LST(HH:MM)	03:20	03:20	03:20	03:20	03:20	03:20
LAT (DEG)	-59.36	-51.48	-43.53	-35.50	-27.42	-19.29
LONG(DEG)	-78.20	-78.68	-79.18	-79.67	-80.17	-80.66
SAT.	DARK					

Figure 9.1: Example of 30 second oscillations

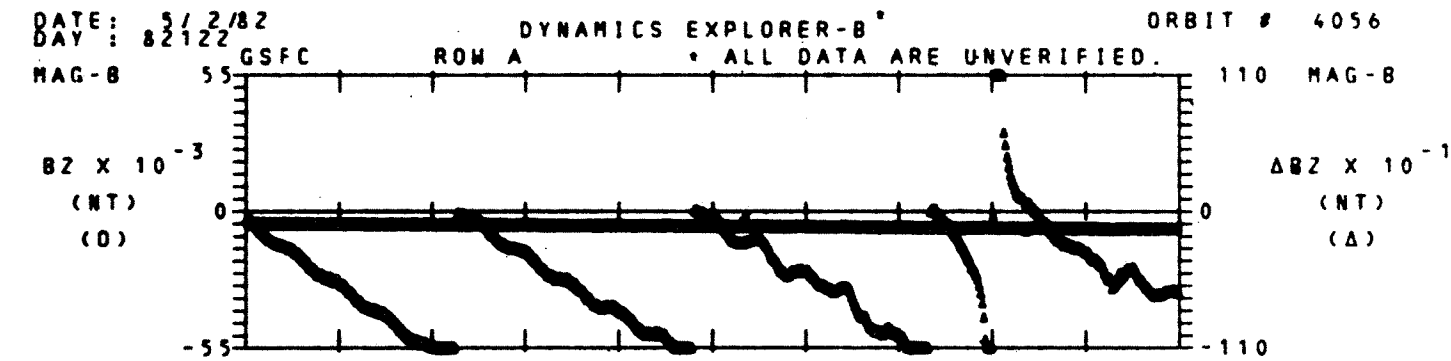

UT (HH:MM)	07:40	07:42	07:44	07:46	07:48	07:50
IL (DEG)	55.83	60.12	64.82	70.08	74.99	77.41
MLT(HH:MM)	06:54	06:33	06:01	05:02	03:07	00:26
ALT. (KM)	392	372	354	339	328	319
LST(HH:MM)	08:03	08:03	08:04	08:04	18:09	20:02
LAT (DEG)	-58.30	-66.19	-74.11	-82.07	-89.93	-81.93
LONG(DEG)	5.18	4.69	4.23	3.85	154.54	-177.6
SAT.	DARK					

Figure 9.2: Example of 5 second oscillations, renormalization, and North Pole effect

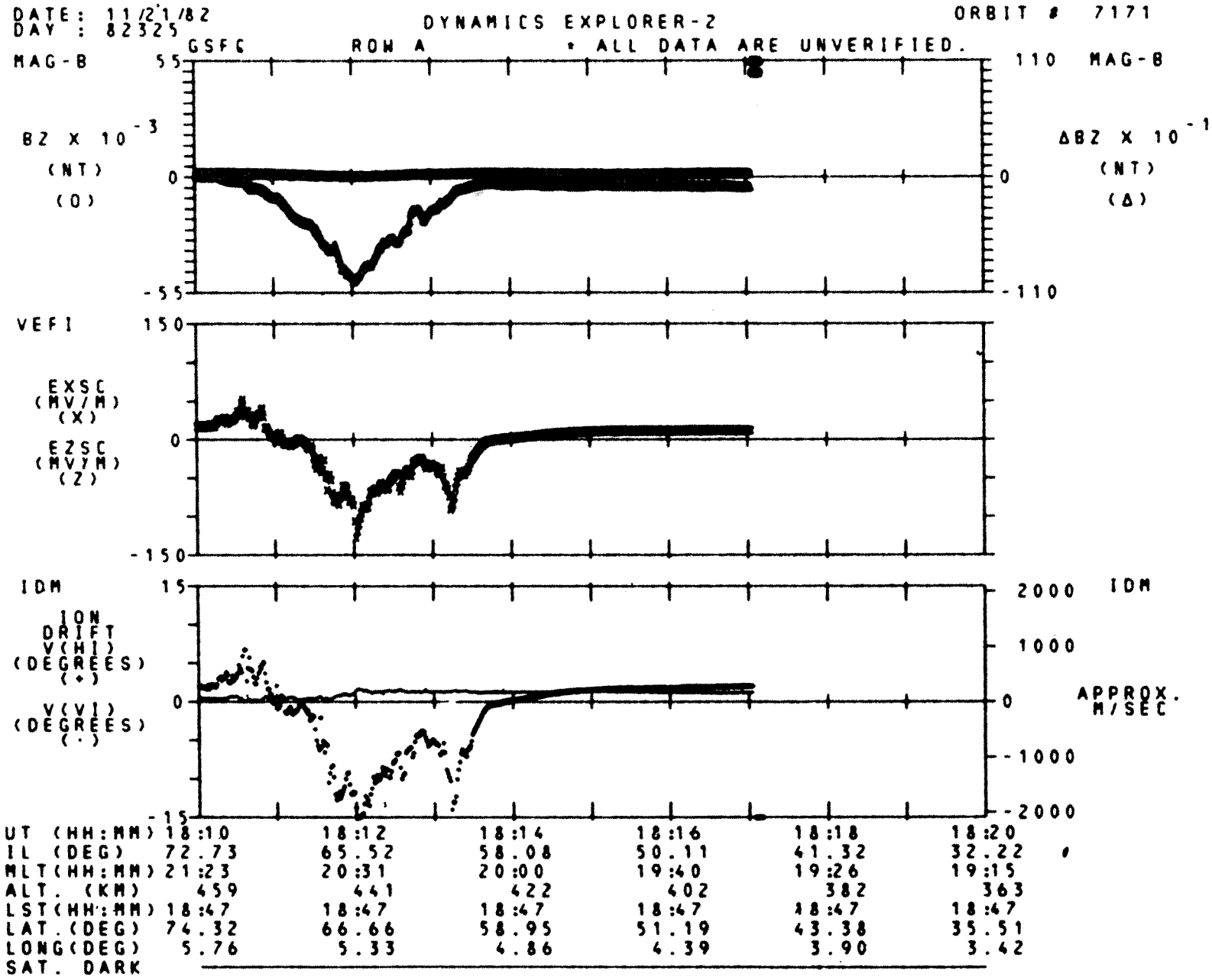

Figure 9.3: Example of field-aligned currents

CHAPTER 10

VECTOR ELECTRIC FIELD INSTRUMENT (VEFI)

10.1 FURTHER INFORMATION:

Contact: N.C. Maynard (301) 344-6328
Code 696
Goddard Space Flight Center
Greenbelt, MD 20771

References: Maynard, N.C., E.A. Bielecki, and H.F. Burdick, "Instrumentation for Vector Electric Field Measurements from DE-B", Space Science Instrumentation, 5, 523 (1981).

Maynard, N.C., J.P. Heppner, and A. Egeland, "Intense, Variable Electric Fields at Ionospheric Altitudes in the High Latitude Regions as Observed by DE-2", Geophysical Research Letters, 9, 981 (1982).

10.2 SUMMARY PLOT PARAMETERS:

- o Ex_{sc} DC electric field components in the spacecraft X direction
  --provides a measurement of the North-South electric field and hence the principle component of convection over most of the orbits through the high latitude regions.

- o AC electric field components 8-16 Hz
  --provides an indication of the ULF electrostatic noise caused principally by the spacecraft moving through spatial ionospheric irregularities.

- o AC electric field components 4-16 kHz
  --provides an indication of auroral hiss, which accompanies particle precipitation in the high latitude regions.

- o GAIN
  --Amplifier gain; GAIN = N indicates the gain status is not available.

10.3 PARAMETERS NOT PLOTTED:

- o Ez_{sc} Electric field components in the Z direction
  --One Z-axis antenna did not deploy. E_z can be estimated using $E \cdot B = 0$ only when B is significantly directed away from the orbit plane. This never occurs in the northern hemisphere and is only possible at limited longitudes in the southern hemisphere.

- o Ey_{sc} Electric field components in the Y direction
  --At high latitudes, Ey_{sc} is nearly parallel to B and is expected to be near zero.

- o Other AC spectrometer filter data
  --18 channels covering 4 Hz to 500 kHz band.

10.4 MEASUREMENT UNITS

- o Geophysical Units: DC components are in millivolts/meter. AC components can be approximately converted to geophysical units by using the gain tables in the glossary.

- o Summary Plot Range: $\pm$150 mV/m for Ex_{sc} and 10^{-4} to 10^{0} V for AC plots.

- o Summary Plot Sampling Rate: Half second averages of data which was sampled 16 times a second for DC data and 1 sample per second for AC data.

- o Summary Plot Resolution: For the AC plots, 10 degrees is equivalant to 10 mV/m rms for low gain and 0.5 mV/m rms for high gain.

- o Accuracy of Trends on Plots: For qualitative use only.

- o Instrument Orientation: See Figure 8.2. E_x is in spacecraft coordinates, positive in the direction of motion. The AC data is in the instrument sensor coordinates, in which X_i is at -45 degrees from X_{sc} and Y_i is at +45 degrees from X_{sc}.

- o Summary Plot Algorithm: A crude approximation of the DC field is derived by multiplying the differences of the opposite sensors in the horizontal plane by a matrix that converts to spacecraft coordinates and then subtracting a rough v x B component.

10.5 MODES

- o None for Ex_{sc}.

- o AC data may be in low or high gain and connected to instrument X or Y axes as specified by status symbols (see Glossary). In general, the AC channels plotted will be looking at the axis most nearly perpendicular to B.

10.6 CORRECTED FOR:

- o Electric field induced by the spacecraft crossing the magnetic field through a crude v x B subtraction, without using definitive attitude.

10.7 UNCORRECTED FOR:

- o Curvature of a fraction of a degree in the antennas
  --Insignificant effect on the summary plots.

- o Contact potential differences
  --Small effect for the summary plot scales.

- o Spacecraft oscillations
  --Oscillations in B (see MAG-B instrument Figure 9.1) are on rare occasions strong enough to affect the E data also. Ignore such artifacts.

10.8 DISPLAY ANOMALIES:

- o Slowly varying slopes in E_x
  --Should be ignored since the v x B subtraction used in the summary plots is very crude and does not use definitive attitude. Rapid or large variations are real.

- o Internal calibration (once or twice per orbit for 32 or 64 seconds)
  --Looks like a square wave in E_x and as a constant level on the 8-16 Hz filter channel. See Figures 10.1A and B, day 81300, orbit 1262, from 2112:20 to 2112:50 UT, for example.

- o Saturated plot points at beginning and end of passes
  --Plotting when the instrument was not on. E_x will be saturated and the filters will be at the zero level. This problem was eliminated in Version 4.5.

- o Unusual cycloidal signature
  --Due to spacecraft interference in the high gain filters. See Figure 10.2, day 81265, orbit 743, from 2110 to 2117 UT, for example.

- o Axis labels and Gain status for the AC filters corrected in Version 3.0
  --Use prior versions with caution. The most common problems were mislabeling the 4-16 kHz channel gain and the axis used for both channels.

- o Scale changes (see scale factors in Glossary)
  --Step function changes in the filter gains can cause shift of the axis scale in mid-plot, generally over the pole or near the equator. This is not generally noticeable and will occur only once per 10 minute plot, at most.

10.9 INTERPRETATIONS:

Substantial variation in "standard" patterns exist. The following are given only as possible cases and should not be construed as definitive. Note that noon-midnight passes across the polar caps do not measure the principle component of the convection electric field; hence patterns vary greatly.

- o Dawn/dusk auroral zone to polar cap demarcation
  --See Figures 10.3 and 10.4, day 81322, orbit 1583, for examples. There are morning auroral effects from 1142 to 1145, polar cap quiet from 1148 to 1155, and evening auroral zone from 1155 to 1159 UT. Note that there are other sources of signals in the 4-16 kHz range besides auroral hiss, such as low frequency irregularities and a mid-latitude VLF signal from 1158 to 1159 UT.

- o Mid-latitude sub-auroral ion drift events
  --See Figure 10.5, day 81284, orbit 1020, from 1324 to 1325 UT, for example. Distinguished from auroral arc fields by small field-aligned currents (ΔB_z small by comparison).

10.10 COMMENTS

- o VEFI data is useful in comparison with all other plasma and field data for understanding electro-dynamical processes. Comparisons with wind data are useful in aeronomic studies. Note that the ion-drift data usually mirrors the electric field data.

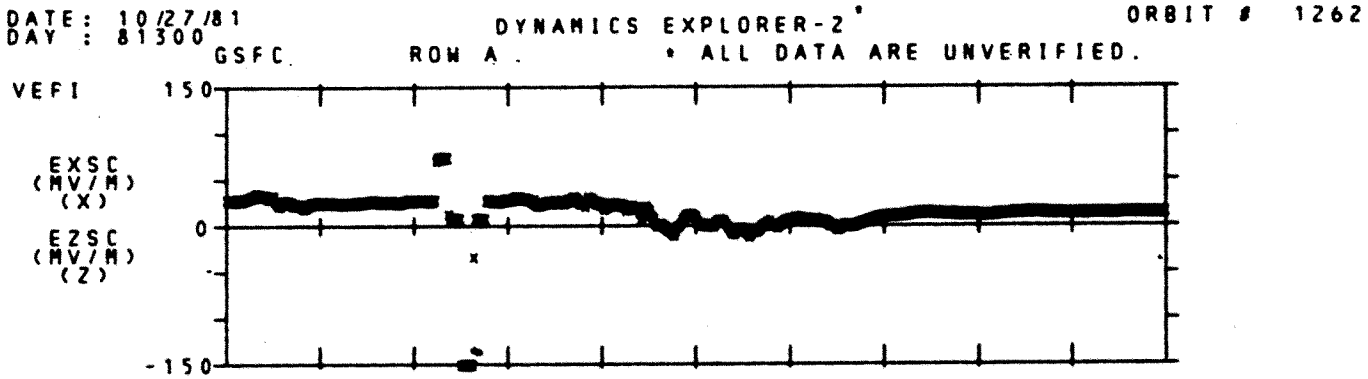

Figure 10.1A: Example of calibration anomaly in Exsc plot

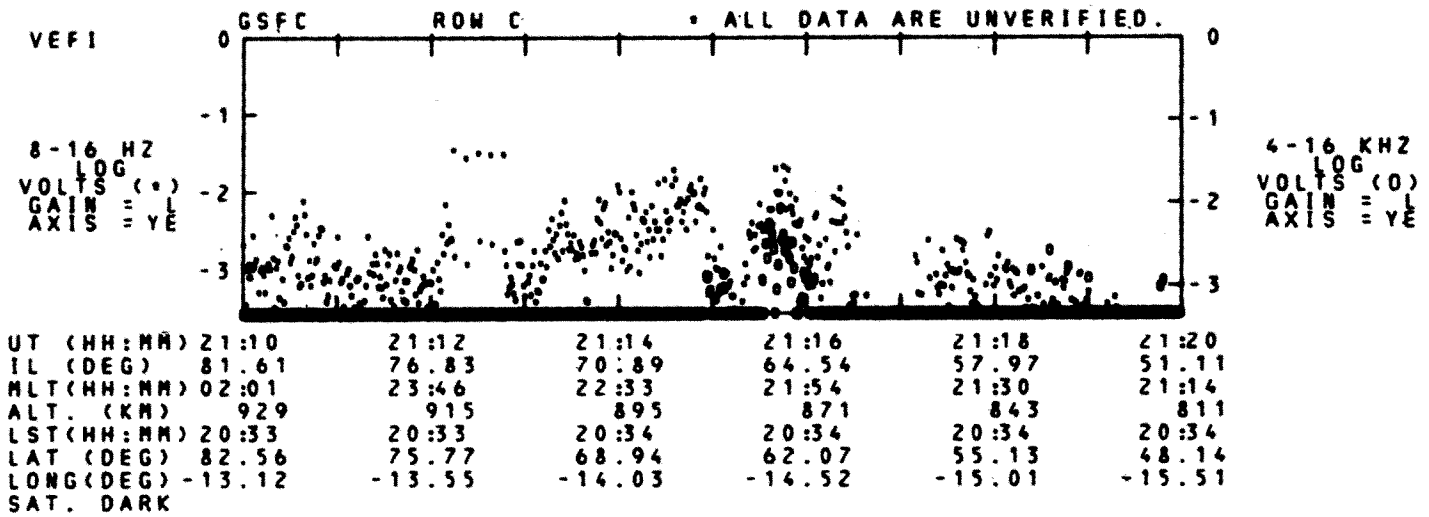

Figure 10.1B: Example of calibration anomaly in 8-16 Hz plot

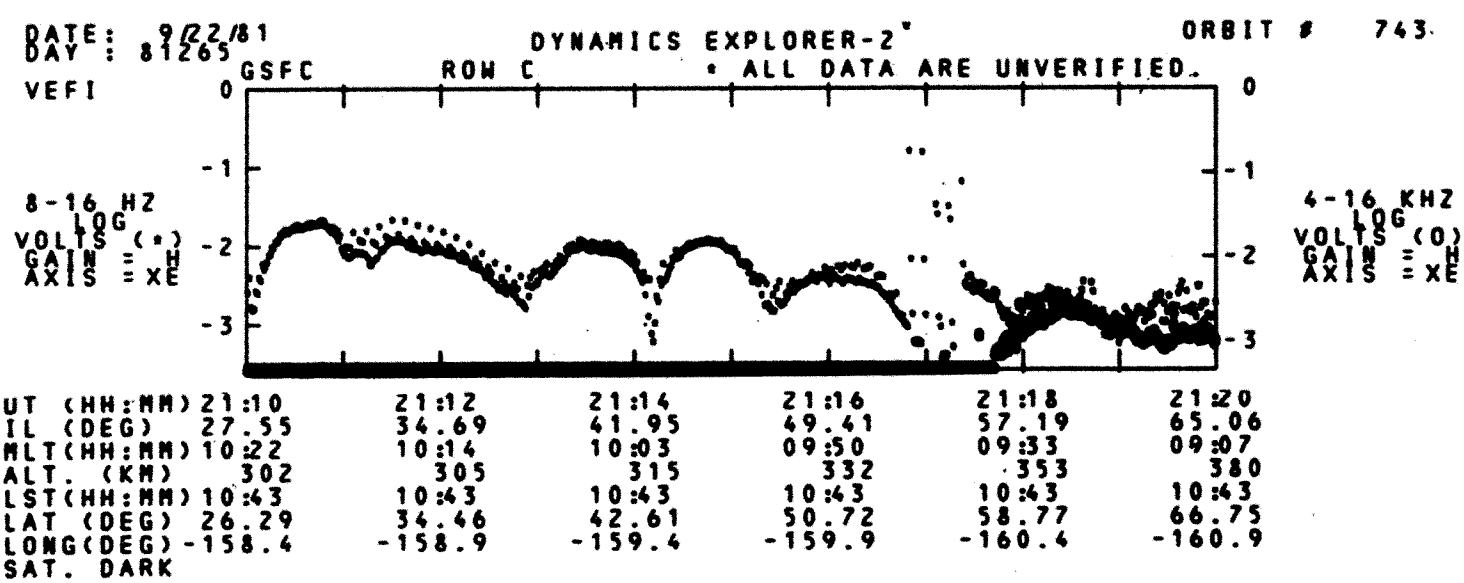

Figure 10.2: Example of cycloidal signature

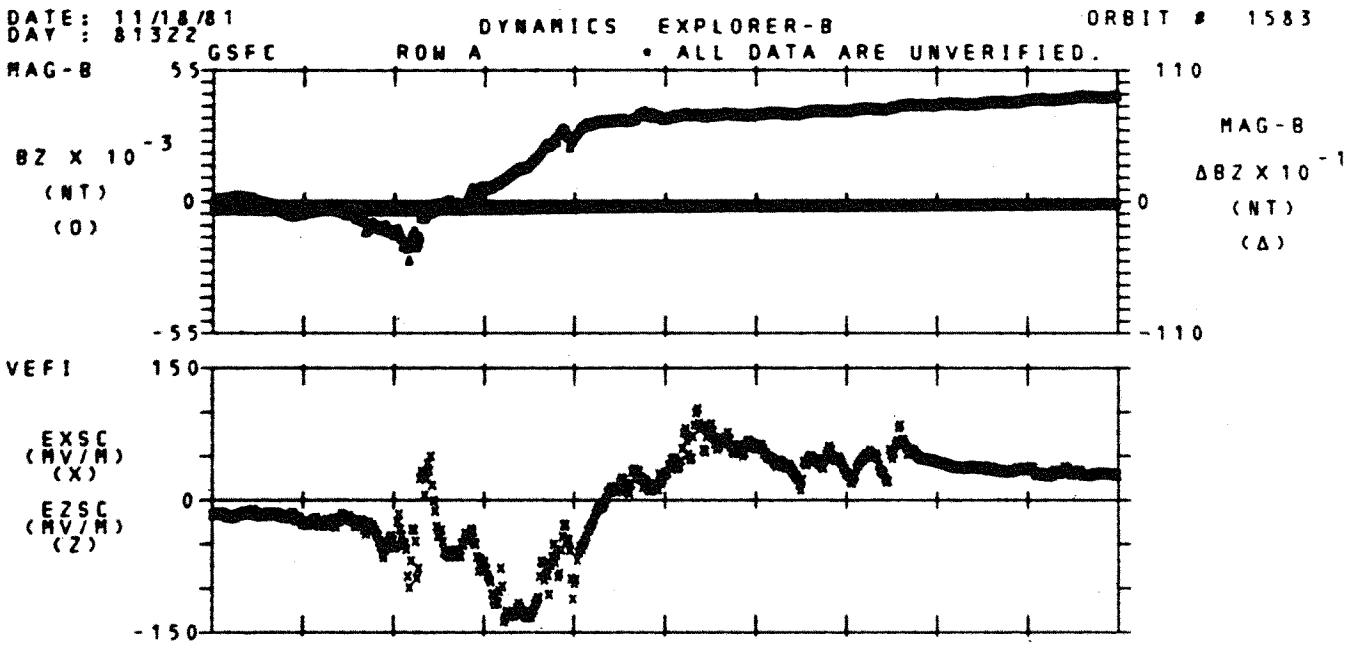

Figure 10.3A: Example of dawn aurora demarcation in Exsc plot

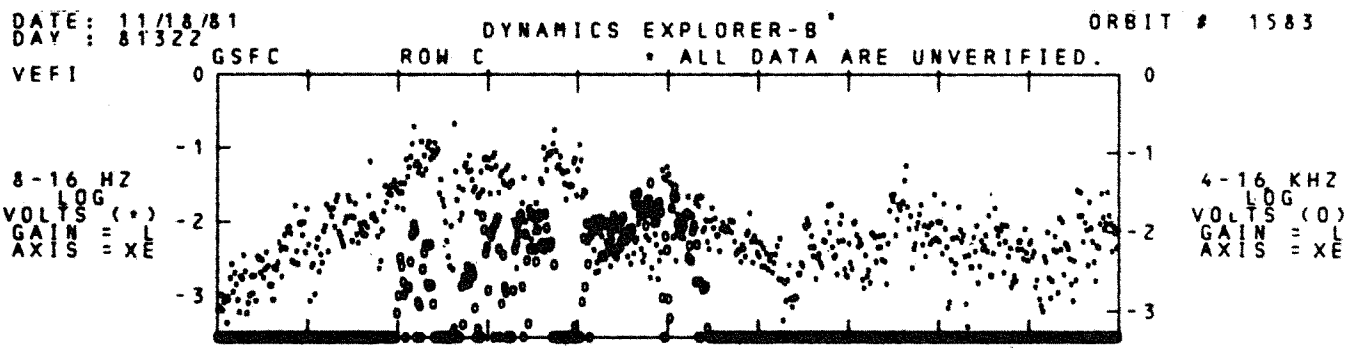

UT (HH:MM)	11:40	11:42	11:44	11:46	11:48	11:50
IL (DEG)	62.70	68.84	75.06	81.25	87.32	86.09
MLT(HH:MM)	07:17	07:14	07:09	06:56	03:23	19:55
ALT. (KM)	811	782	749	714	677	639
LST(HH:MM)	07:07	07:07	07:07	07:07	07:08	07:08
LAT (DEG)	49.51	56.56	63.67	70.83	78.06	85.37
LONG(DEG)	-71.80	-72.30	-72.78	-73.26	-73.72	-74.02

SAT. DARK

Figure 10.3B: Example of dawn aurora demarcation in 8-16 Hz plot

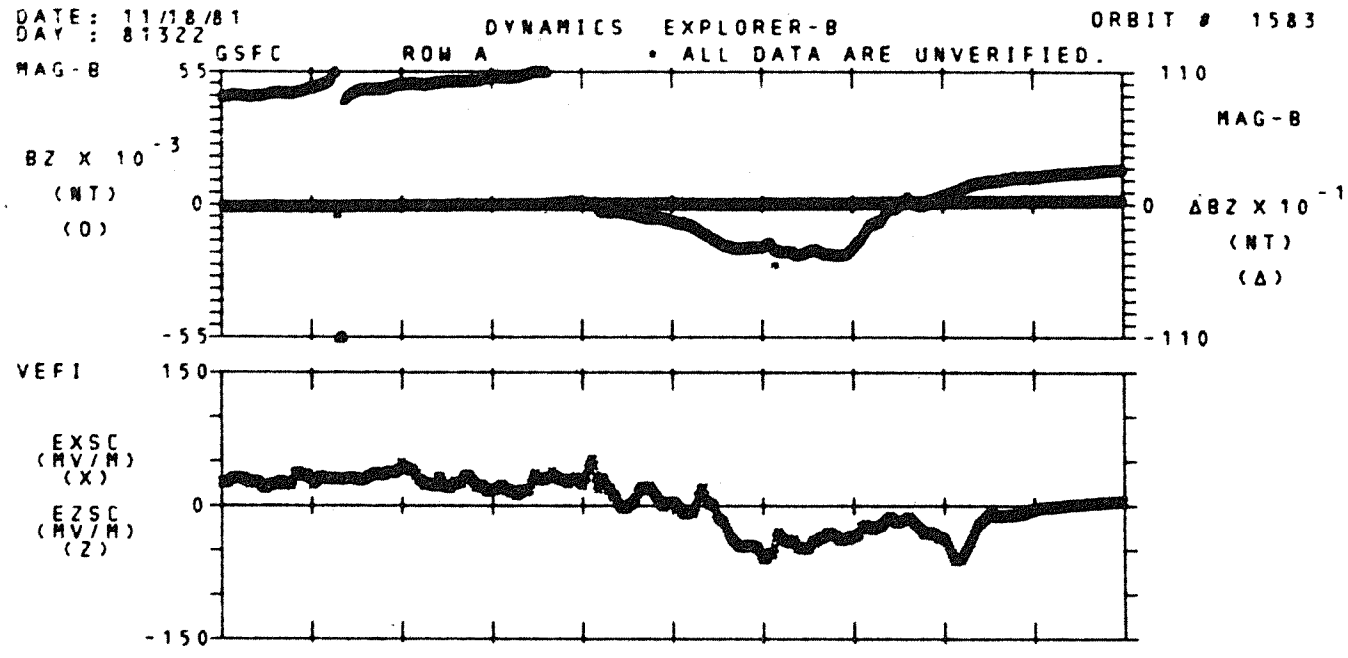

Figure 10.4A: Example of dusk aurora demarcation in Exsc plot

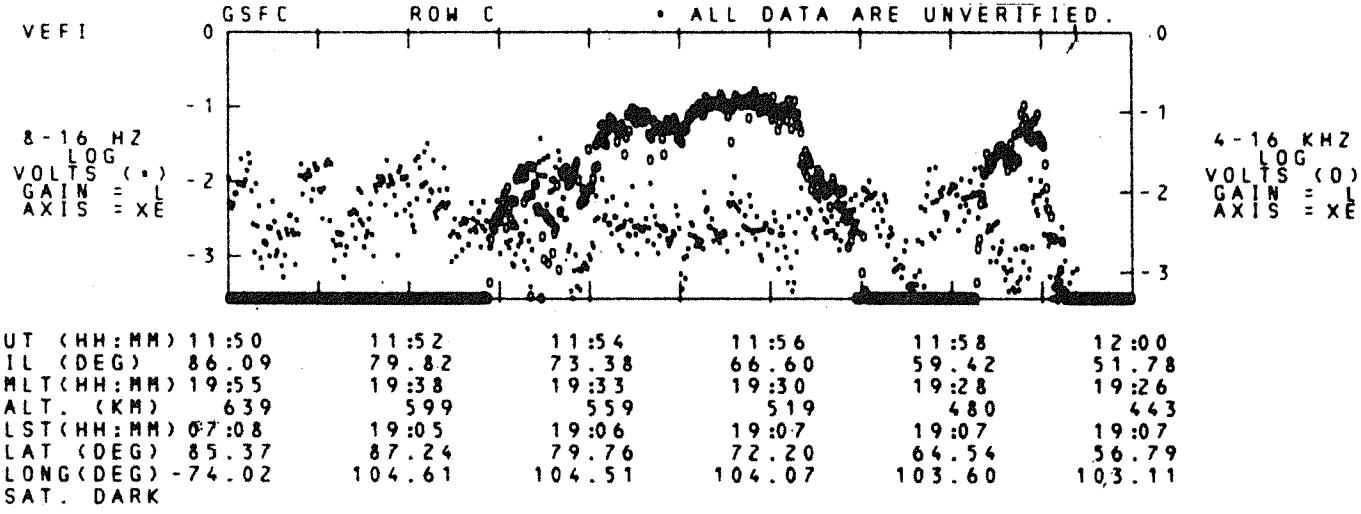

Figure 10.4B: Example of dusk aurora demarcation in 8-16 Hz plot

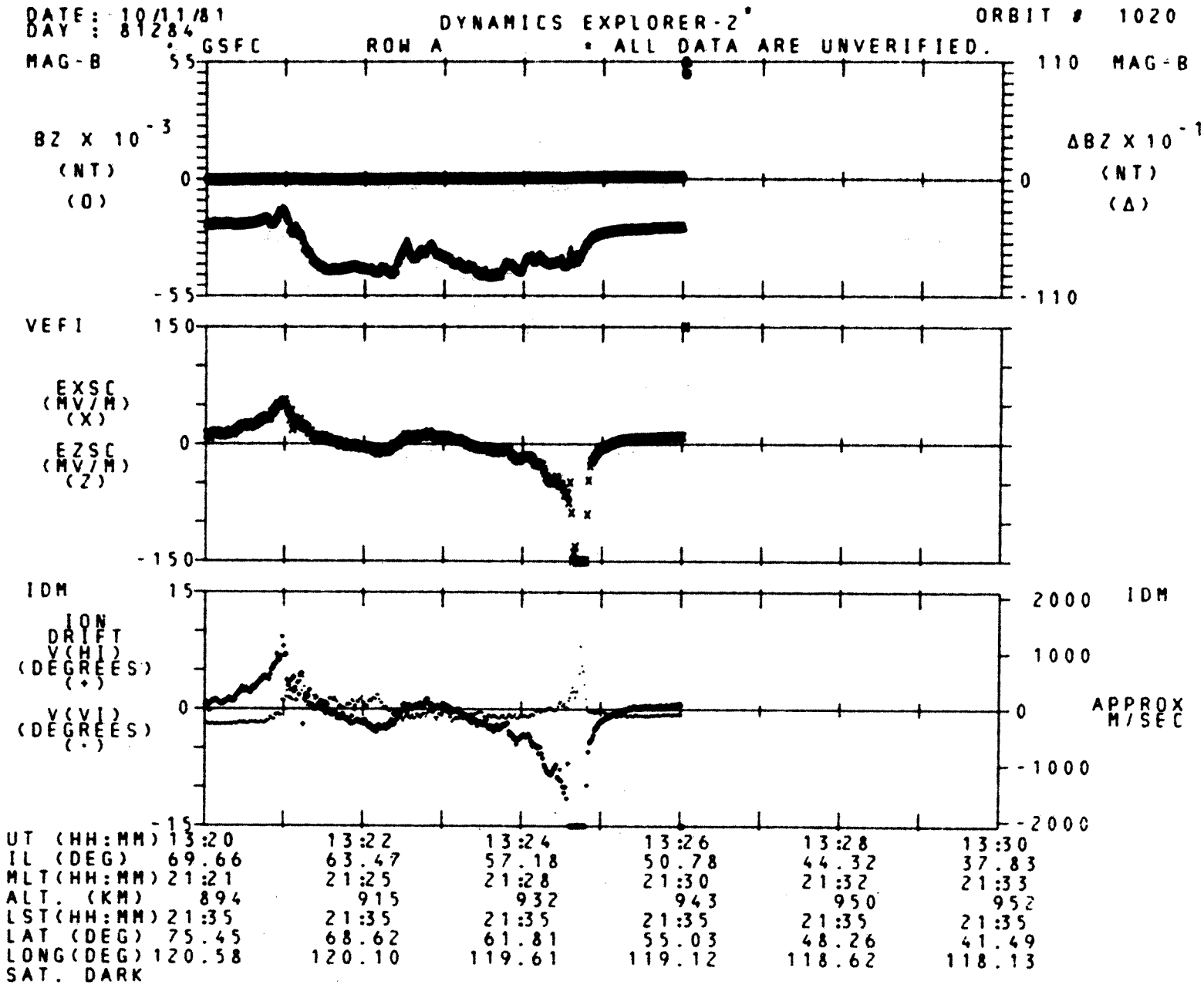

Figure 10.5: Example of sub-auroral ion drift event in Exsc plot

CHAPTER 11

ION DRIFT METER (IDM)

11.1 FURTHER INFORMATION:

Contact: R.A. Heelis (214) 690-2851
Center for Space Sciences
University of Texas at Dallas
Box 688
Richardson, TX 75080

References: Heelis, R.A., W.B. Hanson, C.R. Lippincott, D.R. Zuccaro, L.H. Harmon, B.J. Holt, J.E. Doherty, and R.A. Power, "The Ion Drift Meter for Dynamics Explorer-B", Space Science Instrumentation, 5, 511 (1981).

11.2 SUMMARY PLOT PARAMETERS:

- o V(HI) Transverse ion arrival angle in the horizontal plane, from the orbit plane, relative to the spacecraft
  --Directly derivable without requiring attitude data.
- o V(VI) Transverse ion arrival angle in the orbit plane, from the horizontal plane, relative to the spacecraft
  --Also directly derivable without requiring attitude data.

11.3 PARAMETERS NOT PLOTTED:

- o The number of parameters is limited by summary plot space and computation time.

11.4 MEASUREMENT UNITS

- o Geophysical Units: Approximate angle relative to the spacecraft.
- o Range of Valid Data: $\pm$15 degrees and $\pm$2000 approximate m/sec for altitudes from perigee to about 1500 kilometers where N_i is less than 3000 cm^{-3}.
- o Summary Plot Sampling Rate: Four points are selected in each second.
- o Summary Plot Resolution: Instrument resolution (0.03 degrees) is finer than a visible pixel (more than 0.06 degrees) in the summary plots.
- o Accuracy of Trends on Plots: Although the instrument measured angles are accurate to less than 0.1 degree, attitude data limit the plot accuracy to only about 0.5 degrees or roughly 50 m/sec.

- Instrument Orientation: See Figure 8.2. V(VI) and V(HI) are positive with drift along the -Y and -Z axes, respectively. Both V(VI) and V(HI) reverse direction when the spacecraft is inverted.

- Summary Plot Algorithm: The ion drift relative to the spacecraft along the spacecraft Y and Z axes is given by $V_{z}^{y} = V_{x} \tan \frac{\alpha}{\beta}$, where V_x is the total ion drift relative to the spacecraft along the X axis and α and β are vertical and horizontal arrival angles. The arrival angle is a constant times the range factor times the telemetered voltage.

11.5 MODES

- Only Standard Drift Sensor data are plotted
  --Sometimes fixed in vertical or horizontal.

11.6 CORRECTED FOR:

- Nothing.

11.7 UNCORRECTED FOR:

- Spacecraft inversion
  --A given inertial convection direction will appear with opposite signs.

- Spacecraft spinning
  --See Section 8.6.2.

- Calculation of components of the spacecraft velocity parallel to the sensor look direction (spacecraft radial direction)
  --Affects absolute drift velocity magnitude but not interpretations.

- Spacecraft attitude offsets in Pitch (affects V(VI))
  --See Figure 11.1, day 82325, orbit 7161, from 0117 to 0120 UT, for example. Appears as a DC signal superimposed on the ambient ion drift signal baseline. The ambient signal baseline is a sinewave with amplitude about 6 degrees with zeros at perigee and apogee.

- Spacecraft attitude offsets in Yaw (affects V(Hl))
  --A yaw angle at the equator appears as a sinewave with amplitude equal to the yaw angle and zeros at the north and south poles superimposed on the ambient drift signal baseline.

- Spacecraft attitude offsets in Roll (affects V(Hl))
  --A roll angle at the equator appears as a sinewave with amplitude equal to the roll angle and zeros at the north and south bound equators superimposed on the ambient drift signal baseline.

- o Atmospheric corotation
  --The ambient drift signal baseline is a sinewave with amplitude about 5 degrees with zeros at north and south poles.

- o Ram component of the ambient ion drift velocity
  --Assumed to be zero, affects only the absolute drift velocity.

- o Spacecraft electric fields
  --Small effect.

- o Thermal effects
  --Negligible.

11.8 DISPLAY ANOMALIES:

- o Saturated plot points at beginning and end of passes
  --Eliminated in Version 4.5.

- o Scattered points
  --See Figure 11.2, day 82105, orbit 3808, from 2311 to 2316 UT, for example. Signal can be noisy if N_i is less than 3×10^3 cm^{-3}. See LANG N_i plots.

11.9 INTERPRETATIONS:

Substantial variation in "standard" patterns exist. The following are given only as possible cases and should not be construed as definitive.

- o Small drifts at the equator in V(VI) and high latitude convection signatures during both day and night
  --Atmosphere corotation is the dominant signal in the plasmasphere and is used to determine the inertial direction of the horizontal ion drifts at high latitudes. See Figure 11.3, day 82325, orbit 7171, from 1740 to 1750 UT, for an example.

- o Mid-latitude sub-auroral ion drift events
  --See VEFI Figure 10.5 for an example.

11.10 COMMENTS

- o The right hand scale on the plots shows an approximation to velocity, applying the algorithm V(ions) = 8000 x Angle(radians) in m/s.

- o The third component of ion drift can be derived from RPA data.

- o VEFI and IDM plots are usually very similar; although only IDM is inverted during spacecraft inverted periods.

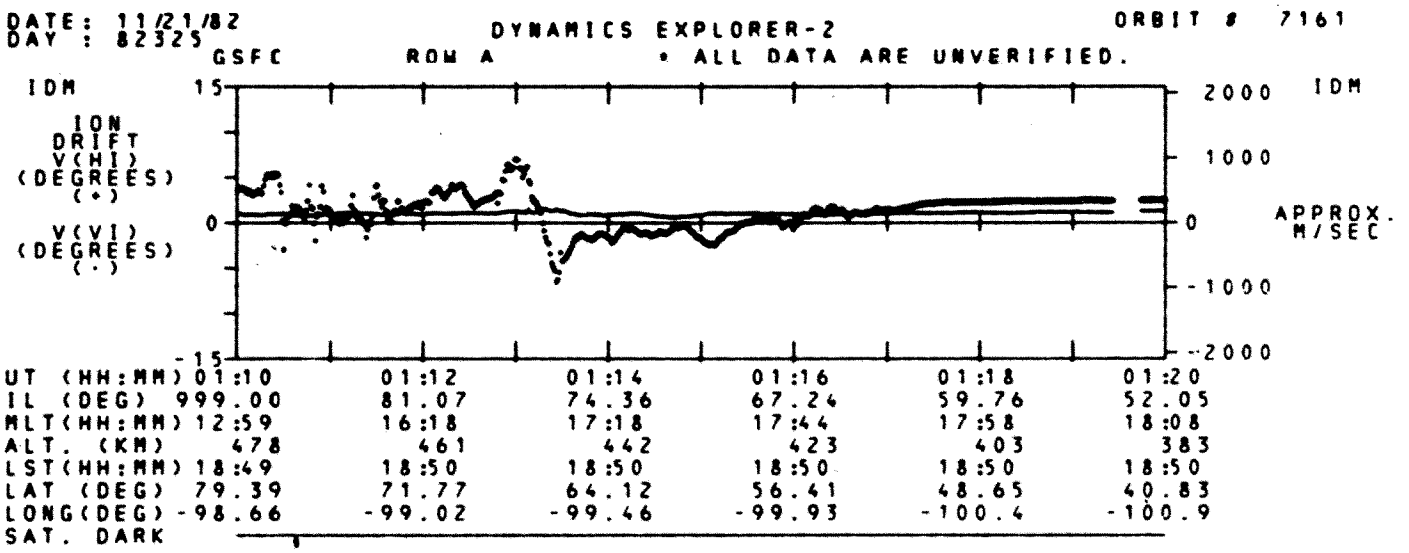

Figure 11.1: Example of spacecraft attitude offsets

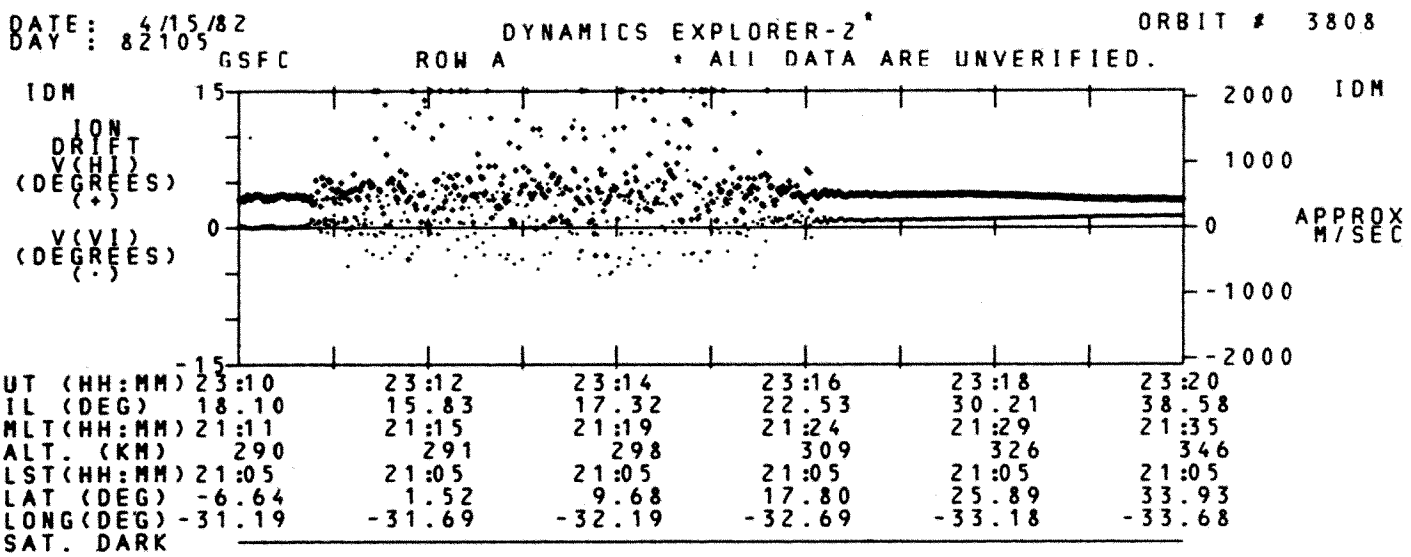

Figure 11.2: Example of scattered points on the plots

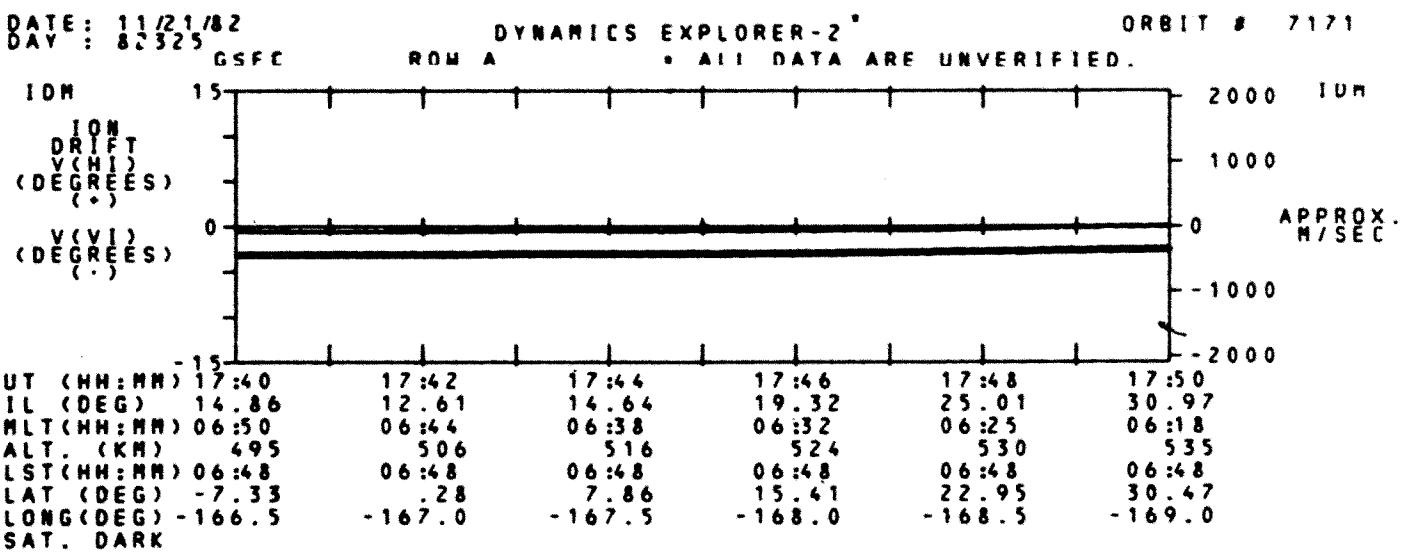

Figure 11.3: Example of small drifts at the equator

CHAPTER 12

LOW ALTITUDE PLASMA INSTRUMENT (LAPI)

12.1 FURTHER INFORMATION:

Contact: J.D. Winningham (512) 684-5111 x3075
Southwest Research Institute
P.O. Drawer 28510
San Antonio, TX 78284

References: Winningham, J.D., J.L. Burch, N. Eaker, V.A. Blevins, and R.A. Hoffman, "The Low Altitude Plasma Instrument (LAPI)", Space Science Instrumentation, 5, 465 (1981).

12.2 SUMMARY PLOT PARAMETERS:

- Spectrogram of electron energy flux from the 7.5 or 15 degree electron detector
  --Provides a measure of the energy disposition, for flux between 5 eV and 32 keV on log scale.

- Spectrogram of ion energy flux from the 97.5 or 112.5 degree ion detector
  --Detects ionic events unique to this angular range, for flux between 5 eV and 32 keV on log scale.

- Integral particle flux of electrons above 35 keV for 0 and 90 degree pitch angles
  --Provides a measure of various trapping boundaries.

12.3 PARAMETERS NOT PLOTTED:

- Data from the remaining 28 sensors at different pitch angles
  --Not plotted due to limited summary plot space and computation time.

12.4 MEASUREMENT UNITS

- Geophysical Units: The log electron and ion spectrograms show energy in electron volts and flux in ergs/(cm^2 sec sr eV). The plot for the integration of particle flux above 35 keV is in electrons per cm^2 per second per steradian.

- Range of Valid Data: Energy 5 to 3 x 10^4 eV, flux 10^{-7} to 10^0 ergs/(cm^2 sec sr eV), and total flux 10^2 to 10^8 electrons/(cm^2 sec sr).

- Summary Plot Sampling Rate: One sequence of energies each 1.0 or 1.7 seconds. The instrument samples every 1/32 or 1/64 second.

- o Summary Plot Resolution: Between launch and day 81327, there were 32 energy levels per scan; after that, there were 16 levels per scan.

- o Accuracy of Trends on Plots: There is about 5 percent error in the calibrations.

- o Instrument Orientation: See Figure 8.2. Pitch angle is defined as the angle between the particle velocity vector and the magnetic field in the northern hemisphere and is shifted 180 degree in the southern hemisphere. Thus downward moving particles always have a pitch angle between 0 and 90 degrees. The scan platform on which LAPI is mounted rotates about 180 degrees when the spacecraft crosses the equator to maintain the same detector orientation with respect to pitch angle.

- o Summary Plot Algorithm: The algorithm changed on day 82124 to handle the spacecraft telemetry word enable failure that occured on day 81327; there was another change on day 82137 to account for the failure in the High Voltage Power Supply (HVPS). Simple algorithms are employed to plot the differential flux from the number of counts as the gray level on the spectrograms.

12.5 MODES

- o Deflector voltage levels vary to give a sweep in energy; the plotted density width of the sample changes vertically for changes in the number of steps.

12.6 CORRECTED FOR:

- o Nothing.

12.7 UNCORRECTED FOR:

- o Spacecraft spinning
  --Produces a space/time aliased pitch angle roll modulation. See Section 8.6.2.

12.8 DISPLAY ANOMALIES:

- o Transients of the scan platform rotating to find the magnetic field
  --Occurs when the platform is turned-on and at the equatorial turn-around. These appear as rammed ions and spurious neutral effects on the electron detectors that are altitude dependent. See Figure 12.1, day 82184, orbit 5001, at 1316 UT, for an example at the equator, and Figure 12.2, day 82194, orbit 5160 at 2206 UT, for an example at turn-on.

- o Geiger-Mueller scale changes
  --Occurred when the preceeding plot frame had saturated on high counts. This was corrected in Version 3.0.

- o Corrections to the plots due to a spacecraft telemetry word enable failure
  --Version 3.0 includes the loss of one sensor and reduction to 16 energy levels from a nominal 32.

- o Loss of half the sensors spaced uniformly in angle
  --Version 4.0 compensates for the High Voltage Power Supply (HVPS) failure.

- o Increase in noise pick-up from the spacecraft
  --Appears and disappears abruptly for data received after the cosmic ray damage to the RCA data word encoder on 81327 and the failure of the HVPS on 81355. Between 81327 and 81355 there was a gradual background noise build-up in some sensors. Plots from such sensors should be ignored. Data from other pitch angles are still valid. Examine plots of this time period carefully.

12.9 INTERPRETATIONS:

Substantial variation in "standard" patterns exist. The following are given only as possible cases and should not be construed as definitive.

- o General background caused by trapped radiation in the Van Allen belts
  --Shown as background that is latitude specific and independent of energy. See Figure 12.3, day 81235, orbit 289, from 0140 to 0141 UT, for example.

- o Enhanced energy independent background
  --Produced by solar protons. See Figure 12.4, day 81285, orbit 1039, after 1956 UT, in both ion and electron spectrograms. Note the Geiger counters show isotropy and fairly high fluxes. The plotted data may be too faint to show in the printed example.

- o Dark band at the bottom of the plots
  --Produced by atmospheric photoelectrons from the ionosphere. See Figure 12.4, day 81285, orbit 1039, from 1954 to 1959 UT, for example.

12.10 COMMENTS

- o Duty cycle
  --About 95 percent when the spacecraft was operating above 55 degrees latitude, otherwise usually off.

- o LAPI was turned off from orbit 3355 (day 82075) to orbit 3643 (day 82094).

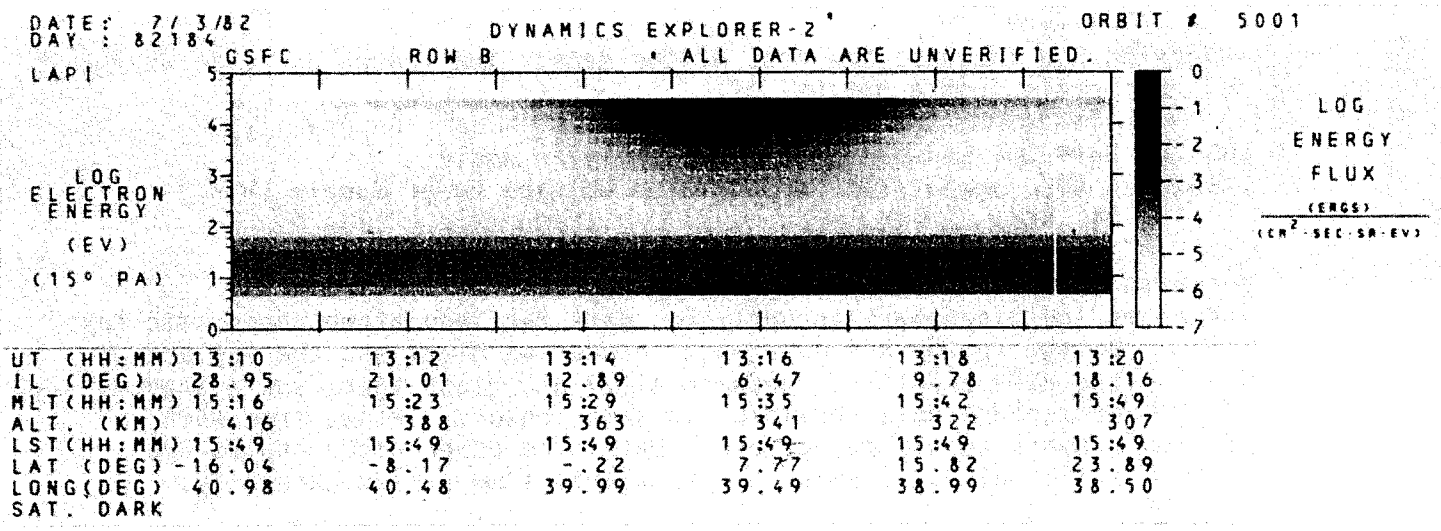

Figure 12.1: Example of platform turn-around transients at the equator

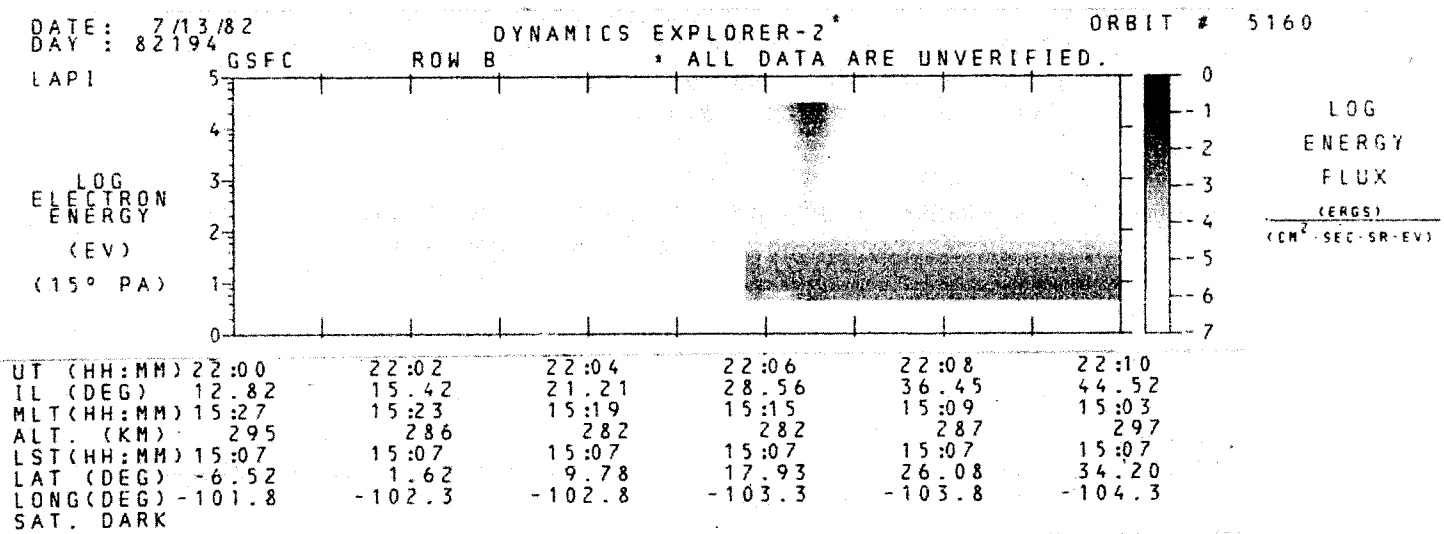

Figure 12.2: Example of platform turn-around transients at turn-on

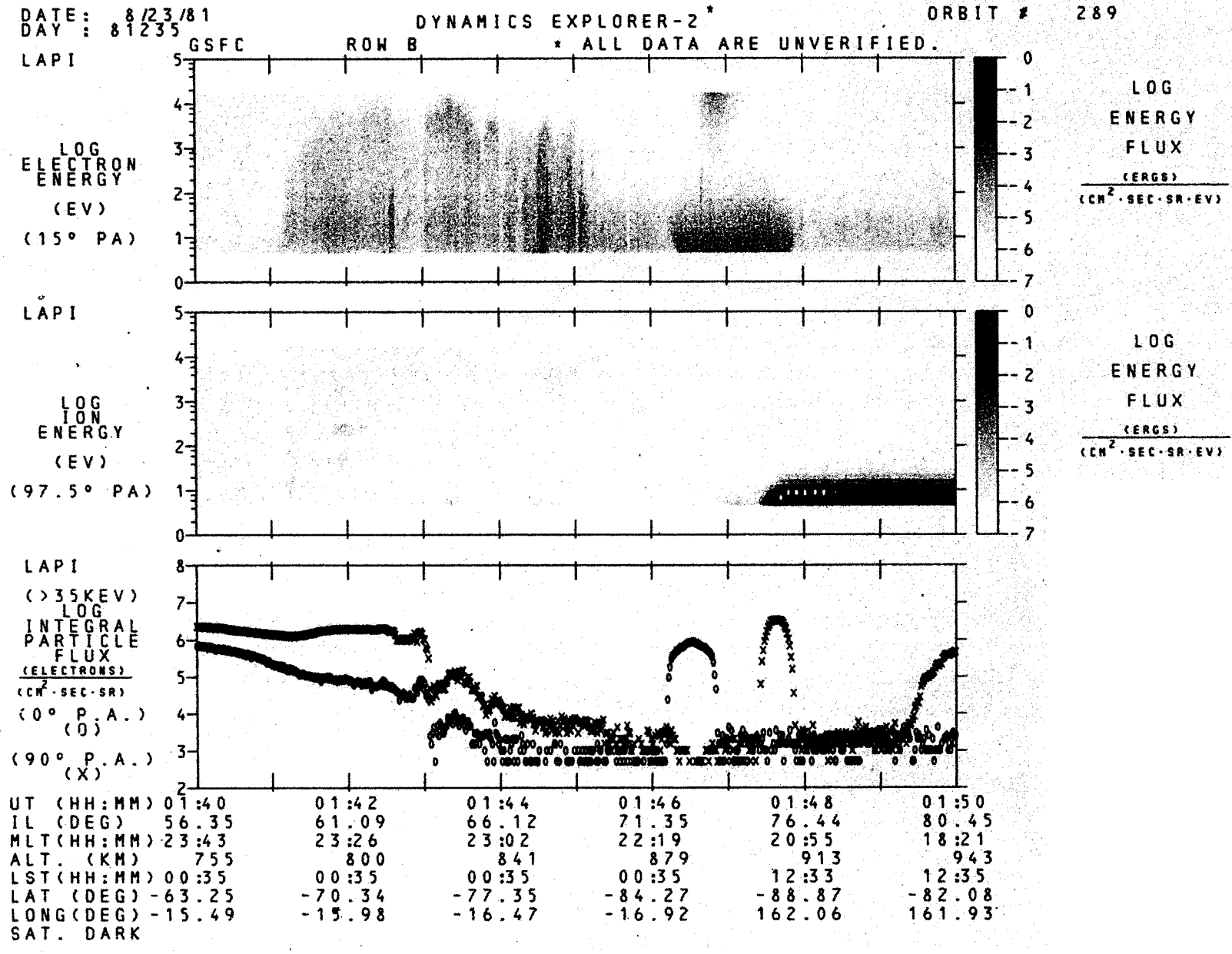

Figure 12.3: Example of trapped radiation background

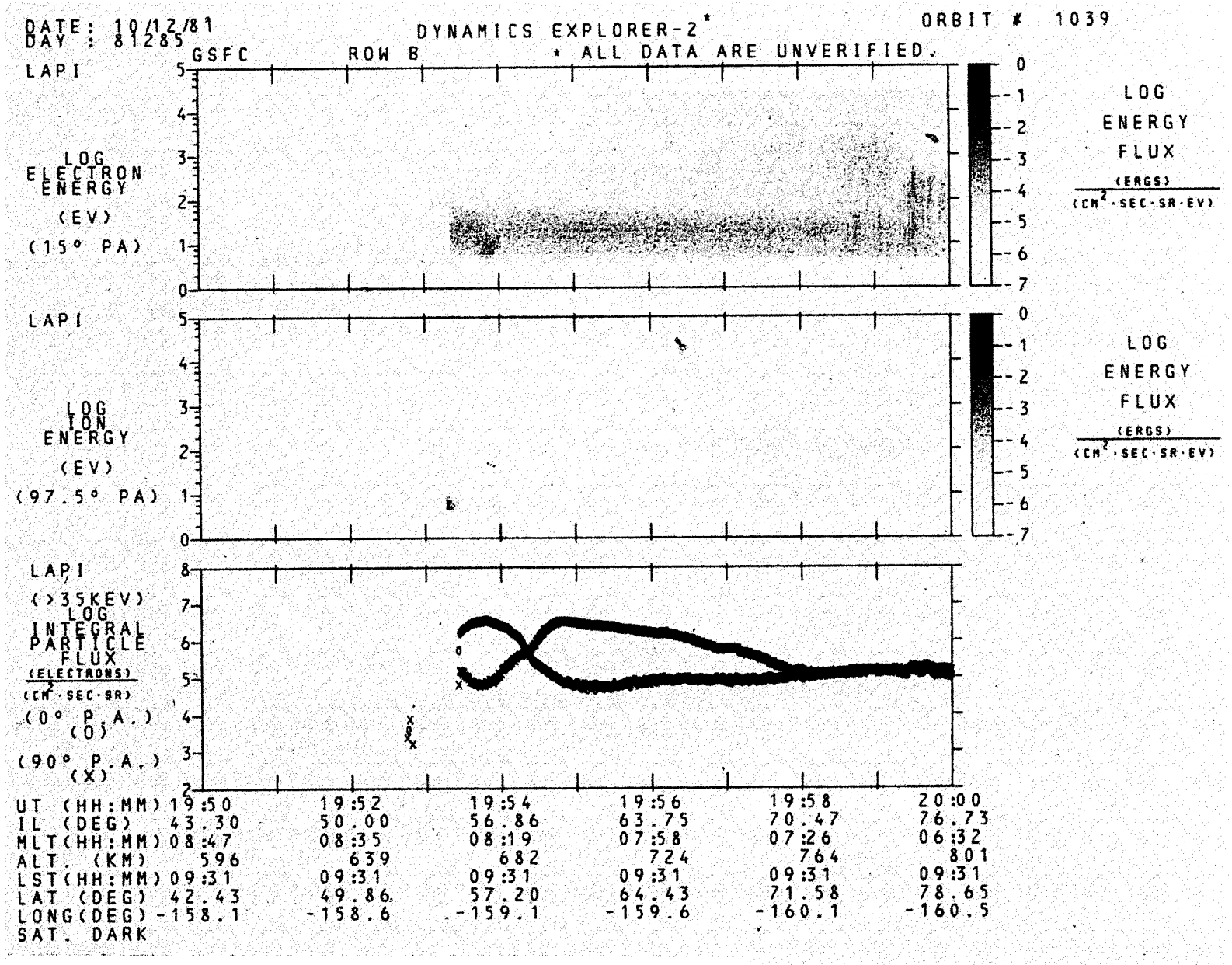

Figure 12.4: Example of solar protons and photoelectrons

CHAPTER 13

LANGMUIR PROBE (LANG)

13.1 FURTHER INFORMATION:

Contact: L.H. Brace (301) 344-8575
Code 961
Goddard Space Flight Center
Greenbelt, MD 20771

References: Krehbiel, J.P., L.H. Brace, R.F. Thies, W.H. Pinkus, and R.B. Kaplan, "The Dynamics Explorer Langmuir Probe Instrument", Space Science Instrumentation, 5, 493 (1981).

Brace, L.H., R.F. Theis, and W.R. Hoegy, "A Global View of the F-Region Electron Density and Temperature at Solar Maximum", Geophysical Research Letters, 9, 989 (1982).

13.2 SUMMARY PLOT PARAMETERS:

- o T_e Electron temperature
  --Primary geophysical parameter measured only by LANG.
- o N_i Ion density
  --Provides the simplest way of measuring plasma density.

13.3 PARAMETERS NOT PLOTTED:

- o N_e Electron density
  --Requires too much processing and is equal to N_i anyway.

13.4 MEASUREMENT UNITS

- o Geophysical Units: Temperature in degrees Kelvin and densities in ions per cm^3.
- o Range of Valid Data: Temperature 10^3 to 10^4 degrees Kelvin and ion density 10^4 to 10^7 ions/cm^3.
- o Summary Plot Sampling Rate: Two per second; the instrument samples half second int·
- o Summary Plot Resolution: Roughly 1/500 of full scale.
- o Accuracy of Trends on Plots: Around 10 percent (except where noted) with the relative accuracy around 1-2 percent (except in ionospheric structure).

- o Instrument Orientation: See Figure 8.2.

- o Summary Plot Algorithm: Multiplication of telemetry output of the in-flight processor by suitable constants.

13.5 MODES

- o Only the adaptive mode is used to get N_i and T_e for the summary plots.

- o Other modes are used for certain science data.

13.6 CORRECTED FOR:

- o Nothing.

13.7 UNCORRECTED FOR:

- o Spacecraft spinning
  --Most values are not valid during spinning.

13.8 DISPLAY ANOMALIES:

- o Plots prior to Version 3.0 are invalid due to programming error
  --N_i was a factor of 10 too low and the T_e scale was 100 to 10,000 degrees Kelvin; now the T_e scale is 1000 to 10,000 degrees and the N_i scale is 10,000 to 10,000,000 cm^{-3}.

13.9 INTERPRETATIONS:

Substantial variation in "standard" patterns exist. The following are given only as possible cases and should not be construed as definitive.

- o Intense particle precipitation regions
  --Shows as structure in N_i and T_e. See Figure 13.1, day 81317, orbit 1502, from 0113 to 0114 UT, for example.

13.10 COMMENTS

- o T_e and N_i are in error if plotted below $N_i = 1 \times 10^4$ cm^{-3} and T_e should also be ignored below 1000 degrees Kelvin, the lower boundary of the summary plot scale.

- o LAPI data are particularly useful in evaluating LANG data since low energy electrons (less than 1 keV) are associated with elevated T_e and structure in N_i.

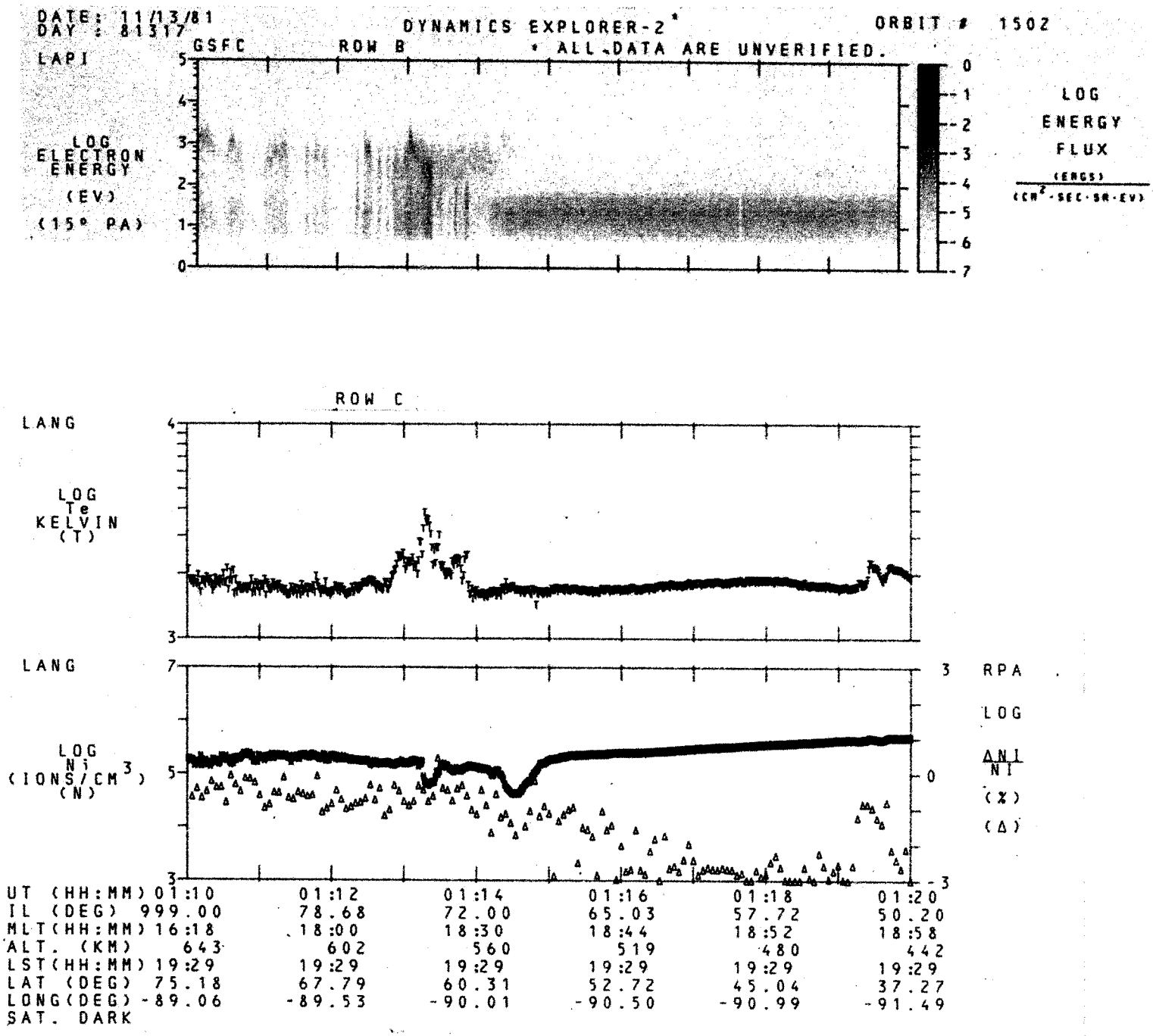

Figure 13.1: Example of effects of intense particle precipitation region

CHAPTER 14

RETARDING POTENTIAL ANALYZER (RPA)

14.1 FURTHER INFORMATION:

Contact: R. A. Power (214) 690-2852
B. J. Holt (214) 690-2832
University of Texas at Dallas
Box 688
Mail Stop FU22
Richardson, TX 75080

References: Hanson, H.B., R.A. Heelis, R.A. Power, C.K. Lippincott, D.R. Zuccaro, B.J. Holt, L.H. Harmon, and S. Sanatani, "The Retarding Potential Analyzer for Dynamics Explorer-B", Space Science Instrumentation, 5, 503 (1981).

Valladares, C.E., W.B. Hanson, J.P. McClure, and B.L. Cragin, "Bottom Side Sinusoidal Irregularities in the Equatorial F Region", Geophysical Research Letters, (accepted 1983).

14.2 SUMMARY PLOT PARAMETERS:

o $\Delta N_i/N_i$ Fractional change in ion density
--Indicates the roughness of the ionosphere, which is an excellent indicator of where plasma instabilities are operating. The quantity actually plotted is proportional to the output of the lowest frequency channel (32-86 Hz) of a six comb filter that detects ionospheric irregularities. The plotted quantity is proportional to the noise on the duct electrometer in the frequency range from 32 to 86 Hz. These signals are amplified by the wide band amplifier and by the detector itself. Thus

$$[\Delta N_i/N_i]_{rms}(\%) = [100\ V_{rms}(32\text{-}86\ Hz)]/V_{de}$$
$$= [100 * 10(R_{wb}-1)/2]\ V_{f1}/(G_{r1}*V_{de})$$
$$= [0.018 * 10(R_{wb}-1)/2](V_{f1}/V_{de})$$

where R_{wb} is the sensitivity range of the wide band amplifier, V_{f1} is the measured voltage output of filter #1, and V_{de} is the voltage output of the duct electrometer. G_{r1} is the end-to-end gain of the system with the wide band amplifier on Range 1 (its most sensitive range) which is equal to 5600.

14.3 PARAMETERS NOT PLOTTED:

- Bulk ion velocity in the direction of spacecraft motion
- Constituent ion concentrations
- Ion temperature along the spacecraft path
- Fractional change in electron density
  --Equals $\Delta N_i/N_i$

14.4 MEASUREMENT UNITS

- Geophysical Units: $\Delta N_i/N_i$ (%) in the 32 - 86 Hz range can only be related to the total broadband if one knows the spectral characteristics of the noise.
- Range of Valid Data: Quality control limits the lower end of the range to 0.001; the plot limits the upper end to 1000.
- Summary Plot Sampling Rate: The filter banks are sampled at least every 2 seconds and every other filter bank channel is plotted on the summary plots.
- Summary Plot Resolution: Roughly 1/500th of the plot range, which is larger than the resolution of the instrument.
- Accuracy of Trends on Plots: On the order of $\pm$10%.
- Instrument Orientation: See Figure 8.2. Data are not applicable if the angle of attack is greater than 45 degrees.
- Summary Plot Algorithm: The ratio is calculated after N_i is approximated by multiplying a constant by the telemetered voltage.

14.5 MODES

- None to affect the plots.

14.6 CORRECTED FOR:

- Nothing to affect the summary plots.

14.7 UNCORRECTED FOR:

- Spacecraft electric fields
  --No detectable problems.

- o Spacecraft attitude oscillations
  --No effect for angle of attack less than 45 degrees and frequencies between 32 and 86 Hz.

14.8 DISPLAY ANOMALIES:

- o None.

14.9 INTERPRETATIONS:

Substantial variation in "standard" patterns exist. The following are given only as possible cases and should not be construed as definitive.

- o Always disturbed ionosphere over the polar regions. See Figure 14.1, day 82032, orbit 2700, from 0811 to 0815 UT, for example; note the similar behavior of the 8-16 Hz VEFI data and the RPA data.

- o Often disturbed region in night time ionosphere that could occur at any latitude. See Figure 14.2, day 82005, orbit 2298, from 1150 to 1200 UT, for example.

- o Usually very quiet in sunlight except for cusp and auroral zones. See Figure 14.3, day 81330, orbit 1700, from 0924 to 0930 UT, for example; note the transition from the auroral zone to low latitude at 0924:45 UT.

14.10 COMMENTS

- o VEFI output in the 8 - 16 Hz octave indicates essentially the same characteristics as $\Delta N_i/N_i$. This should be expected since gradients in N_i generally have electric fields associated with them.

- o Very low N_i could give rise to instrumental noise.

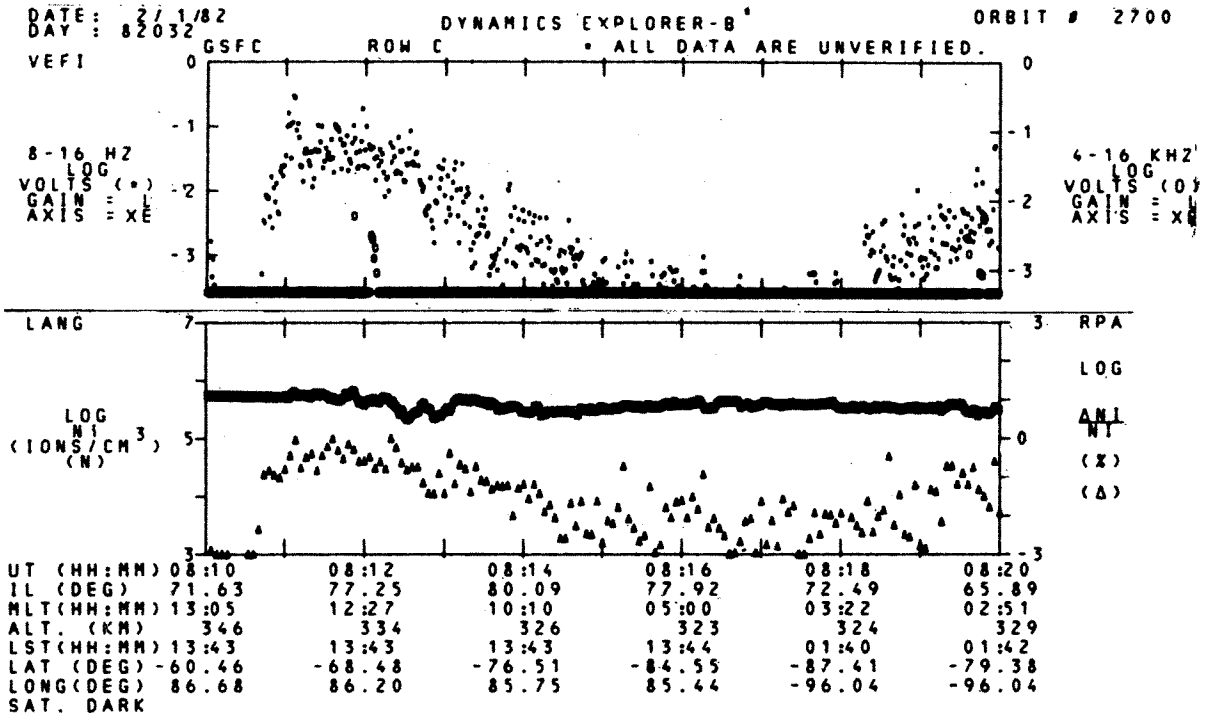

Figure 14.1: Example of disturbed ionosphere over the polar regions

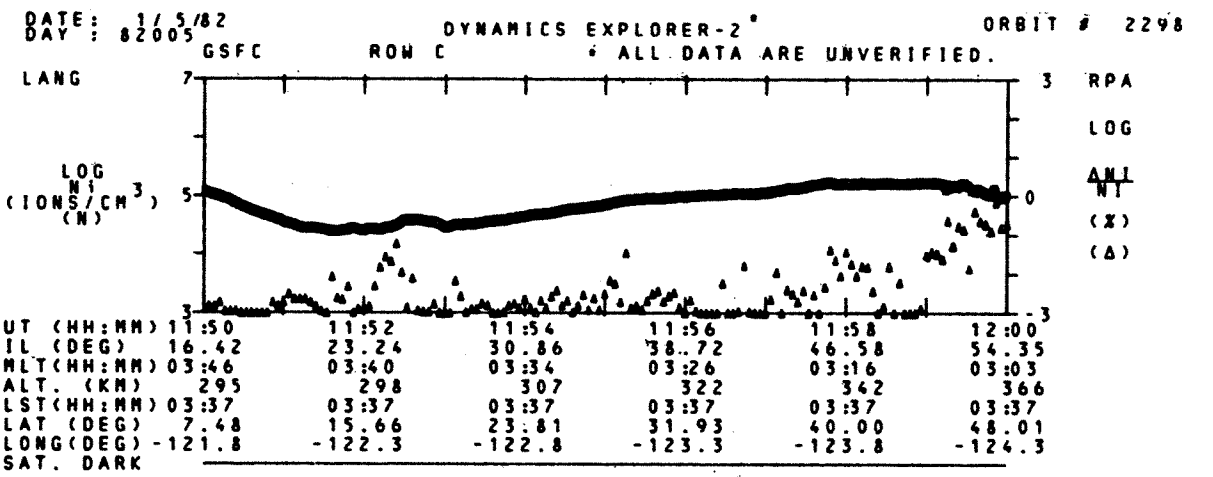

Figure 14.2: Example of disturbed night time ionosphere

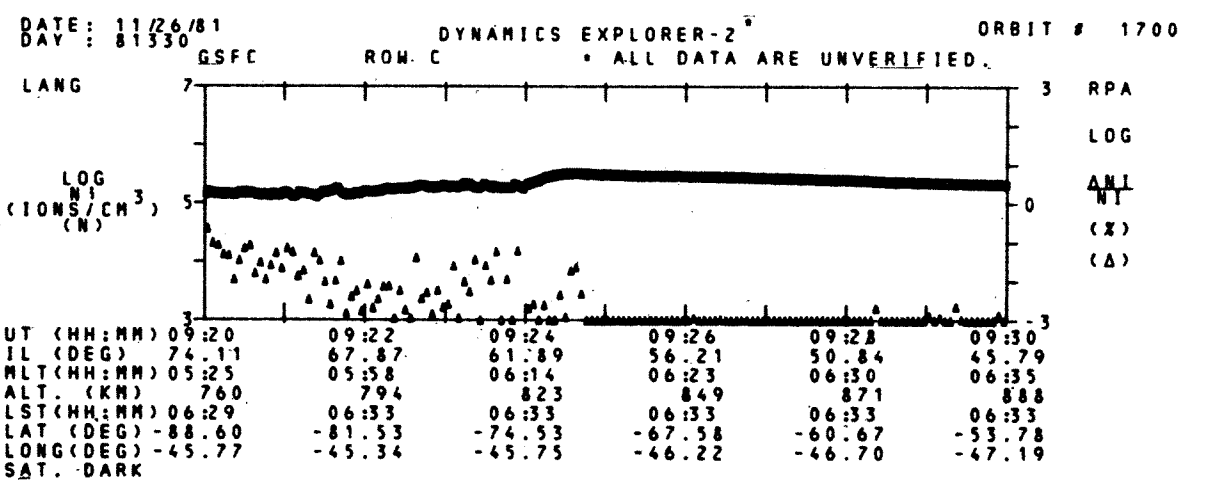

Figure 14.3: Example of quiet sunlit ionosphere

CHAPTER 15

WIND AND TEMPERATURE SPECTROMETER (WATS)

15.1 FURTHER INFORMATION:

Contact: Nelson W. Spencer (301) 344-5001
Code 960
Goddard Space Flight Center
Greenbelt, MD 20771

References: Spencer, N.W., L.E. Wharton, H.B. Niemann, A.E. Hedin, G.R. Carignan, and J.C. Maurer, "The Dynamics Explorer Wind and Temperature Spectrometer", Space Science Instrumentation, 5, 417 (1981).

15.2 SUMMARY PLOT PARAMETERS:

- o V(H) Zonal Neutral Wind
  --Velocity of transverse winds horizontal to the spacecraft direction of motion. V(H) > 0 for winds to the East in the horizontal plane.

- o V(V) Vertical Neutral Wind
  --Velocity of transverse winds vertical to the spacecraft direction of motion. V(V) > 0 for winds upward in the orbit plane.

15.3 PARAMETERS NOT PLOTTED:

- o Neutral atmosphere temperature
  --Simple plotting algorithms are not available.

15.4 MEASUREMENT UNITS

- o Geophysical Units: Given by rotating from spacecraft to geophysical coordinates for values in meters per second.

- o Range of Valid Data: V(H) $\pm$800 m/sec and V(V) $\pm$400 m/sec and only for altitudes below about 600 kilometers.

- o Summary Plot Sampling Rate: 7.5 per minute or less; the amount of time for one major frame of telemetry.

- o Summary Plot Resolution: Vertical velocity of the spacecraft times 8 seconds.

- o Accuracy of Trends on Plots: Roughly 20 m/s trends
  --Poisson noise roughly 10 m/s, attitude error roughly 15 m/s, and optical pulse digitization round-off roughly 20 m/s.

- o Instrument Orientation: See Figure 8.2. The instrument faces into the +X spacecraft axis. V(H) and V(V) are transverse winds horizontal and vertical to the direction of motion in spacecraft coordinates.

- o Summary Plot Algorithm: The average shaft angle of the baffle wake is evaluated; the angle is then converted into a velocity by substitution into a Taylor series.

15.5 MODES

- o Only one mode plotted.

15.6 CORRECTED FOR:

- o Nothing to affect the summary plots.

15.7 UNCORRECTED FOR:

- o Spacecraft attitude and flight path angle error
  --Except for gravity waves, the vertical wind component is usually zero; spacecraft attitude and flight path angle error introduce a long range deflection that slopes to zero at perigee and apogee.

- o Changes in meridional velocity
  --The error is less than 6 m/s in the horizontal direction and insignificant in the vertical direction.

15.8 DISPLAY ANOMALIES:

- o Zonal wind changes sign crossing the poles
  --Convention is positive to the East and the direction East changes on crossing the poles. See Figure 15.1, day 82262, orbit 6195, at 1438 UT and Figure 15.2, day 81337, orbit 1810 at 1925:55 UT, for examples.

- o Scatter of points at high altitudes and low densities (above about 600 kilometers)
  --Low densities decrease counting rate and increase error according to counting statistics.

- o Scale changes with Version 4.3
  --Needed to bring horizontal (zonal) velocity on scale.

- o Wrap-around of data on the plots
  --Off-scale velocity wraps around one time. Since the majority of velocities are on-scale the wrap-around velocities can usually be recognized. See Figure 15.2, day 81337, orbit 1810 at 1923:15 UT, for example.

- o Discontinuity of data especially in V(V)
  --Odd numbers of sweeps in Oxygen causes error of up to 150 m/s because of the gas-surface interaction. When the instrument switches to N2 the error goes away, causing a discontinuity. See Figure 15.2, day 81337, orbit 1810, at 1923:45 UT, for example.

15.9 INTERPRETATIONS:

Substantial variation in "standard" patterns exist. The following are given only as possible cases and should not be construed as definitive.

- o Polar gravity waves
  --Except for spacecraft attitude effects, vertical winds are usually zero on the plots. Cyclic effects are probably gravity waves. See Figure 15.3, day 82032, orbit 2708, from 2110 to 2116 UT, for example.

- o Polar E x B driven winds
  --Exhibited as large values for horizontal winds. See Figure 15.1, day 82262, orbit 6195 from 1431 to 1435 UT, for example. 1432:30 UT is a clear crossing of the auroral zone.

15.10 COMMENTS

- o Valid only for altitudes below 700 kilometers.

- o Ignore discontinuities on the order of 150 m/s. Ignore the long range slope of the vertical velocity plots (not corrected for changes in the flight path angle).

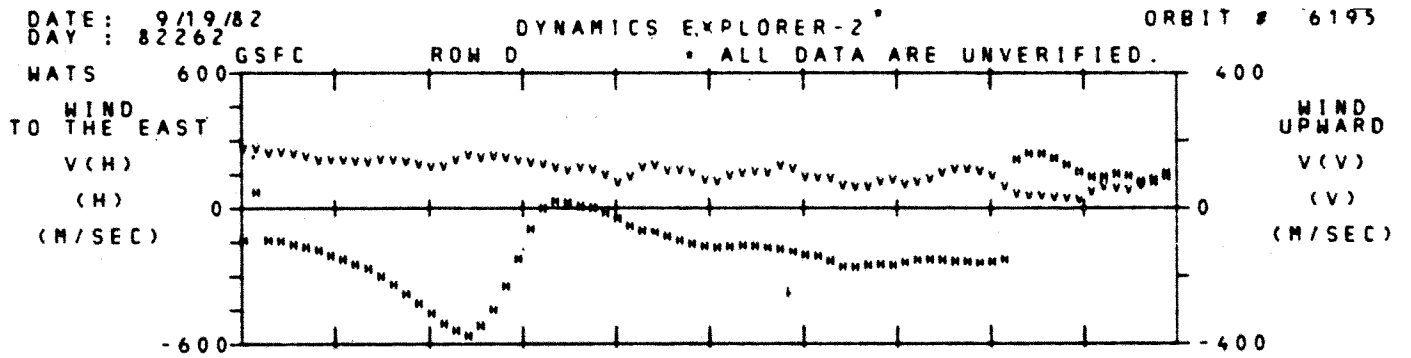

UT (HH:MM)	14:30	14:32	14:34	14:36	14:38	14:40
IL (DEG)	65.98	73.35	80.42	999.00	83.28	76.41
MLT(HH:MM)	11:12	11:25	12:10	19:30	21:59	22:22
ALT. (KM)	350	333	319	307	297	290
LST(HH:MM)	10:51	10:51	10:51	10:51	10:58	22:49
LAT (DEG)	56.69	64.64	72.61	80.62	88.64	83.31
LONG(DEG)	-56.29	-56.76	-57.22	-57.60	-56.54	120.78
SAT.	DARK					

Figure 15.1: Example of sign change in V(H) at the poles and E x B driven winds

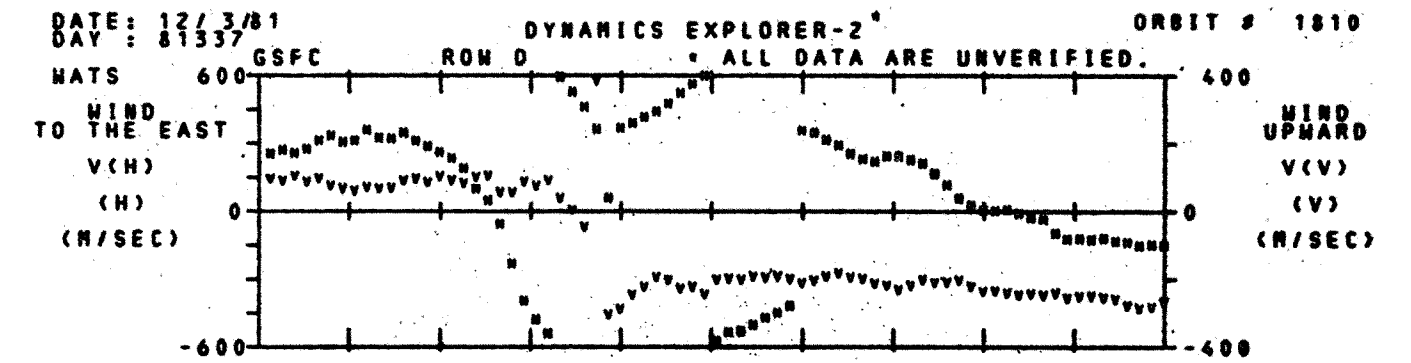

UT (HH:MM)	19:20	19:22	19:24	19:26	19:28	19:30
IL (DEG)	60.18	68.00	75.62	81.83	82.36	76.66
MLT(HH:MM)	04:57	04:39	04:07	02:58	00:13	21:01
ALT. (KM)	448	417	388	363	341	324
LST(HH:MM)	06:02	06:02	06:02	06:11	18:01	18:01
LAT (DEG)	65.78	73.58	81.45	89.38	82.64	74.60
LONG(DEG)	158.07	157.60	157.19	158.93	-24.19	-24.59
SAT.	DARK					

Figure 15.2: Example of data wrap-around, discontinuity of data, and polar sign change

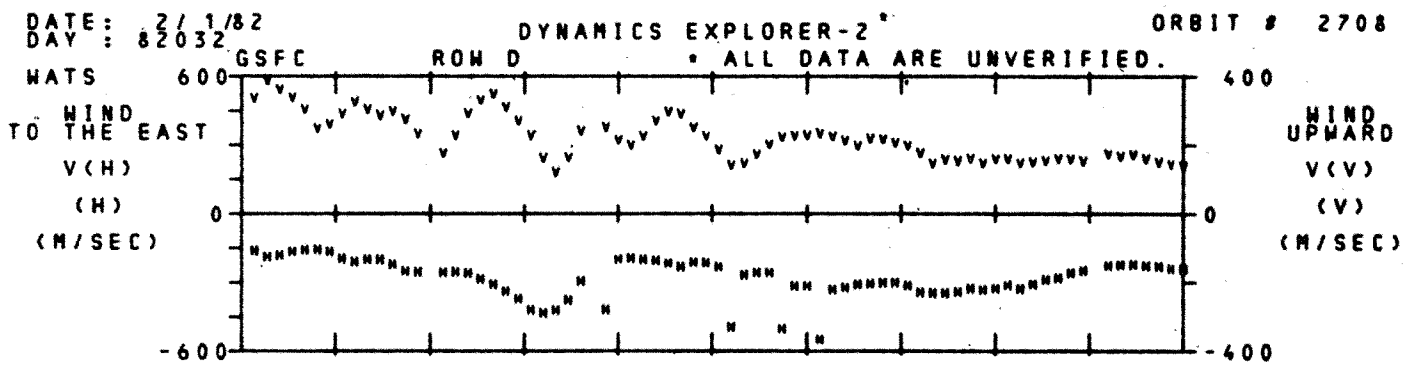

UT (HH:MM)	21:10	21:12	21:14	21:16	21:18	21:20
IL (DEG)	76.92	73.28	67.89	61.69	55.05	48.05
MLT(HH:MM)	21:46	23:34	00:16	00:38	00:51	01:00
ALT. (KM)	335	347	363	382	406	432
LST(HH:MM)	01:40	01:40	01:40	01:40	01:40	01:40
LAT (DEG)	-76.23	-68.22	-60.24	-52.30	-44.40	-36.54
LONG(DEG)	70.96	70.51	70.03	69.54	69.05	68.56
SAT.	DARK					

Figure 15.3: Example of polar gravity waves

CHAPTER 16

FABRY-PEROT INTERFEROMETER (FPI)

16.1 FURTHER INFORMATION:

Contact: T.L. Killeen (313) 763-6218
R.J. Theriault (313) 764-7220
Space Physics Research Laboratory
University of Michigan
2455 Hayward Street
Ann Arbor, Michigan 48108

References: Hays, P.B., T.L. Killeen, and B.C. Kennedy, "The Fabry-Perot Interferometer on Dynamics Explorer", Space Science Instrumentation, 5, 395 (1981).

Killeen, T.L., P.B. Hays, N.W. Spencer, and L.E. Wharton, "Neutral Winds in the Polar Thermosphere as Measured from Dynamics Explorer", Geophysical Research Letters, 9, 957 (1982).

16.2 SUMMARY PLOT PARAMETERS:

- o V(0) Horizontal neutral wind velocity in the orbit plane
- o --- Temperature of metastable atoms $O(^1D)$, filter wheel position 3
  --Yields neutral temperature.
- o --- Emission brightness for various wavelengths
  --Only for versions before Version 3.9; related to atmospheric volume emission rate. Not plotted now due to confusion and not central to mission objectives.
- o Since the instrument was tilted downward 15 degrees to baffle against sunlight, FPI data is not valid when the spacecraft was inverted.

16.3 PARAMETERS NOT PLOTTED:

- o Horizontal ion wind velocity
  --Cannot compete with statistical accuracy of RPA for ion drifts. FPI altitude profiles of ion winds require special software for analysis.
- o Velocity and temperature of $O(^1S)$, $O^+(^2P)$, $N(^2D)$, and $Na(^2P)$ metastable atoms
  --Require special programs for analysis.

- o Specific densities
  --Requires inversions of optical remote sensing data too complicated for summary level plotting.

16.4 MEASUREMENT UNITS

- o Geophysical Units: Ion velocity is plotted in meters per second and temperature in degrees Kelvin.

- o Range of Valid Data: Velocity $\pm$500 m/sec and temperature 500 to 2000 degrees Kelvin. Usable data is produced for spacecraft altitudes between 250 and 600 kilometers and 200 to 400 kilometers for tangential measurements.

- o Summary Plot Sampling Rate: 15 second averages to avoid noisy plots due to statistical uncertainties especially on nightside and twilight passes.

- o Summary Plot Resolution: About 30-50 m/s per plotted point and 50-80 degrees Kelvin, depending on the degree of illumination of the atmosphere.

- o Accuracy of Trends on Plots: Roughly 50 m/s due to the simple reduction algorithm used for the summary plots.

- o Instrument Orientation: See Figure 8.2. V(U) is positive away from the spacecraft. All FPI measurements at summary plot level refer to the atmosphere at the tangent point to the earth's surface along the instantaneous line-of-sight of the instrument. There is, therefore, a varying phase shift between the plotted FPI data and the other in-situ measurements. This shift is typically 2 minutes or a few degrees in latitude. The instrument has 16 viewing directions below the X axis from 5 to 15 degrees. Only the top few mirror positions are used in order to both minimize this phase shift and to weight the data to altitudes just below the spacecraft. FPI is tilted down 15 degrees to avoid the sun on the horizon of the Earth. The spacecraft is inverted every six months and FPI is thus tilted 15 degrees away from the earth. Times of inversions are given in the Introduction Section 8.7.

- o Summary Plot Algorithm: Measures Doppler shift and broadening of $O(^1D)$ emission at 630 nm from observed high resolution spectrograms using a linearized least square fit chosen by a simple algorithm from a set of pre-calculated inversion matrices. A simple matrix multiplication gives the estimates of the neutral wind and temperature.

16.5 MODES

- o Only those modes where filter wheel position 3 ($O(^1D)$) is used are plotted.

- o Binary modes where the filter wheel oscillates between two filters
  --Always some summary plot data with fewer points. See Figure 16.1, day 83036, orbit 8364, from 1150 to 1200 UT, for example.

- o A and B modes where the program bins data by scan mirror position
  --Plots only when filter position 3 is used.

- o Plots several scan mirror positions
  --Each position has appropriate correction and is averaged in 15 second bins for each point.

16.6 CORRECTED FOR:

- o First order temperature effects such as drifts in wavelength due to etalon size changes.

- o Angle of view
  --Simple cosine (θ) * spacecraft velocity correction, where θ is the angle of view below the local horizontal.

16.7 UNCORRECTED FOR:

- o Errors and offsets in spacecraft attitude
  --Meridional measurements are less susceptible than WATS or IDM.

- o Spacecraft attitude oscillations
  -- Insignificant error.

16.8 DISPLAY ANOMALIES:

- o Turn-on and turn-off calibration sequence
  --Shows up as a string of off-scale points for about two minutes. See Figure 16.2, day 82032, orbit 2708, from 2117 to 2120 UT, for example.

- o Noisy data
  --Due to poor illumination of the atmosphere (night side) and low counting rates.

16.9 INTERPRETATIONS:

Substantial variation in "standard" patterns exist. The following are given only as possible cases and should not be construed as definitive.

- o Large winds over the polar cap
  --See Figure 16.3, day 81297, orbit 1213, from 1430 to 1440 UT, for an example of a South summer polar pass. Trends are particularly clear over the well-illuminated pole.

- o Low latitude dayside
  --See Figure 16.4, day 81279, orbit 951, from 2230 to 2240 UT and following frames, for example. This is about the best accuracy that can be obtained from the summary plots. Note the small winds over the equator but with a geophysically significant gradient. Off-scale points at the end are due to inclusion of calibration sequence data. The temperature scatter includes a component due to different altitudes sampled and binned together. The user should draw his best line through the temperature data to estimate exospheric temperatures. Most of the scatter is still statistical rather than geophysical.

- o South pole storm pass
  --See Figure 16.2, day 82032, orbit 2708, from 2110 to 2117 UT, for an example of elevated neutral winds and temperatures.

16.10 COMMENTS

- o Trust data only out to solar zenith angles of 100 degrees.

- o Plots made from nightside passes show a lot of scatter but some trends are discernible.

- o Only altitudes below a fixed value are plotted to avoid noisy plots. The FPI cannot view the $O(^1D)$ layer above 650 kilometers.

- o Local time of the orbit indicates the degree of atmospheric illumination.

- o Generally, skip noisy plots where no trend is observable and reject off-scale points. However, full analysis of FPI data may yield useful data.

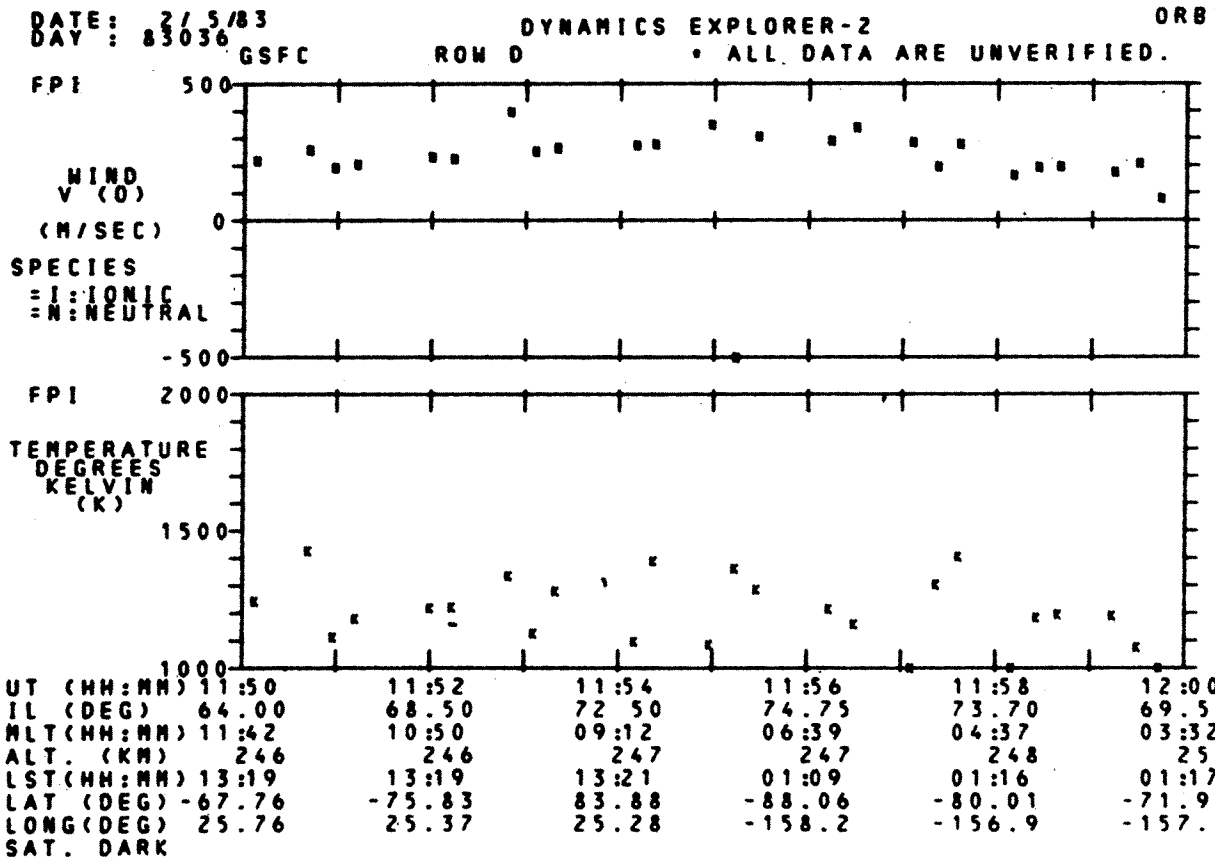

Figure 16.1: Example of binary mode

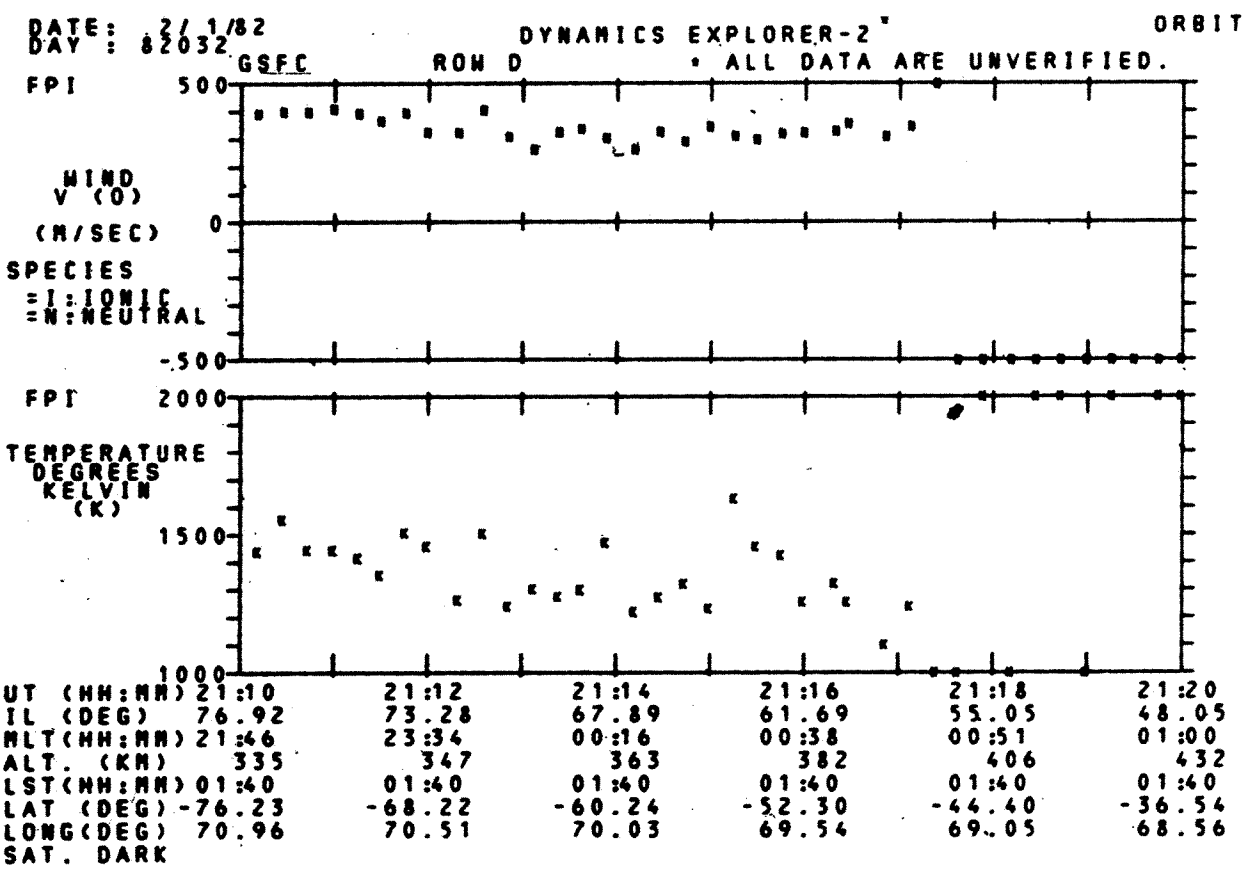

Figure 16.2: Example of South pole storm pass and turn-off calibration

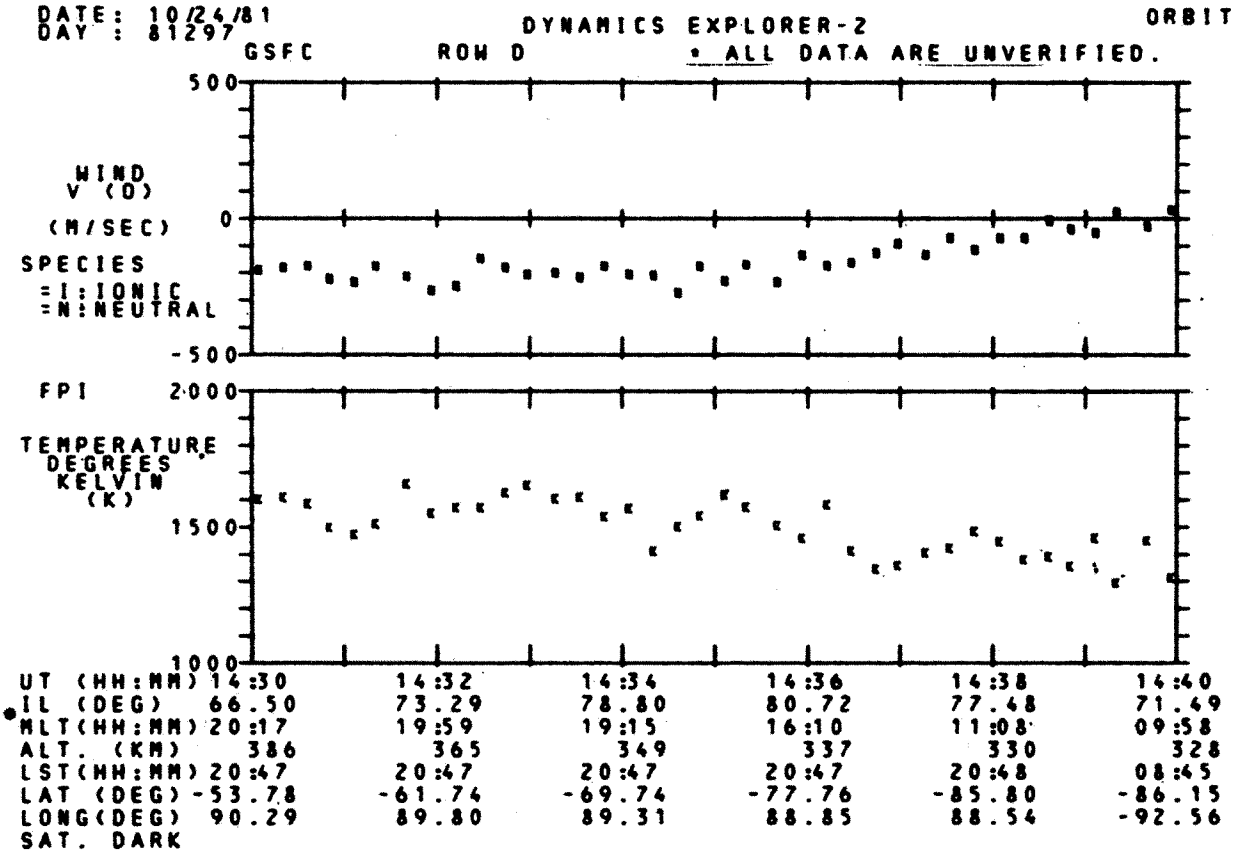

Figure 16.3: Example of large winds over the polar caps

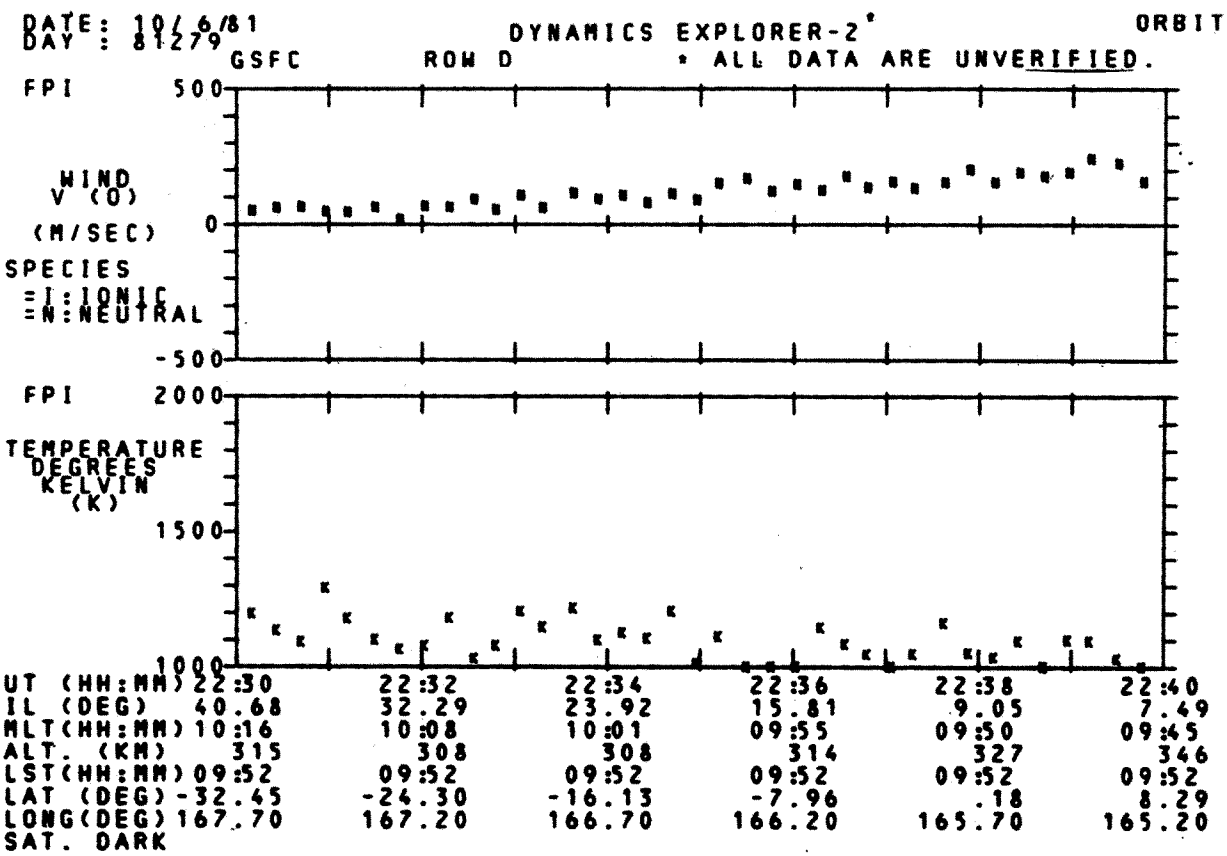

Figure 16.4: Example of low latitude dayside pass

CHAPTER 17

NEUTRAL ATMOSPHERE COMPOSITION SPECTROMETER (NACS)

17.1 FURTHER INFORMATION:

Contact:

G.R. Carignan
Space Physics Research Laboratory
University of Michigan
2455 Hayward Street
Ann Arbor, Michigan 48109
(313) 764-9426

A.E. Hedin
Code 961
Goddard Space Flight Center
Greenbelt, MD 20771
(301) 344-8393

References: Carignan, G.R., B.P. Block, J.C. Maurer, A.E. Hedin, C.A. Reber, and N.W. Spencer, "The Neutral Mass Spectrometer on Dynamics Explorer B", Space Science Instrumentation, 5, 429 (1981).

17.2 SUMMARY PLOT PARAMETERS:

- o N2 Nitrogen Density
  --To a large extent, N2 reflects the thermal state of the atmosphere and is affected relatively little by flow and chemistry processes.

- o TINF Exospheric Temperature
  --Derived from the N2 density; characterizes the N2 density measurements with a height independent quantity which may make it easier to identify areas of neutral heating.

- o N2(300) Nitrogen density normalized to 300 kilometers
  --Alternative to N2 above. See Section 17.10 for comment on normalization.

- o HE(300) Helium density normalized to 300 kilometers
  --Reflects the results of flow processes and thus complements the N2 measurements. "100HE(300)" on the plot indicates the scale for N2(300) must be divided by 100 for Helium.

- o O/N2(300) Oxygen to Nitrogen density ratio normalized to 300 kilometers
  --Important in ionospheric processes (F-region electron density).

17.3 PARAMETERS NOT PLOTTED:

- o Argon density
  --Too low to be detectable much of the time.

- o Atomic Nitrogen density
  --Estimates are so uncertain it would cause confusion to plot it.

17.4 MEASUREMENT UNITS

- o Geophysical Units: Densities are in molecules per cm^3. Temperature is in degrees Kelvin.
- o Range of Valid Data: N2 density 10^5 to 10^9 cm^{-3}, normalized N2 10^7 to 10^{11} cm^{-3}, normalized HE 10^5 to 10^9 cm^{-3}, O/N2 density ratio 1 to 10 percent, and TINF 400 to 2100 degrees Kelvin.
- o Summary Plot Sampling Rate: Once every two seconds. The instrument samples 8 times per second.
- o Summary Plot Resolution: Roughly 1/500th of the scale range.
- o Accuracy of Trends on Plots: The relative accuracy of individual points is better than 5 percent.
- o Instrument Orientation: See Figure 8.2.
- o Summary Plot Algorithm: The data are multiplied by a calibration constant; a diffusive equilibrium equation produces temperature and extrapolation data.

17.5 MODES

- o Only one plotted.

17.6 CORRECTED FOR:

- o Nothing to affect the summary plots.

17.7 UNCORRECTED FOR:

- o Spacecraft Attitude
  --Insensitive to attitude if spacecraft was within a few degrees of ram direction.
- o Spacecraft Velocity
  --Measurements are directly proportional to velocity, but only a single nominal speed is assumed for the summary plots.
- o Gas background within the instrument
  --Leads to increasingly inaccurate N2 and O densities at high altitudes.

17.8 DISPLAY ANOMALIES:

- o Plotting when the spacecraft was pointed away from direction of motion
  --Produces low densities on the summary plots; these periods have no geophysical significance.

o Plotting when the spacecraft was spinning
  --Produces modulation of densities at the spin rate; only the envelope corresponding to the ram direction is comparable to despun data.

o Initial downward drift after instrument turn-on
  --Outgassing while instrument warms up. Normally the instrument is warmed-up prior to operations.

o High altitude inaccuracies
  --N2 and O are asymptotic toward a residual background reading and estimated temperature rises to unrealistic values. See Figure 17.1, day 81290, orbit 1103, from 0400 to 0410 UT, for an example when leaving high altitudes.

o Off-cycle during passes
  --Plotting turned off with LAPI flag (i.e., when LAPI turned off); corrected with Version 4.6.

o O/N2 ratio sometimes off-scale
  --Narrow scale range was chosen to show detail. This ratio is not too meaningful at high altitudes anyway.

o N2 density goes off-scale at low altitudes
  --Near the end of the mission only.

17.9 INTERPRETATIONS:

Substantial variation in "standard" patterns exist. The following are given only as possible cases and should not be construed as definitive.

o Neutral heating signature
  --Increases in N2 and TINF correlated with decreases in He and O/N2 in almost every orbit with perigee at high latitudes. See Figure 17.2, day 81290, orbit 1103, from 0430 to 0440 UT, for example.

o Oscillatory patterns
  --May be gravity waves. See Figure 17.3, day 82018, orbit 2497, from 1850 to 1858 UT, for example.

o Summer
  --Seasonal increases in temperature and N2(300) toward the summer pole with a decrease in He and O/N2 for orbits with perigee near the equator around the solstices. See Figure 17.4, day 81326, orbit 1636, from 0140 to 0150 UT, for example.

17.10 COMMENTS

- Normalization is intended to provide height independent quantities. Normalization assumes diffusive equilibrium and a temperature equal to the exospheric temperature estimated from N2. The 300 kilometer altitude was chosen because it would remain near or within the altitude range of actual measurements for most of the flight and thus minimize extrapolation errors.

- Mass resolution is at least 1 AMU.

- High latitude heating is often coincident with particle precipitation on the LAPI plot or increases in electron temperature on the LANG plot.

- Ignore data at high altitudes, especially N2 and O.

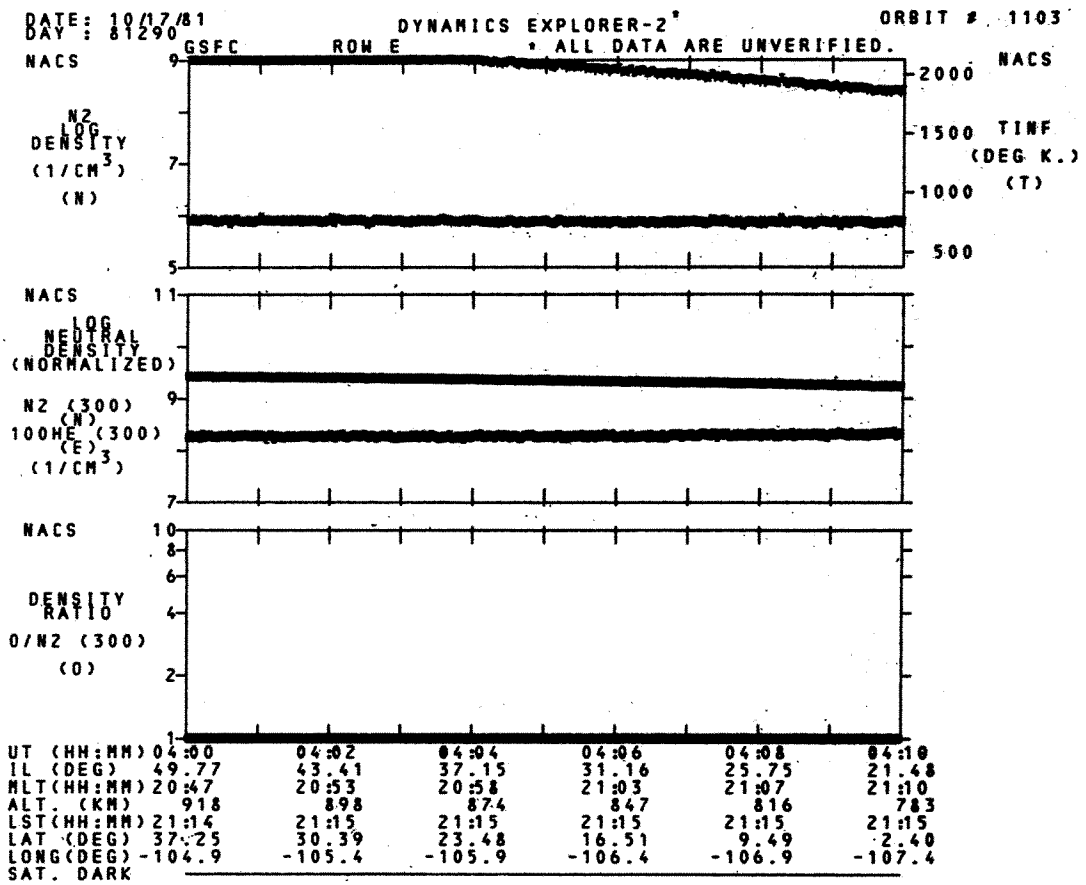

Figure 17.1: Example of high altitude inaccuracies

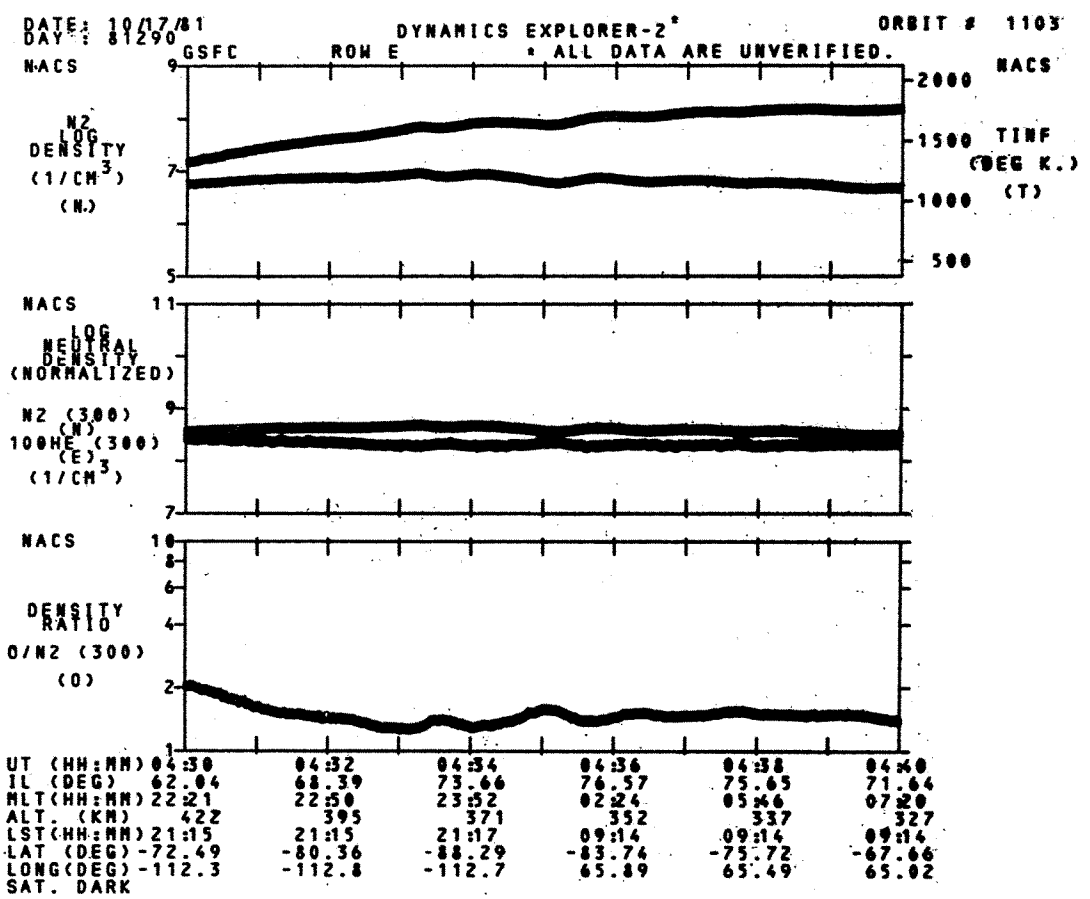

Figure 17.2: Example of neutral heating

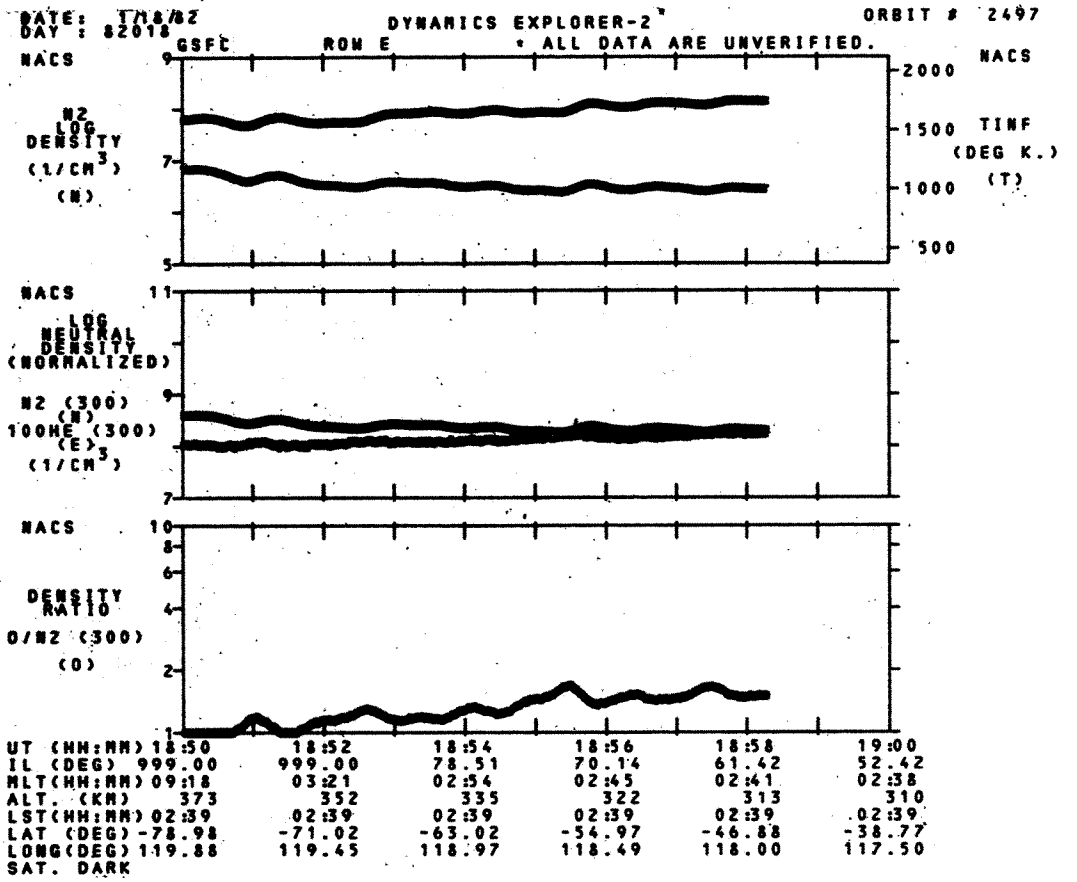

Figure 17.3: Example of possible gravity waves

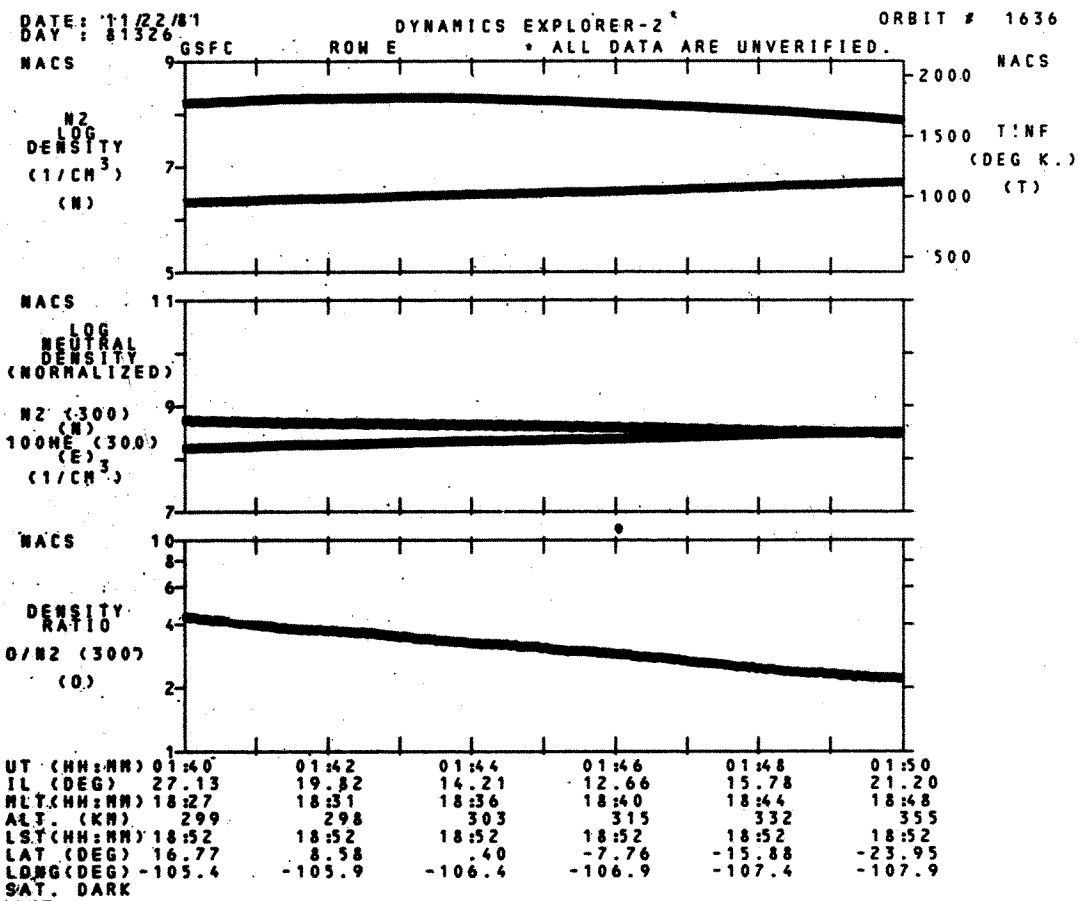

Figure 17.4: Example of seasonal heating